5-2018

Studies on High-Performance Sustainable Blends from Lignin, a Low- Cost Renewable Feedstock

Kokouvi Mawuko Akato
University of Tennessee

To the Graduate Council:

I am submitting herewith a dissertation written by Kokouvi Mawuko Akato entitled "Studies on High-Performance Sustainable Blends from Lignin, a Low- Cost Renewable Feedstock." I have examined the final electronic copy of this dissertation for form and content and recommend that it be accepted in partial fulfillment of the requirements for the degree of Doctor of Philosophy, with a major in Energy Science and Engineering.

Amit K. Naskar, Major Professor

We have read this dissertation and recommend its acceptance:

Roberto S. Benson, David P. Harper, Nicole Labbe

Accepted for the Council:

Dixie L. Thompson

Vice Provost and Dean of the Graduate School

(Original signatures are on file with official student records.)

Studies on High-Performance Sustainable Blends from Lignin, a Low-Cost Renewable Feedstock

A Dissertation Presented for the
Doctor of Philosophy
Degree
The University of Tennessee, Knoxville

Kokouvi Mawuko Akato
May 2018

DEDICATION

This work is dedicated to my parents especially my mother, Ayawa Kossivi, who cherishes education but has not gotten the opportunity to attend school.

ACKNOWLEDGEMENTS

I would like to thank my principal supervisor and mentor, Dr. Amit Naskar for his timely advice, academic advice, reading and improving of drafts of journals and dissertation-related documents, and meticulous scrutiny that have helped me to a very great extend to accomplish my dissertation works.

I owe a deep sense of gratitude to my committee members. Dr. Nicole Labbe for her continuous support; Dr. David Harper for his help, brilliant suggestions and teaching with kindness, and Dr. Roberto Benson, for his fatherly guidance and advices, and making sure I continue to improve.

I am thankful for the opportunity at Oak Ridge National Laboratory and at the University of TN, Knoxville. Learning under all professors will forever impact my professional career. I will take the lessons I learned with me for the rest of my life.

My sincere thanks to members of the carbon and composites group at Oak Ridge National Laboratory, in particular Dr. Ngoc A. Nguyen and Fue Xiong for their invaluable help in material characterization, the Center for Renewable Carbon (CRC) and the Bredesen Center for Interdisciplinary Research and Graduate Education at the University of TN, Knoxville during my appointment duration, especially Dr. Timothy Rials, who gave me the opportunity to prove myself in graduate school.

I would like to thank my family and friends who continuously encouraged me for every challenge I choose in my life.

It is a privilege to thank my wife Ida Ayivor-Akato, for her grace, her strength, her constant encouragement and for being my backbone throughout my research. To my son Christopher E. Akato, I love you!

Lastly, I offer my regards and blessings to all of those who have supported me in any respect during the completion of the project.

ABSTRACT

Demand for plant-derived materials has increased in recent years not only to boost the economics in US Agricultural and Forestry sectors, but also to address environmental concerns. Lignin, an aromatic polymer, extracted from biomass has the potential to be used for preparing innovative materials. Developing high-performance polymers from lignin is attractive, but often requires additional lignin modification and cost-intensive functionalization that creates chemical wastes. The overarching goal of this study was the development of sustainable high-performance alloys from thermoplastic and lignin without chemical modification using melt-blending technique, which is technically the most convenient and inexpensive method. Thus, the approach aimed to find value for lignin, a low-cost byproduct of modern biorefineries and woody biomass pulping industry. More specifically, we conducted comprehensive study on thermal, rheological, morphological, and structural properties of the thermoplastic-lignin blends together with lignin's chemistry and thermal behavior to understand and improve the materials' performance.

The first part of the study involved exploiting lignin's miscibility with polyethylene oxide (PEO) to enhance the compatibility between lignin and acrylonitrile-butadiene-styrene (ABS) polymer under reactive mixing conditions and develop a recyclable renewable matrix for sustainable composite applications.

The second part consisted on manipulating the melt behavior of polyethylene terephthalate (PET) polyester from pre-consumer wastes using a renewable plasticizer tall oil fatty acid (TOFA). To avoid lignin degradation and devolatilization during amalgamation with plasticized PET we devised thermal treatment of lignin that not only improved the stability but also reduced dispersed lignin domains in the matrix.

The last part was based on understanding the effect of source-dependent lignin chemistry on its compatibility with a renewable polyester. Organosolv lignin from oak, methanol fractionated Kraft pine lignin, and methanol fractionated acetic acid extracted wheat straw lignin give equivalent melt processability. Blends of these lignins with polylactic acid (PLA) were studied to understand the relationship between the lignin chemistry and resulting blends' thermal stability, mechanical properties, and melt-rheology.

This study answered questions on the role of lignin chemistry that affects the properties of thermoplastic/lignin blends and developed methods to modify melting behavior of both thermoplastic matrices and lignin without thermal degradation.

PREFACE

This dissertation is structured to cover six main chapters. An overall introduction, four research articles, and an overall conclusion. This dissertation manuscript is prepared to cover the main research objective and the approach to answer the research questions.

Chapter 1 covers the state of the art in lignin structure characterization and lignin-derived thermoplastics focusing primarily on the blends of lignin and thermoplastics. We used available background and literature to give readers detailed insight on lignin structure, biomass sources and extraction methods, and relate them to the structure and properties of thermoplastics-lignin blends. A quick overview was presented on the reactive aspect of producing polymeric materials from lignin. Finally, we discussed application and processing engineering of the thermoplastic-lignin blends.

Chapter 2 is a version of an article published in “ACS sustainable chemistry and engineering”. It focuses on self-assembly of lignin in acrylonitrile-butadiene-styrene (ABS), a polymer heavily used in the automotive industry. Due to lack of miscibility between lignin and ABS, polyethylene oxide PEO was added. We evaluated the blends in term of mechanical properties, rheology and morphology. Composites produced from the high lignin content blends and carbon fibers have performance of the one used currently in 3 D applications.

Chapter 3 and 4 are paired together. First, renewable plasticizer tall oil fatty acid (TOFA) was used to modify engineering polyethylene terephthalate (PET). We present detailed characterization of effects of different concentration of TOFA on PET structure, morphology and performance. Such modification reduced PET normal working temperature and viscosity, which allows to expand PET use to other applications, such as melt blending with thermally unstable lignin. In chapter 4, we controlled the dispersion in plasticized PET and characterized phase dispersion of lignin. Interfacial interactions between lignin and PET were assessed by evaluating the molecular dynamics around the glass transition.

Chapter 5 addresses the influence of lignin from different biomass source and extraction methods on interactions with polylactic acid (PLA) matrix. Lignin complex chemical structure was characterized in detail to understand how their features are important to development of PLA/lignin blends.

Chapter 6 comprises an overall conclusion related to lignin thermoplastic blends using different techniques and matrices and future research.

TABLE OF CONTENTS

CHAPTER 1 Literature review 1
1.1. Lignin as a renewable macromolecule 2
1.1.1. Lignin structure and chemistry. 2
1.1.2. Extraction methods of lignin. 4
1.1.3. Characterization of lignin. 5
1.2. Renewable blends of thermoplastic/lignin 6
1.2.1. Polyolefins. 6
1.2.2. Polymers with aromatic rings. 7
1.2.3. Other polymers. 7
1.2.4. Polyesters. 8
1.3. Modification of lignin for improvement of interfacial interaction in blends 11
1.3.1. Chemical modification. 11
1.3.2. Addition of compatibilizers. 12
1.3.3. Plasticization route. 12
1.4. Lignin as a reactive component for preparation of polymeric materials 12
1.5 Applications of lignin-based thermoplastics 13
1.6. Process engineering of thermoplastic/lignin blends 14
1.7. Motivation and Objectives 15
References 18
CHAPTER 2 Poly(ethylene oxide)-Assisted Macromolecular Self-assembly of Lignin in ABS Matrix for Sustainable Composite Applications 25
Abstract 26
2.1. Introduction. 26
2.2. Experimental section. 29
2.2.1. Materials 29
2.2.2. Blend Preparation. 29
2.2.3. Thermal Analysis. 29
2.2.4. Tensile Testing and Morphology Analysis. 29
2.2.5. Rheological Properties. 30
2.3. Results and discussion 30
2.3.1. Tensile Properties. 30
2.3.2. Morphology Analysis by SEM and TEM. 30
2.3.3. Capillary Rheology Study. 35
2.3.4. Effect of PEO on Thermal Degradation. 36
2.3.5. Dynamic Mechanical Analysis. 36
2.3.6. Carbon Fiber Composites. 38
2.4. Conclusion 40
References 41

Appendix A 43
CHAPTER 3 Recycling Waste Polyester via Modification with a Renewable Fatty Acid for Enhanced Processability 49
Abstract 50
3.1. Introduction 50
3.2. Experimental section 52
3.2.1. Materials 52
3.2.2. Blending of Post-industrial Polyester and TOFA. 52
3.2.3. Blends Characterization. 52
3.2.4. Fiber Melt-spinning and Characterization. 53
3.3. Results and discussion 53
3.3.1. Thermal characteristics. 53
3.3.2. Crystallization behavior 56
3.3.3. Flow characteristics. 57
3.3.4. Morphological evaluation 57
3.3.5. Properties of fibers spun from plasticized polyester resins 60
3.4. Conclusion 62
References 63
Appendix B 65
CHAPTER 4 Controlling Lignin Dispersion and Interfacial Interactions in Recycled Polyester Renewable Composites 67
Abstract 68
4.1. Introduction 68
4.2. Experimental section 70
4.2.1 Materials 70
4.2.2. Lignin thermal treatment and characterization. 70
4.2.3. Blend preparation. 70
4.2.4. Thermal analysis. 71
4.2.5. Scanning electron microscopy and morphology analysis. 71
4.2.6 Tensile and dynamic mechanical testing. 71
4.2.7 Rheological evaluation. 71
4.3. Results and discussion 71
4.3.1. Lignin structural transformation. 71
4.3.2. Thermal and morphological properties of the compositions 76
4.3.3. Interfacial interactions-performance relationships 77
4.3.4. Processing engineering and degradation parameters of partially renewable blends 80
4.4. Conclusion 84
References 85
Appendix C 90

CHAPTER 5 Influence of lignin functionalities on intermolecular interactions in polylactic acid blends 95
Abstract 96
5.1. Introduction 96
5.2. Experimental section 98
5.2.1. Materials 98
5.2.2 Lignin characterization 99
5.2.3 Blend preparation and compression molding 99
5.2.4. Thermal analyses 99
5.2.5. Tensile testing and morphology analysis 99
5.3. Results and discussion 100
5.3.1. Survey of lignins variability. 100
5.3.2 Thermal stability. 100
5.3.3. Mechanical properties. 104
5.3.4. Glass transition behavior and activation energy for thermal relaxation. 107
5.4. Conclusion 109
References 110
Appendix D 113
CHAPTER 6 Conclusion 122
6.1. Conclusions 123
6.2. Future research 124
VITA 126

LIST OF TABLES

Table 1-1. H/G/S ratio from various sources 2
Table 2-1 Temperatures corresponding to the loss tangent peak (T_g) at different frequencies from the dynamic mechanical analysis, and the activation energy (E_a) associated with thermal relaxation at T_g..... .37
Table 3-1. Thermal and crystalline properties of neat PET and its plasticized derivatives 54
Table 3-2. Mechanical properties of the plasticized fibers..... 61
Table 4-1. Functional groups of the L lignin and thermally treated lignin (L_{HT}) as determined by the quantitative ^{31}P NMR method (mmol/g)..... 73
Table 4-2. Quantitative estimation of interactions computed from mechanical properties of the blends ..... .79
Table 4-3. Temperatures corresponding to the loss tangent peak (T_g) at different frequencies from the dynamic mechanical analysis, and the activation energy (E_a) associated with thermal relaxation at T_g..... 81
Table 4-4. Thermal degradation parameters of neat PET, PET_{PL}/30L and PET_{PL}/30 L_{HT}. 83
Table C-1. Assignment of hydroxyl groups peaks in ^{31}P NMR spectroscopy 89
Table C-2.^{13}C and ^{1}H assignments of the lignin signals in 2D HSQC spectra..... 91
Table C-3.Thermal behavior temperatures, calorimetric values, and degree of crystallinity of PET and it lignin derived blends..... 93
Table 5-1. Isolation method, content in hydroxyl groups quantified by ^{31}P NMR, Average molar mass indexes measured by GPC of the lignins used for blending with PLA. 101
Table 5-2. Temperatures corresponding to the loss tangent peak (T_g) at different frequencies from the dynamic mechanical analysis, and the activation energy (E_a) associated with thermal relaxation at T_g..... 108
Table D-1 The extraction method, biomass type, melting temperature (T_m) and flow temperature (T_{flow}) determined by hot stage..... 114
Table D-2 ^{13}C and ^{1}H assignments of the lignin signals in 2D HSQC spectra..... 116
Table D-3 Tensile properties of PLA and its lignin derived blends at 30 wt. % lignin contents. 119

LIST OF FIGURES

Figure 1-1. Phenylpropanoid monomers of lignin: p-coumaryl, coniferyl, and sinapyl alcohols 3
Figure 1-2. Empirical model structure of spruce lignin with two different structures: The random branching model (a), the linear lignin model (b). 3
Figure 1-3. Illustration of an extended straightening of a hardwood lignin molecule (top) and softwood lignin (bottom) in the presence of PEO. 9
Figure 1-4. Tensile strength as a function of lignin content for PET, PS, PP, LDPE. 10
Figure 1-5 Chemical esterification of lignin by acetic anhydride 11
Figure 2-1. Schematic diagram of compositions of lignin-extended ABS resins and their fiber-reinforced composites created from a blend modified with poly(ethylene oxide). 28
Figure 2-2. Ratios of tensile strength (a), tensile modulus (b), and ultimate elongation (c) of lignin-loaded matrices over those of neat ABS at different lignin concentrations. 32
Figure 2-3. Scanning electron micrographs of the cryofractured surface of molded ABS/lignin (70/30) (a) and the corresponding performance-enhanced blend of ABS/lignin/PEO (70/27/3) (b) 33
Figure 2-4. Transmission electron micrographs of neat ABS (a), ABS/lignin (70/30) (b), and ABS/lignin/PEO (70/27/3) (c) blends. 34
Figure 2-5. Capillary rheology data of neat ABS, its selected lignin-loaded compositions, and the corresponding PEO compatibilized formulation studied at 200°C. 35
Figure 2-6. Storage modulus data for neat ABS, ABS/lignin, and ABS/ (lignin/PEO) compositions at 1 Hz frequency (inset figure show expanded storage modulus axis). 39
Figure 2-7. Loss tangent peak of the rubbery phase (a) and of the hard phase (b) in different ABS compositions at 1 Hz frequency. 39
Figure A-1. Micrographs of tensile fractured surfaces; (a) neat ABS, (b) ABS/10% lignin, (c) ABS/10% lignin–PEO, (d) ABS/30% lignin, and (e) ABS/30% lignin–PEO 44
Figure A-2. Micrographs of cryofractured surfaces; (a) neat ABS, (b) ABS/10% lignin, (c) ABS/10% lignin–PEO, (d) ABS/20% lignin, (e) ABS/20% lignin–PEO, (f) ABS/30% lignin, and (g) ABS/30% lignin–PEO 45
Figure A-3. Capillary rheology data of the neat ABS, its selected lignin-loaded compositions [10% (a), 20% (b), and 30% (c) lignin loadings], and corresponding PEO compatibilized formulation studied at 200°C. 46
Figure A-4.Thermogravimetric analysis data of neat lignin and lignin–PEO (10 wt. % PEO) mix. 47

Figure A-5. Ratio of tensile strength (a), tensile modulus (b), and ultimate elongation (c) of organosolv Alcell lignin-loaded matrices over those of neat ABS at different lignin concentrations. 48
Figure 3-1. Thermal characterization of as-received recycled PET and it plasticized derivatives. (a) DSC second heating thermograms, (b) DSC cooling thermograms, (C) DMA storage modulus E' and (d) DMA loss factor Tan δ. 55
Figure 3-2. (a) Crystallization peak temperatures T_{rec} and (b) crystallization enthalpy ΔH_{rec} as a function of log cooling rate 56
Figure 3-3. Frequency-dependent complex viscosity η* at T_{ref} = 240C (a) and 250C (b) and Frequency-dependent storage modulus G' at T_{ref} = 240C (c) and 250C (d) of recycled PET and its TOFA plasticized derivatives. 58
Figure 3-4. Micrographs of cryofractured surfaces; (a) neat PET, (b) PET/10% TOFA, (c) PET/20% TOFA, (d) PET/30% TOFA. 59
Figure 3-5. SEM micrographs of fibers from (a) Recycled PET/10 wt.% TOFA, (b) Recycled PET/30 wt.% TOFA and (c) Recycled PET/30 wt.% TOFA. 61
Figure B-1. FTIR spectra of TOFA, neat PET and its blends with different renewable plasticizer content (from 10 wt.% to 30 wt.%). 64
Figure B-2. DSC thermograms of the fibers spun from plasticized PET matrices. (a) The first heating cycle, (b) the consequent cooling cycle, and (c) the second heating cycle indicating similar characteristics of the bulk samples. 66
Figure 4-1. Functional groups identified by quantitative ^{31}P NMR measurements after phosphorylation of lignins L and L_{HT} 74
Figure 4-2. Two-dimensional 2D NMR heteronuclear single quantum coherence (HSQC) spectra of both L and L_{HT} lignins. The top two images are the aliphatic oxygenated side chain region (δ_C/δ_H 90-150/2.5-6) and the bottom two images represent the aromatic/unsaturated region (δ_C/δ_H 90-150/5-8). 75
Figure 4-3. Scanning electron micrographs of cryo-fractured and NaOH etched surfaces of PET_{PL}/30L (a) and PET_{PL}/30L_{HT} (b) blends. 77
Figure 4-4. Ratios of tensile strength of lignin-loaded matrices over those of neat PET at different lignin weight fraction (a), and the natural logarithm of reduced tensile strength as a function of volume fraction of lignin (b). 79
Figure 4-5. Loss tangent peak of PET, plasticized PET and its derived blends with L and LHT at in different compositions at 10 Hz frequency. 81
Figure 4-6. Frequency-dependent complex viscosity (η*) at Tref = 240°C (a) and 250°C (b) and Frequency-dependent storage modulus (G') at Tref = 240°C (c) and 250°C (d) of recycled PET, its plasticized resin (PET_{PL}), and its lignin-derived blends (PET_{PL}/30L and PET_{PL}/30L_{HT}). 83
Figure C-1. Lignin substructures detected by 2D HSQC NMR. (A) β-O-4'; (B) β-5' (phenylcoumaran structure); (C) β-β' (resinol structures); (G) guaiacylpropane unit;

(S) syringyl propane unit; (S') syringyl propane unit with carbonyl at Cα; (H) p-hydroxyphenolpropane unit. 90
Figure C-2 DSC thermograms of L and L_{HT} in nitrogen atmosphere showing the glass transition temperatures T_g. 92
Figure C-3 TGA and derivative weight thermograms of L and L_{HT} in nitrogen atmosphere showing the effect of thermal treatment on lignin thermal stability. 92
Figure C-4 Ratios of tensile strength (a), tensile modulus (b), and ultimate elongation (c) of lignin-loaded matrices over those of neat PET at different lignin concentrations. 94
Figure C-5 Thermal decomposition of PET and it lignin derived blends at 30 wt.% lignin contents in oxidative atmosphere at 20°C/min. 94
Figure 5-1 . Phenylpropanoid monomers of lignin: p-coumaryl (H-type), coniferyl (G-type), and sinapyl (S-type) alcohols. 98
Figure 5-2. Oxygenated Aliphatic side chain (δ_C/δ_H = 50-90/2.5-6) and aromatic (δ_C/δ_H = 100-145/6-8) regions of 2D NMR heteronuclear single quantum coherence HSQC spectra of OLH, MKS, MOW lignins. 102
Figure 5-3. TGA and derivative weight change (DTG) thermograms in nitrogen atmosphere of OLH, MKS, MOW lignins. 103
Figure 5-4. Bar chart shows the tensile strength and elongation at break of PLA and its lignin derived blends. 106
Figure 5-5. Micrographs of tensile fractured surfaces the samples. (a) PLA, (b)PLA-OLH, (c) PLA-MKS and (d) PLA-MOW showing the samples fracture pattern and single-phase blends. 106
Figure 5-6.The loss factor tan δ of PLA and its lignin derived blends at 1 Hz in the α-relaxation region. 108
Figure D-1. Molecular weight distribution OLH, MKS and MOW dissolved in THF115
Figure D-2. Functional groups identified by quantitative ^{31}P NMR measurements after phosphorylation the lignins studied. 115
Figure D-3. Major lignin substructures detected by 2D HSQC NMR. 117
Figure D-4. TGA and DTG of PLA, lignin and PLA-lignin blend of OLH, MKS and MOW 118
Figure D-5. Micrographs of tensile fractured surfaces the samples. (a) PLA, (b)PLA-OLH, (c) PLA-MKS and (d) PLA-MOW showing aggregates of lignin in random locations. 120
Figure D-6. Storage modulus E and loss modulus E" data for neat PLA and PLA-lignin derived blends at 1 Hz. 121

CHAPTER 1
LITERATURE REVIEW

1.1. Lignin as a renewable macromolecule

1.1.1. Lignin structure and chemistry.

Lignin, the amorphous matrix of wood, is produced from lignocellulosic biomass as a byproduct of the paper industry in massive quantities [1]. The very complex structure of lignin is described as a highly irregular assembly of different building blocks, and it varies as a function of sources and extraction technologies. A typical model structure shows that lignin is a polyphenol dominated mostly by three types of phenylpropanoid monomer units connected to each other through various covalent bonds [2]. These monomers are also called monolignols and are classified as para-coumaryl alcohol (H-type), coniferyl alcohol (G-type) and sinapyl alcohol (S-type) (Figure 1-1). The p-coumaryl alcohol, which is low in hardwood and softwood lignin, is prevalent in lignin from grasses. Softwood lignin is almost exclusively comprised of coniferyl alcohol, and hardwood lignin is made of varying ratios of both coniferyl and sinapyl alcohol (Table 1-1).

Researchers have relied heavily on analytical chemistry to elucidate the complex structure of lignin but to date the schematic formula has been limited to empirical model structures based on their findings and conclusions, but it should be noted that many structural questions remain. For instance, hardwood spruce lignin structure is presented in Figure 1-2. Adler [3] used dehydrogenation theory to construct lignin structure. His efforts generated one of the first generations of statistical lignin structures in which phenylpropanes units are linked together to form a macromolecule with random branching (Figure 1-2a). Gellerstedt [4], on the other hand, used size exclusion chromatography (SEC) to obtain an understanding of spruce lignin structure. His model suggested that the lignin structure contains a high proportion of S-type units which results in a high percentage of linear lignin (Figure 1-2b). Brunow [5] relied on oxidative coupling of phenol and lignin biosynthesis pathways to gain valuable knowledge about softwood lignin structure and chemistry. A combination of data from oxidative coupling experiments and 2-D NMR spectroscopy helped to define a random branched structural unit model like the Adler model (Figure 1-2a).

Table 1-1. H/G/S ratio from various sources [6].

Sources	H/G/S ratio
Softwood	0-5/95-100/0
Hardwood	0-8/25-50/46-75
Grasses	5-33/33-80/20-54

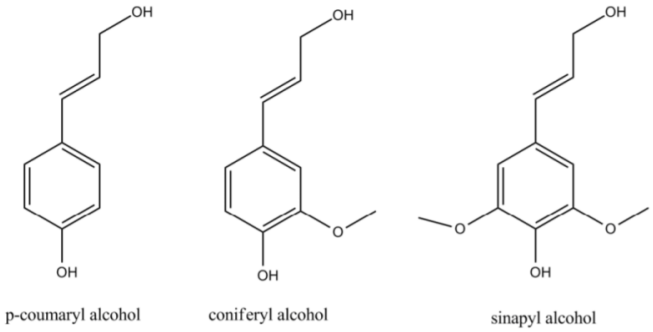

Figure 1-1. Phenylpropanoid monomers of lignin: p-coumaryl, coniferyl, and sinapyl alcohols [7].

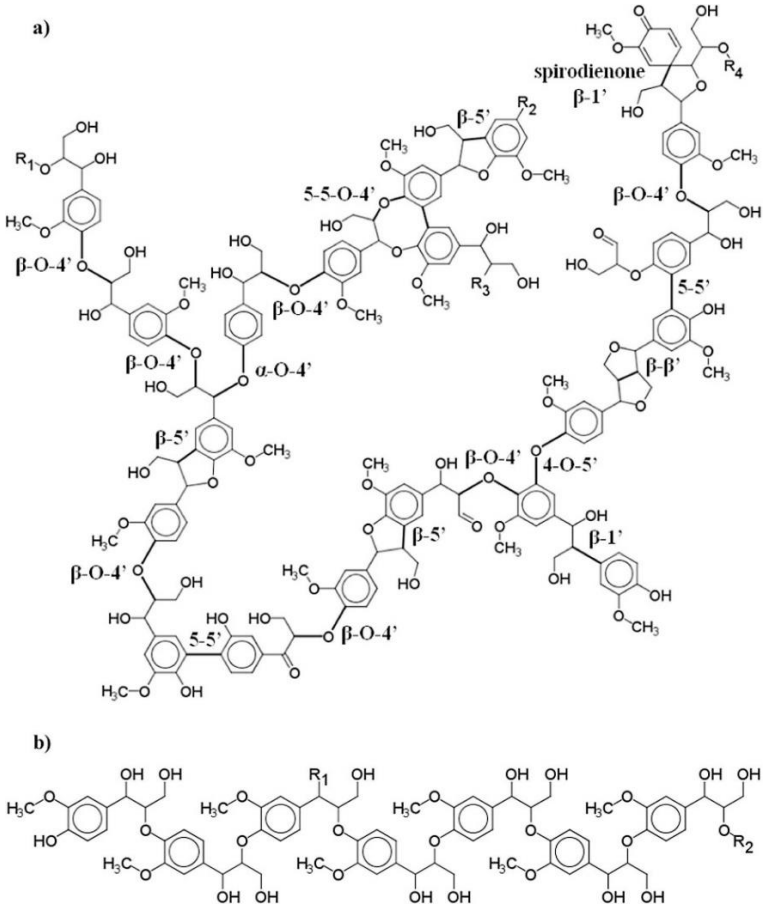

Figure 1-2. Empirical model structure of spruce lignin with two different structures: The random branching model (a), the linear lignin model (b) [3, 4].

Today, new emerging chemical approaches are used to obtain information on the chemical structure of lignin. One of the methods is wet chemistry analysis. In summary, the wet chemistry method provides information about the structure but is deemed semi-quantitative. In that scope, Erickson [8] pioneered oxidation with KM_nO_4-H_2O_2 method based on the oxidative elimination of side chains principle to generate a structural scheme of lignin. Also, approaches employing thioacidolysis [9] and acidolysis [10] both based on hydrolytic cleavage of ethers were used to analyze functional groups and linkage of the structural construction of lignin. Nuclear Magnetic resonance (NMR) has been used extensively to elucidate lignin structure. This method is proven to be more reliable than the wet chemistry methods. Gosselink [11] developed analytical protocols for characterization of sulfur-free lignin from five laboratories. The technique uses quantitative analysis of ^{13}C NMR spectra to provide the number of distinct types of carbon atoms. The summary of the results helped to develop protocols that can be used for reproducible determination of the chemical composition and functional groups, such as phenolic hydroxyl and carboxyl groups of alkaline lignin from various sources.

1.1.2. Extraction methods of lignin.

Physical and chemical properties of lignin depend on the lignin extraction or isolation method. For example, lignin is isolated as the byproduct of the paper and pulping industry. During paper manufacturing, lignin is extracted and separated from the target cellulose pulps. To date, techniques involving alkali-based dissolution of lignin (soda or Kraft pulping), organic solvent-based extraction (organosolv pulping) and steam explosion along with a few new emerging techniques such as alcohol and organic acids extraction are used to produce lignin.

The soda process, first patented in 1854, used an alkaline aqueous medium of sodium hydroxide to deprotonate the phenolic hydroxyl groups of lignin, leading to successive reactions and mostly cleavage of the α-O-4-ether and β-O-4-ether bonds [12]. The Kraft process is known as the most often used pulping method. The technique uses a combination of sodium hydroxide and sodium sulfide to accelerate the depolymerization reaction of lignin [13]. However, the technique does present a drawback to lignin availability on the market as most of the lignin produced is burnt and not offered commercially. Fortunately, there is the sulfite process that can generate up to 1 million tons/year of commercially offered lignin. The process depends on the change in pH to initiate the lignin depolymerization [14]. The main reaction recorded is the cleavage of the α-O-4-ether bonds resulting from sulfonation of the α-carbon atoms of lignin. It was reported that a minimal part of the β-O-4-ether bonds participate in the reaction compared to the soda and Kraft processes. The solvent extraction method or organosolv pulping [15-18] has gained attention at the laboratory level in recent years. Polar organic solvents are used for the extraction and the resulting lignin polarity, structure, and properties depend on the solvent type. The steam explosion method is yet another novel extraction method of lignin. Unlike the methods discussed above that are heavily used in pulping,

steam explosion is used in bioethanol production. Hot steam treatment coupled with explosive decompression followed by enzymatic treatment gives a slurry of sugar and lignin where the lignin can be filtered out with ease [19]. Innovations of the isolation process in recent days have produced lower molecular weight lignin with higher solubility to facilitate deconstruction of biomass components.

1.1.3. Characterization of lignin.

Characterization of lignin is important in terms of side groups arrangement, type, and the number of functional groups so a potential route can be established to take advantage of the groups to produce novel materials. Different methods have been used for quantitative determination of groups such as aromatic hydroxyl, total hydroxyl, methoxyl, carboxyl, carbonyl, and sulfonate. Granata [20] and Angyropoulos [21] used ^{31}P NMR to determine aromatic hydroxyl groups of lignin. Granata carried out his experiment on six standard lignins by evaluating the effect of a reagent on the uncondensed and condensed phenolic moieties in lignins. Angyropoulos called his technique a new tool for lignin chemistry but used a relaxation reagent. Both techniques were simple and novel and provided information about soluble lignin sample. Landucci [22] on other hand used ^{13}C NMR to determine the aromatic hydroxyl group content of lignin. This method developed a rapid analysis of various peak clusters in ^{13}C NMR spectra of lignin and established a procedure for reproducible analysis.

Jakab [23] used thermogravimetry/mass spectrometry (TG-MS) to study lignin isolated from grasses, hardwoods and softwoods. The study evaluated the total hydroxyl, methoxyl and aromatic hydroxyl groups of the lignins. The samples were thermally decomposed in an inert atmosphere. By monitoring the weight loss and evolution of decomposition products, he assigned the gaseous products to functional groups. Faix [24] used a modified oximation and FTIR to determine the carbonyl group of lignin. The oximation reaction occurred at 80°C and helped to yield higher CO content compared to common oximation at 20°C. The oximation results were correlated to the total carbonyl region of the FTIR spectra to allow reproduction of the CO groups that were previously reported. The sulfonate group content of lignin has also been extensively researched. The most convenient method to procure direct measure of the sulfonate content is titrimetry [25]. The most proven, however, is the conductimetric titration where electrical conductivity of the solution is measured after successive additions of reagent.

The available methods for characterization of lignin functional groups are improving. Beside the examples listed above, gas chromatography (GC) [26, 27], ^{1}H NMR [28, 29], and ultraviolet-visible spectrophotometry (UV-VIS) [30, 31] were also reported as techniques used. The complexity of lignin structure and its diverse sources affect, to some extent, the method to employ for chemical characterization. In addition, gel permeation chromatography (GPC) [32, 33] can be used to determine molecular weight distribution of lignin. The distribution is important for lignin usage as it affects physicochemical changes of lignin during processing. For example, conversion of lignin

to carbon fiber starts with melt-spinning of fibers, followed by oxidative thermostabilization, and later carbonization. High molecular weight lignin exhibiting high glass transition temperature is usually difficult to spin. Softwood and grasses derived lignins are denser and possess more crosslinked structures which impede their thermal mobility and spinnability. The hardwood lignin, on other hand, spins with ease due to the ethoxylation of its side chains but does not perform well during thermostabilization [34].

1.2. Renewable blends of thermoplastic/lignin

Extensive research is currently ongoing to utilize lignin as a renewable polymeric material component [35-37]. Lignin can be introduced as a filler or blend component into natural or synthetic polymers. Pristine or chemically modified lignins were subject to a vast number of studies but with a common goal to develop innovative technologies and manufacturing processes.

1.2.1. Polyolefins.

Lignin is an amphiphilic macromolecule with strong inter- and intramolecular interactions because of the functional OH group in the molecule. The polar character of lignin affects the selection of polymers that can be blended with the structure, and properties of the blends depend on it. For example, apolar polyethylene (PE) and polypropylene (PP) and their derivatives can only enter weak dispersion interaction with lignin. Mechanical performances of these blends are weak because they lack polar functional groups in polyolefins chains and high interfacial energy, but impressive aging resistance was reported. Levon [38] reported enhancement of PE thermal stability when lignosulphonate was added. He also reported that a reaction occurred during mixing and identified a reaction temperature by analyzing the rheological properties of the blends. Gregorova [39] studied the free radical scavenging capability of lignin phenolic OH groups in both pristine and recycled resins. He evaluated the stabilization efficiency of lignin and compared it to commercial synthetic antioxidant. The results showed that lignin is a potential processing stabilizer for PP. Others evaluated lignin as UV protector of polyolefins [40, 41]. The conclusions were all supportive of the idea that lignin can act as a stabilizer against degradation mechanisms and prevent changes involving free radical-based reactions during processing or end-use. Such reactivity subsequently improves the performance (e.g., light and thermal resistance) of the final product. In the scope of stabilization improvement, a very little amount of lignin was added. However, addition of substantial amounts of lignin to polyolefins, with hopes to modify mechanical properties, often leads to different observations. Modulus is usually increased but strength and deformability often decrease. The improved modulus is related to the lignin stiffness, but other diminishing performances were attributed to the lack of homogenization and compatibility. Jeong [42] studied acetylated softwood Kraft lignin as a filler in synthetic polymers. A complete miscibility was claimed even though performances were retained only at 12.5 wt.% lignin content. Maldhure [43] used modified lignin to improve its solubility

and compatibility toward PP. The study also claimed success even though continuous deterioration of mechanical properties was detected up to 25 wt. %. The key here is that Jeong and Maldhure both used lignins that were chemically modified to gain these encouraging results. We will discuss chemical modification of lignin in a subsequent section.

1.2.2. Polymers with aromatic rings.

The approach of blending lignin with polymers with aromatic rings is plausible due to the stronger π stacking interactions between them. One would expect some degree of compatibility and better properties from such blends. However, the contribution of Barzegari [44] to the topic showed different observations. He blended polystyrene (PS), an aromatic polymer, with lignin and showed that flexural and torsional moduli both increased, while tensile properties decreased with increasing lignin content. The study indicates a weak interaction between lignin and PS as the basis for poor performances. Pacciarielo [40] also studied PS/lignin blends. The primary aim of this research was to develop thermoplastic material in which cost, and availability of lignin can provide less expensive materials in the field of packaging, health care products, agricultural films, and disposable household objects. The study evaluated a range of polymers, but the PS/lignin blends showed poor properties due to poor compatibility of the components. However, image analysis of different polymers, including PS, blended with lignin by Pouteau [45] produced contrasting results. They found that PS and lignin had the better compatibility compared to the rest of the polymers. The study suggested the existence of solubility and suspected some chemical reaction between PS and lignin.

1.2.3. Other polymers.

Other petroleum-based aliphatic polymers like polyvinyl chloride, engineered polymers like acrylonitrile butadiene styrene (ABS) resin, nitrile rubber, polyvinyl alcohol, and renewable bio-derived polyesters like polylactic acid (PLA) and poly(3-hydroxybutyrate) (PHB) have been blended with lignin. Some of these systems require modification of lignin or use of compatibilizer to improve interfacial adhesion. Gordobil [46] used commercial alkaline lignin and lignin derived from almond shells as PLA fillers. To address the absence of compatibility, acetylated lignins were used. The results showed an improvement in PLA thermal stability but a deficiency in the rate of crystallization. Nonetheless, the PLA /acetylated lignin blends maintained mechanical properties equivalent to neat PLA. Mousavion [47] successfully studied blends of PHB and soda lignin. The study claimed to achieve miscibility and suggested bonding between the carbonyl groups of the PHB and the OH groups of lignin. It also concluded that soda lignin enhanced PHB stability and increased the matrix decomposition temperatures. Tran [37] used a temperature-induced miscibility approach to develop a new green polymer from a blend of nitrile rubber and lignin. The excellent performance of the blend (yield stress 15-45 MPa) and dispersion would not be achieved if some type of interfacial interaction did

not exist between nitrile rubber and the lignin. Most of these reported results show interaction between the host polymer and lignin. A group of researchers claimed partial compatibility between blend components, whereas some went further to conclude complete miscibility. The contradiction relates to the interpretation of the experimental results and a standard is yet to be established for lignin-based thermoplastic blend systems. Some of these results are based on the polymer type and available functional groups present on the macromolecule chains, lignin type, lignin modification, the extent of modification, and addition of compatibilizers.

1.2.4. Polyesters.

A wide array of polyesters was blended with lignin. Investigation of blends of organosolv lignin with poly (ethylene oxide) PEO by Kubo [48] showed solubility in all proportions. The study used unmodified lignin to obtain perfect homogeneity throughout. These results are further supported by a systematic study of the interaction between PEO and lignin in solution by Imel et al. [49]. This interaction is schematically represented in (Figure 1-3). It was concluded that the addition of PEO changed the local and global length scales of the lignin structure as well as the diameter of cylindrical building blocks. These changes resulted in anisotropic lengthening of the cylinders. The interaction between lignin and PEO is simply based on strong hydrogen bonding of the phenolic–OH group of lignin and PEO ether groups. These findings suggest the potential to strategic selection of an appropriate host matrix for efficient lignin dispersion.

Blends of polyethylene terephthalate (PET) and lignin have attracted a good deal of attention. Kadla [50] analyzed the intermolecular interaction in lignin and synthetic polymers including PET. The study reported immiscibility between lignin and PET. The lack of hydrogen bonding in the PET/lignin blend [compared to a PEO/lignin blend] caused weak specific intermolecular interactions. Canneti [51] extensively examined PET/lignin blends in respect to morphology, thermal behavior and supramolecular structure. The study reported “good” dispersion of lignin in PET but did not report mechanical properties of the blends. Lignin addition to PET, in a different report by Jeong [42], suggests improved miscibility although the blends exhibit a diminishing trend of the tensile strength as a function of the amount of lignin loading. Jeong’s work also covered PS, PP and HDPE as host polymers for lignin. Figure 1-4 summarizes composition dependence of the tensile strength of all four polymers when lignin is added. It is also important to point out that the results reported in figure 1-4 were from lignin that was acetylated using the esterification reaction reported in figure 1-5. His work covered some polymers we discuss throughout the present review and can serve as a good summary.

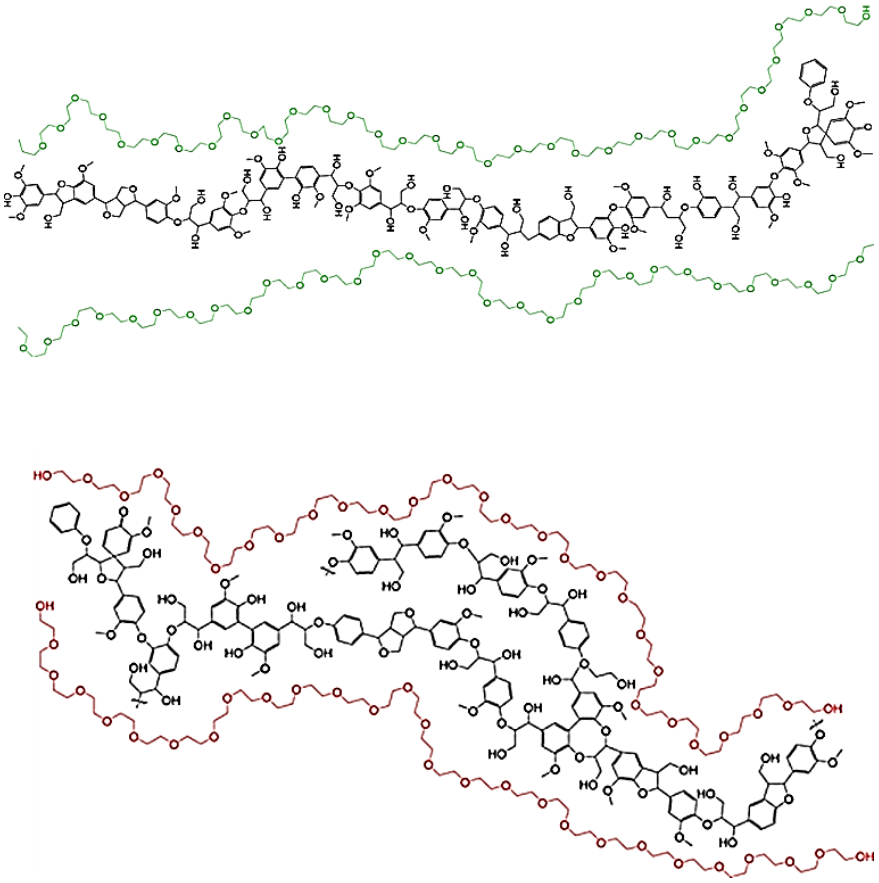

Figure 1-3. Illustration of an extended straightening of a hardwood lignin molecule (top) and softwood lignin (bottom) in the presence of PEO [49].

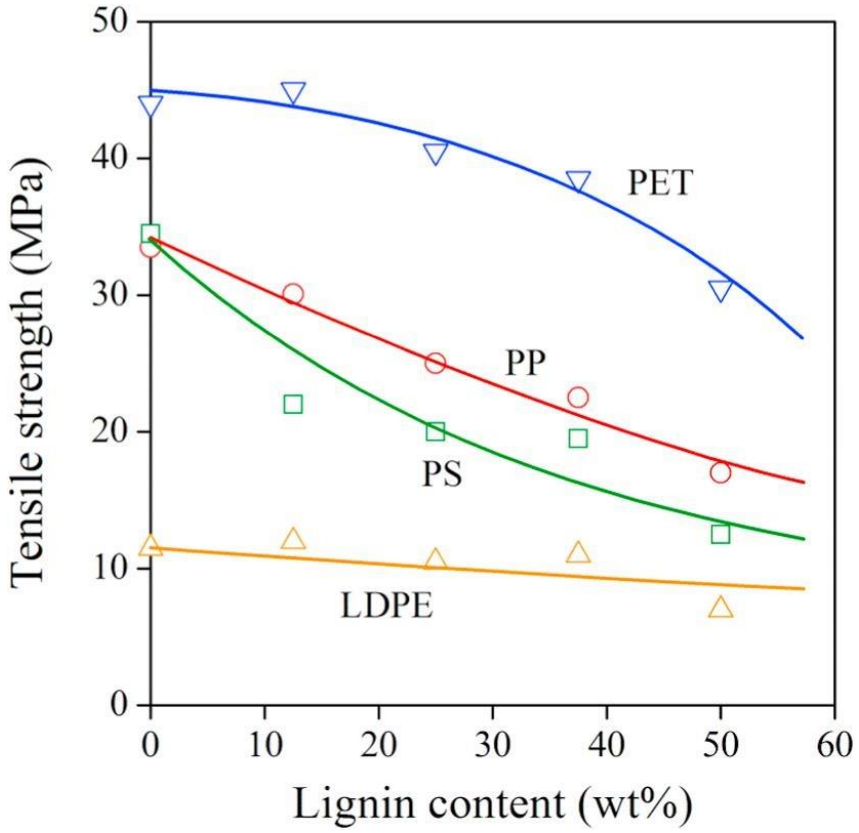

Figure 1-4. Tensile strength as a function of lignin content for PET, PS, PP, LDPE [42].

1.3. Modification of lignin for improvement of interfacial interaction in blends

Researchers have reported functionalization or modification of lignin, and addition of compatibilizers or plasticizers to improve lignin miscibility with the host thermoplastic matrices to tailor the morphology of the blends and to improve the properties of the blends. However, such approaches usually increase material cost and require use of chemicals and an associated need for waste disposal.

1.3.1. Chemical modification.

A survey of chemical modification of lignin shows that lignin can be acetylated [46, 52], esterified with stearoyl chloride [53], phthalic and maleic anhydride [43, 54], arylated in chlorobenzene [55], reacted with propylene oxide [56, 57], and grafted with the host polymer matrices [58]. Not only is the modification aimed to improve the interaction between host polymer and lignin, but also, it must reduce the interaction between lignin molecules to be effective. Acetylation of lignin which is accomplished by reacting lignin with acetic anhydride/pyridine (1/1, v/v) at room temperature for at least 24 hours is the most used modification reported. The esterification reaction is presented in Figure 1-5. Monteil-Rivera [59] developed a greener way to acetylate lignin without solvent or catalyst. The process used a microwave to assist the reaction and reduced the time of reaction considerably. However, the lignin produced from the process was not blended with thermoplastics. Systematic studies related to different lignin modifications by Maldhure [43, 55] were aimed to optimize the interfacial energy and enhancement of lignin compatibility with PP. The study compared lignins that were arylated with chlorobenzene, alkylated with dichloroethane, dichloromethane and esterified with maleic anhydride, respectively. The intermolecular interaction between the PP matrix and the lignin improved regardless of the modification method. Nevertheless, some modifications were more pronounced than others in terms of thermal stability, melting characteristics and mechanical properties. The study, however, lacked a direct comparison between unmodified lignin and PP blends.

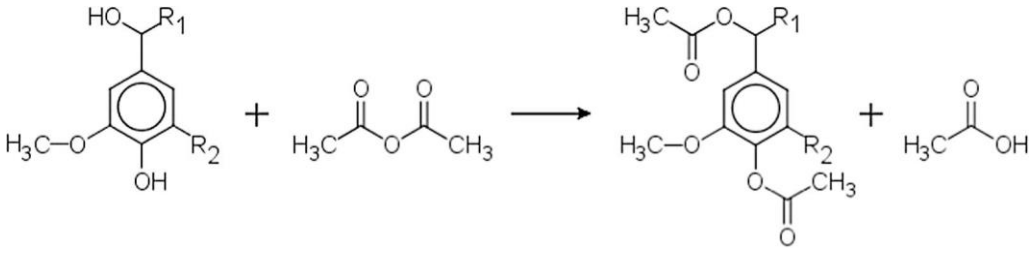

Figure 1-5 Chemical esterification of lignin by acetic anhydride.

1.3.2. Addition of compatibilizers.

The cost associated with chemical functionalization of lignin has redirected researchers to evaluate newer and simpler approaches to improve interfacial interactions in thermoplastic/lignin blends. The addition of phase compatibilizers has significantly increased to address such issue. A report by Alexy [60] on the use of compatibilizers claimed a breakthrough in LDPE/lignin thermoplastic blend development. The addition of 10 wt.% of ethylene-vinyl acetate (EVA) to LDPE/lignin at high lignin content doubled the tensile strength and showed 1300% increase in elongation at break. In the same scope, Barzegari [44], used linear styrene-hydrogenated butylene-styrene block copolymer as a compatibilizer for PS/lignin system. The results showed an improvement of dispersion and performance when compared with blends without a compatibilizer.

1.3.3. Plasticization route.

Lignin is a rigid macromolecule by nature. That characteristic alone can make it difficult to blend with thermoplastics. One way to address such limitation is a thorough plasticization. Plasticization is accomplished by adding dispersant that helps increase plasticity or flow of a material. One can expect a decrease in intermolecular interactions between the lignin macromolecules by use of a plasticizer and it can lead to a fine dispersion of lignin in specific thermoplastic matrices. Some of the reported plasticizers for lignin include: water, ethylene carbonate, ethylene glycol, and glycerol. Rahman [61] used polyethylene glycol (PEG) to plasticize PLA/lignin blends. It used two binary systems of PLA/PEG and PLA/lignin as control to understand the effectiveness of the PEG in the ternary system of PLA/PEG/lignin. The study showed higher deformability of PLA/PEG/lignin system than the PLA/lignin system; thus, PEG increased the flexibility of the matrix molecules. Precise study by Feldan [62] addressed the efficiency of a plasticizer in thermoplastic lignin systems. An attempt to blend rigid polymer poly vinyl chloride (PVC) and lignin could only be possible at low loadings of lignin. Higher lignin loadings formed lignin agglomerates. By introducing a plasticizer to the system, the work showed an improved dispersion of lignin. Lignin particles were found to be finer after plasticization and the results were supported by the improved performance of the PVC/plasticizer/lignin blends. Still, the efficiency of a plasticizer remains unknown when sources of lignin and their isolation methods vary.

1.4. Lignin as a reactive component for preparation of polymeric materials

The reactive route is an important approach to exploit lignin's functional groups to prepare new polymeric materials. The ideal situation for such application is to utilize unmodified lignin directly as a substitute in a resin system. Tachon [63] pioneered an approach to use organosolv wheat straw unmodified lignin as a substitute of phenol in phenol-formaldehyde-resol system. The direct substitution is appealing due to lignin polyphenolic structure. The reported limit of substitution was 70% and the resulting resin met the

standard to be used in industrial scale to fabricate plywood panels. The drawback of lignin as a substitute in the phenol-formaldehyde system is that lignin only offers limited reactivate aromatic sites compared to phenol [64]. That often leads to weakening of properties proportionally to lignin content. Unmodified lignin was also used in other applications. For example, unmodified lignin was added as a third component in urea-formaldehyde systems for its hydrophobic influence on the crosslinking reaction [65]. Other researchers contributed to the field by using unmodified lignin to prepare polyurethanes (PU) [66, 67], PU-urea [68], epoxy resins [69] and polyester [70] . However, the quality of the final product depends mostly on the reactivity of lignin.

In order to prepare better products and extend the range of lignin as a reactive component, chemical modification is carried out in which phenolation, oxypropylation, and esterification, to name only a few, were used to improve the reactivity of lignin [71]. An investigation carried out by Bernadini [72], used oxypropylated lignin to prepare flexible polyurethane foam. The work was based on green synthetic pathways to produce the PU foam. The idea of using lignin to replace polyol in preparation of polyurethane was methodically studied by Xue [73]. The lignin-based polyurethane matrix was reinforced by cellulose nanocrystals to improve performance. The results showed the effect of lignin content on the films tensile properties, most importantly the effectiveness of altering the stoichiometry to control favorable films properties. In a different vein, chemical modification of lignin by attaching polymer chains and using the graft copolymer as a suitable polymerization monomer has been developed. Laurichesse [74] used ring opening polymerization to graft lignin to caprolactone by using hydroxyl functions of lignin. The resulting product was a long-branched polyester with OH groups that can be used for other applications. Liu [75] has also used similar polymerization routes to synthesis lignin graft poly (ε- caprolactone) copolymers. The graft copolymers were evaluated for UV absorption coating.

1.5 Applications of lignin-based thermoplastics

Lignin is a very versatile material with a lot of potential in preparation of bio-derived materials. Lignin finds applications in adhesives, production of chemicals, carbon fiber and carbonaceous materials for insulation and energy storage, and composites. Lignin as a precursor for carbon fiber production is a viable alternative to petroleum derived precursors in terms of cost, environmental protection and energy security [76-78]. At this time lignin-derived carbon fibers are continuous works and no structural carbon fiber derived from lignin is commercially available [76, 78].

The recent industrial revolution along with high impact research create unprecedented opportunity for preparation of novel value-added polymeric materials based on lignin [36, 37]. The goal is to produce thermoplastic/lignin blends that are processable with ease using available processing techniques such as injection molding, blow molding, compression and transfer molding and thermoforming and extrusion so they can be transformed and shaped into finished products with superior quality.

Thermoplastic/lignin can be used as antioxidant and stabilizer for most commodity polymers [41, 79]. The abundance of phenolic hydroxyl groups in lignin structure is the source of the radical scavenging and stabilization significance of lignin. Lignin was also blended with PEO to produce fibrous materials that can be used in energy storage and insulating materials [80]. This application is debatable in terms of thermoplastic lignin products as PEO was added to help with fiber spinning. Understanding of the interaction between components in such systems is important for research and development as the knowledge of the interfacial interaction can be translated to other systems.

The field of thermoplastic lignin blends is still growing. Very little of these materials are commercially available. Tecnaro, a German company, has an engineered structural bioplastic available under trade mark Arboform. The bioplastic is reinforced with natural fibers to improve performance and expand its usage [81]. The company reports that it is thermally stable from 95°C to 105°C and moldable at temperatures below 160°C. Arboform is currently used in electronics, jewelry, furniture, musical instruments and construction applications. For thermoplastic lignin blends to rival the supremacies of oil-based thermoplastics [82], the cost-performance index must be improved significantly. It is believed that once that threshold is achieved, the bioplastics can totally replace the petroleum-based counterparts and applications can be expanded from short-life and disposable products to long-life applications.

1.6. Process engineering of thermoplastic/lignin blends

Achieving improved mechanical properties in lignin-based thermoplastic blends requires efficient dispersion of lignin with reduced domain sizes of lignin macromolecules in the host polymer matrix [83]. To control the degree of dispersion of lignin, a significant enhancement in interfacial interaction between lignin and the soft matrices is desired. Interaction between lignin and polymers can be categorized by dipolar or ionic interactions, covalent or hydrogen bonding, and electron donor-acceptor complexes [62, 84]. The presence of these chemical or physical interactions is an advantage as they can readily increase loading of lignin in the matrix with increased rigidity of the blend. The goal remains to accomplish these without compromising the blend's ductility. Achieving higher mechanical stiffness without compromising the material's ductility is a classical grand challenge in materials research. The approach must consider a precise ability to control lignin self-assembly in the host polymer matrix and a proficiency to tune parameters associated with process engineering.

Blending of polymers at their molten state by mechanical mixing often requires proper selection of the process parameters. Since lignin is not miscible with most polymers, extra steps are often required to render it miscible, so that the thermodynamic condition $\Delta G_m \leq 0$ is achieved [85]. The effect of mixing temperature, rheological properties and chemical reactions is important in terms of controlling and defining ideal morphology of the blend for enhanced performance. Often miscibility is increased by increasing melt temperature; however, this approach often causes lignin degradation during shear mixing. Viscous

heating is another cause of lignin degradation during melt-mixing [86]. Thus, rheological behaviors of the components and the blends are important. Ultimately the process depends on the molecular structures of the components. Therefore, differences in lignin molecular structure are expected to affect rheological behaviors of the resulting polymer blends. The structural characteristics of lignin include: molecular weight, molecular weight distribution, monomer ratio, and associated thermal stability [87]. Although numerous lignin-based compositions have been studied, there is still a tremendous need for a low-cost, commercially deployable high-performance lignin-based thermoplastic for our sustainable future.

1.7. Motivation and Objectives

Demand for plant-derived materials has increased in recent years not only to boost the economics in US Agricultural and Forestry sectors, but also to address environmental concerns. Particularly, forestry and agricultural residues such as bark, wood chips, corn stover, switchgrass, wheat straw and their derivatives need value-addition for supplementary revenue streams [88]. Lignin, an aromatic polymer, extracted from these sources has the potential to be used for preparing innovative materials.

Recent technological innovations on usage of lignin create unparalleled opportunity for the preparation of novel polymeric materials [37, 82, 89, 90]. Lignin can be used as a filler macromonomer, as a diluent, or in more complex ways, as a reactive component because of the plentiful aliphatic and phenolic hydroxyl groups. The possibility to produce new polymer composites by either chemically or physically incorporating lignin in existing petroleum based or renewable thermoplastics addresses the need for environment-friendly and cost-effective renewable materials. Most of the above-mentioned applications require some physical modification or chemical functionalization of lignin because of its lack of miscibility with common thermoplastics [91]. However, the additional functionalization steps increase cost and create need for disposal of chemical wastes. Amalgamation of lignin in blend formulations creates another challenge as most lignins are not thermally malleable and reprocessable, which limits melt mixing with thermoplastics. On the other hand, lignin is a mixture of heterogeneous polyaromatic molecules that also differ by source and isolation method [92]. Interaction and dispersion of lignin are in part governed by the chemical functionalities in sourced lignin.

Systematic studies were done on the development of lignin/soft matrices, such as commodity rubber, to produce high performance elastomers to compete with petroleum-derived materials [37, 83, 93]. In the automotive applications, they can only be used for interior applications mainly because of their low modulus and soft networked structure. Blending high melting thermoplastic matrices with lignin imposes additional process engineering issue. For instance, polyether ether ketone (PEEK), a thermoplastic with outstanding mechanical and chemical resistance, that melts at 343°C [94] cannot be used for lignin melt-blending because lignin significantly degrades above 240°C [95].

The overarching goal of this study is the development of sustainable high-performance composites from thermoplastic blends of lignin without chemical modification. Thus, the approach aims to find value for lignin, a low-cost byproduct of woody biomass pulping industry. The research evaluates the physicochemical properties of lignin and helps establishing suitable processing conditions for blends preparation. This work analyzes lignin sourced from various biomass such as oak, pine, and wheat straw on the properties of commodity plastics. More specifically, we aim to address the following research questions:

1- What are the thermoplastic matrices that can accommodate lignin without deleterious effect on properties?
2- How can we manipulate melting behavior of thermoplastic matrices to mix lignin without thermal degradation and obtain controlled dispersed morphology?
3- How does lignin chemistry affect the properties of thermoplastic/lignin blends?

The above research questions will be answered in separate detailed chapters addressing specific aims that establish a common objective of lignin valorization to thermoplastic high-performance materials.

Research aim #1: Reactive compatibilization of lignin in automotive thermoplastic matrix

In chapter 2, our goal is to exploit lignin's miscibility with polyethylene oxide (PEO) to enhance the compatibility between lignin and acrylonitrile-butadiene-styrene (ABS) polymer under reactive mixing conditions, and develop a melt-extrudable, recyclable, partially renewable matrix with relatively high lignin content for sustainable composite applications.

Research aim #2: Modification of melting behaviors of engineered polymer to control dispersion of lignin phase without degradation

This research is divided in two segments. First, we conduct modification of engineering polyethylene terephthalate (PET) polyester matrix through plasticization. Chapter 3 discusses the use of a renewable plasticizer tall oil fatty acid (TOFA) to reduce melting temperature and viscosity of a waste PET melt. This plasticization improves the processability of PET and broadens applications of PET scraps from the manufacturing floor. Then in Chapter 4 we explore controlling lignin phase dispersion and interfacial interactions in TOFA-plasticized recycled PET matrix using simple melt-blending techniques. To avoid lignin degradation and devolatilization during amalgamation, it was thermally treated; additionally, as-received lignin was used as reference. Structural transformation of lignin macromolecules during heat treatment improves lignin thermal stability. Interfacial interactions between lignin and PET were assessed from mechanical properties and thermal analyses.

Research aim #3: Understanding the effect of source-dependent lignin chemistry on its compatibility with a renewable polyester

In Chapter 5, we study the interactions of three technical lignins with polylactic acid (PLA) matrix. First, lignin molecular weight and softening points were normalized by adopting alcohol-based fractionation of soluble lignin streams from 3 technical sources. Organosolv lignin from oak, methanol fractionated Kraft pine lignin, and methanol fractionated acetic acid extracted wheat straw lignin give equivalent melt processability. Blends of these lignins with PLA are studied to understand effect of lignin chemistry on the blends' thermal stability, mechanical properties, and melt-rheology.

In summary, this study evaluates plasticization of host thermoplastic matrices and reactive extrusion of their blends with various lignins to produce renewable thermoplastic composites. Different thermoplastic matrices such as ABS, an engineered terpolymer, a recycled engineering polyester and a biodegradable PLA studied in this work address question 1. To undertake question 2, two different matrix systems are investigated. First, in chapter 2, we find PEO improves compatibility between the lignin and ABS. It also reduces the viscosity of the blends and improves dispersion of lignin in ABS matrix. Second in chapter 3, TOFA plasticizes PET to reduce melting temperatures for efficient amalgamation of lignin without thermal degradation. To address question 3, three technical lignins with different chemical profiles but of similar softening points and molecular weights are used in an aliphatic polyester (PLA) to produce high-strength thermoplastics. A series of sustainable lignin thermoplastics exhibiting superior performance compared to state-of-the-art copolymerized lignin derivatives were developed.

References

1. Achyuthan, K.E., et al., *Supramolecular Self-Assembled Chaos: Polyphenolic Lignin's Barrier to Cost-Effective Lignocellulosic Biofuels.* Molecules, 2010. **15**(12): p. 8641.
2. Freudenberg, K., *Lignin - Its Constitution and Formation from P-hydroxycinnamyl Alcohols.* Science, 1965. **148**(3670): p. 595-600.
3. Adler, E., *Lignin chemistry—past, present and future.* Wood Science and Technology, 1977. **11**(3): p. 169-218.
4. Lawoko, M., G. Henriksson, and G. Gellerstedt, *Structural Differences between the Lignin−Carbohydrate Complexes Present in Wood and in Chemical Pulps.* Biomacromolecules, 2005. **6**(6): p. 3467-3473.
5. Brunow, G., et al., *Oxidative Coupling of Phenols and the Biosynthesis of Lignin*, in *Lignin and Lignan Biosynthesis*. 1998, American Chemical Society. p. 131-147.
6. Notley, S.M. and M. Norgren, *Lignin: Functional Biomaterial with Potential in Surface Chemistry and Nanoscience*, in *The Nanoscience and Technology of Renewable Biomaterials*. 2009, John Wiley & Sons, Ltd. p. 173-205.
7. Lupoi, J.S., et al., *Recent innovations in analytical methods for the qualitative and quantitative assessment of lignin.* Renewable and Sustainable Energy Reviews, 2015. **49**(Supplement C): p. 871-906.
8. Erickson, M. and E. Miksche Gerhard, *Charakterisierung der Lignine von Gymnospermen durch oxidativen Abbau*, in *Holzforschung - International Journal of the Biology, Chemistry, Physics and Technology of Wood*. 1974. p. 135.
9. Rolando, C., B. Monties, and C. Lapierre, *Thioacidolysis*, in *Methods in Lignin Chemistry*, S.Y. Lin and C.W. Dence, Editors. 1992, Springer Berlin Heidelberg: Berlin, Heidelberg. p. 334-349.
10. Lapierre, C., C. Rolando, and B. Monties, *Characterization of Poplar Lignins Acidolysis Products: Capillary Gas-Liquid and Liquid-Liquid Chromatography of Monomeric Compounds*, in *Holzforschung - International Journal of the Biology, Chemistry, Physics and Technology of Wood*. 1983. p. 189.
11. Gosselink, R.J.A., et al., *Analytical protocols for characterisation of sulphur-free lignin.* Industrial Crops and Products, 2004. **19**(3): p. 271-281.
12. Prinsen, P., et al., *Modification of the Lignin Structure during Alkaline Delignification of Eucalyptus Wood by Kraft, Soda-AQ, and Soda-O2 Cooking.* Industrial & Engineering Chemistry Research, 2013. **52**(45): p. 15702-15712.
13. Gellerstedt, G., A. Majtnerova, and L. Zhang, *Towards a new concept of lignin condensation in kraft pulping. Initial results.* Comptes Rendus Biologies, 2004. **327**(9): p. 817-826.
14. Restolho, J.A., et al., *Sugars and lignosulphonates recovery from eucalyptus spent sulphite liquor by membrane processes.* Biomass and Bioenergy, 2009. **33**(11): p. 1558-1566.

15. Reza, M., et al., *Accessibility of Cell Wall Lignin in Solvent Extraction of Ultrathin Spruce Wood Sections.* ACS Sustainable Chemistry & Engineering, 2014. **2**(4): p. 804-808.
16. Klein, A.P., et al., *Accelerated Solvent Extraction of Lignin from Aleurites moluccana (Candlenut) Nutshells.* Journal of Agricultural and Food Chemistry, 2010. **58**(18): p. 10045-10048.
17. El Hage, R., et al., *Characterization of milled wood lignin and ethanol organosolv lignin from miscanthus.* Polymer Degradation and Stability, 2009. **94**(10): p. 1632-1638.
18. Pan, X., et al., *Organosolv Ethanol Lignin from Hybrid Poplar as a Radical Scavenger: Relationship between Lignin Structure, Extraction Conditions, and Antioxidant Activity.* Journal of Agricultural and Food Chemistry, 2006. **54**(16): p. 5806-5813.
19. Gravitis, J., et al., *Lignin from steam-exploded wood as binder in wood composites.* Journal of Environmental Engineering and Landscape Management, 2010. **18**(2): p. 75-84.
20. Granata, A. and D.S. Argyropoulos, *2-Chloro-4,4,5,5-tetramethyl-1,3,2-dioxaphospholane, a Reagent for the Accurate Determination of the Uncondensed and Condensed Phenolic Moieties in Lignins.* Journal of Agricultural and Food Chemistry, 1995. **43**(6): p. 1538-1544.
21. Argyropoulos, D.S., *Quantitative Phosphorus-31 NMR Analysis of Lignins, a New Tool for the Lignin Chemist.* Journal of Wood Chemistry and Technology, 1994. **14**(1): p. 45-63.
22. Landucci Lawrence, L., *Quantitative 13C NMR Characterization of Lignin 1. A Methodology for High Precision*, in *Holzforschung - International Journal of the Biology, Chemistry, Physics and Technology of Wood*. 1985. p. 355.
23. Jakab, E., et al., *Thermogravimetry/mass spectrometry study of six lignins within the scope of an international round robin test.* Journal of Analytical and Applied Pyrolysis, 1995. **35**(2): p. 167-179.
24. Faix, O., B. Andersons, and G. Zakis, *Determination of Carbonyl Groups of Six Round Robin Lignins by Modified Oximation and FTIR Spectroscopy*, in *Holzforschung - International Journal of the Biology, Chemistry, Physics and Technology of Wood*. 1998. p. 268.
25. Beatson, R.P., *Determination of Sulfonate Groups and Total Sulfur*, in *Methods in Lignin Chemistry*, S.Y. Lin and C.W. Dence, Editors. 1992, Springer Berlin Heidelberg: Berlin, Heidelberg. p. 473-484.
26. Hodges, K., et al., *Determination of alkoxyl substitution in cellulose ethers by Zeisel gas chromatography.* Analytical Chemistry, 1979. **51**(13): p. 2172-2176.

27. Månsson, P., *Quantitative Determination of Phenolic and Total Hydroxyl Groups in Lignins*, in *Holzforschung - International Journal of the Biology, Chemistry, Physics and Technology of Wood*. 1983. p. 143.
28. Lundquist, K., *Proton (1H) NMR Spectroscopy*, in *Methods in Lignin Chemistry*, S.Y. Lin and C.W. Dence, Editors. 1992, Springer Berlin Heidelberg: Berlin, Heidelberg. p. 242-249.
29. Faix, O., C. Grünwald, and O. Beinhoff, *Determination of Phenolic Hydroxyl Group Content of Milled Wood Lignins (MWL's) from Different Botanical Origins Using Selective Aminolysis, FTIR, 1H-NMR, and UV Spectroscopy*, in *Holzforschung - International Journal of the Biology, Chemistry, Physics and Technology of Wood*. 1992. p. 425.
30. Goldschmid, O., *Determination of Phenolic Hydroxyl Content of Lignin Preparations by Ultraviolet Spectrophotometry.* Analytical Chemistry, 1954. **26**(9): p. 1421-1423.
31. Wexler, A.S., *Characterization of Lignosulfonates by Ultraviolet Spectrometry. Direct and Difference Spectrograms.* Analytical Chemistry, 1964. **36**(1): p. 213-221.
32. Colombini, M.P., et al., *Archaeological wood characterisation by PY/GC/MS, GC/MS, NMR and GPC techniques.* Microchemical Journal, 2007. **85**(1): p. 164-173.
33. Himmel, M.E., et al., *Molecular Weight Distribution of Aspen Lignins Estimated by Universal Calibration*, in *Lignin*. 1989, American Chemical Society. p. 82-99.
34. Hosseinaei, O., et al., *Role of Physicochemical Structure of Organosolv Hardwood and Herbaceous Lignins on Carbon Fiber Performance.* ACS Sustainable Chemistry & Engineering, 2016. **4**(10): p. 5785-5798.
35. Wang, C., S.S. Kelley, and R.A. Venditti, *Lignin-Based Thermoplastic Materials.* ChemSusChem, 2016. **9**(8): p. 770-783.
36. Saito, T., et al., *Development of lignin-based polyurethane thermoplastics.* RSC Advances, 2013. **3**(44): p. 21832-21840.
37. Tran, C.D., et al., *A New Class of Renewable Thermoplastics with Extraordinary Performance from Nanostructured Lignin-Elastomers.* Advanced Functional Materials, 2016. **26**(16): p. 2677-2685.
38. Levon, K., et al., *Improvement of the thermal stabilization of polyethylene with lignosulphonate.* Polymer, 1987. **28**(5): p. 745-750.
39. Gregorova, A., B. Košíková, and A. Staško, *Radical scavenging capacity of lignin and its effect on processing stabilization of virgin and recycled polypropylene.* Journal of Applied Polymer Science, 2007. **106**(3): p. 1626-1631.
40. Pucciariello, R., et al., *Physical properties of straw lignin-based polymer blends.* Polymer, 2004. **45**(12): p. 4159-4169.

41. Ye, D., et al., *Antioxidant and Thermal Stabilization of Polypropylene by Addition of Butylated Lignin at Low Loadings.* ACS Sustainable Chemistry & Engineering, 2016. **4**(10): p. 5248-5257.
42. Jeong, H., et al., *Use of acetylated softwood kraft lignin as filler in synthetic polymers.* Fibers and Polymers, 2012. **13**(10): p. 1310-1318.
43. Maldhure, A.V., J.D. Ekhe, and E. Deenadayalan, *Mechanical properties of polypropylene blended with esterified and alkylated lignin.* Journal of Applied Polymer Science, 2012. **125**(3): p. 1701-1712.
44. Reza Barzegari, M., et al., *Mechanical and rheological behavior of highly filled polystyrene with lignin.* Polymer Composites, 2012. **33**(3): p. 353-361.
45. Pouteau, C., et al., *Lignin–polymer blends: evaluation of compatibility by image analysis.* Comptes Rendus Biologies, 2004. **327**(9): p. 935-943.
46. Gordobil, O., et al., *Physicochemical properties of PLA lignin blends.* Polymer Degradation and Stability, 2014. **108**(Supplement C): p. 330-338.
47. Mousavioun, P., W.O.S. Doherty, and G. George, *Thermal stability and miscibility of poly(hydroxybutyrate) and soda lignin blends.* Industrial Crops and Products, 2010. **32**(3): p. 656-661.
48. Kubo, S. and J.F. Kadla, *Kraft lignin/poly(ethylene oxide) blends: Effect of lignin structure on miscibility and hydrogen bonding.* Journal of Applied Polymer Science, 2005. **98**(3): p. 1437-1444.
49. Imel, A.E., A.K. Naskar, and M.D. Dadmun, *Understanding the Impact of Poly(ethylene oxide) on the Assembly of Lignin in Solution toward Improved Carbon Fiber Production.* ACS Applied Materials & Interfaces, 2016. **8**(5): p. 3200-3207.
50. Kubo, S. and J.F. Kadla, *Lignin-based carbon fibers: Effect of synthetic polymer blending on fiber properties.* Journal of Polymers and the Environment, 2005. **13**(2): p. 97-105.
51. Canetti, M. and F. Bertini, *Supermolecular structure and thermal properties of poly(ethylene terephthalate)/lignin composites.* Composites Science and Technology, 2007. **67**(15): p. 3151-3157.
52. Gordobil, O., et al., *Kraft lignin as filler in PLA to improve ductility and thermal properties.* Industrial Crops and Products, 2015. **72**(Supplement C): p. 46-53.
53. Vasile, C., et al., *Modified lignin/polyethylene blends.* Cellulose Chemistry and Technology, 2006. **40**(5): p. 345-351.
54. Sailaja, R.R.N. and M.V. Deepthi, *Mechanical and thermal properties of compatibilized composites of polyethylene and esterified lignin.* Materials & Design, 2010. **31**(9): p. 4369-4379.
55. Maldhure, A.V. and J.D. Ekhe, *Effect of modifications of lignin on thermal, structural, and mechanical properties of polypropylene/modified lignin blends.* Journal of Thermoplastic Composite Materials, 2015. **30**(5): p. 625-645.

56. Wei, M., et al., *Role of Star-Like Hydroxylpropyl Lignin in Soy-Protein Plastics.* Macromolecular Materials and Engineering, 2006. **291**(5): p. 524-530.
57. Chen, P., et al., *Effects of nanoscale hydroxypropyl lignin on properties of soy protein plastics.* Journal of Applied Polymer Science, 2006. **101**(1): p. 334-341.
58. Casenave, S., A. Aït-Kadi, and B. Riedl, *Mechanical behaviour of highly filled lignin/polyethylene composites made by catalytic grafting.* The Canadian Journal of Chemical Engineering, 1996. **74**(2): p. 308-315.
59. Monteil-Rivera, F. and L. Paquet, *Solvent-free catalyst-free microwave-assisted acylation of lignin.* Industrial Crops and Products, 2015. **65**(Supplement C): p. 446-453.
60. Alexy, P., et al., *Modification of lignin–polyethylene blends with high lignin content using ethylene–vinylacetate copolymer as modifier.* Journal of Applied Polymer Science, 2004. **94**(5): p. 1855-1860.
61. Rahman, M.A., et al., *Biocomposites based on lignin and plasticized poly(L-lactic acid).* Journal of Applied Polymer Science, 2013. **129**(1): p. 202-214.
62. Feldman, D. and D. Banu, *Interactions in poly(vinyl chloride)–lignin blends.* Journal of Adhesion Science and Technology, 2003. **17**(15): p. 2065-2083.
63. Tachon, N., B. Benjelloun-Mlayah, and M. Delmas, *Organosolv Wheat Straw Lignin as a Phenol Substitute for Green Phenolic Resins*. 2016. Vol. 11. 2016.
64. Hu, L., et al., *Methods to Improve Lignin's Reactivity as a Phenol Substitute and as Replacement for Other Phenolic Compounds: a Brief Review*. 2011. Vol. 6. 2011.
65. Fan, D.-B., et al., *Synthesis and Structure Characterization of Phenol-Urea-Formaldehyde Resins in the Presence of Magnesium Oxide as Catalyst.* Polymers, 2014. **6**(8): p. 2221.
66. Li, H., et al., *High Modulus, Strength, and Toughness Polyurethane Elastomer Based on Unmodified Lignin.* ACS Sustainable Chemistry & Engineering, 2017. **5**(9): p. 7942-7949.
67. Griffini, G., et al., *Polyurethane Coatings Based on Chemically Unmodified Fractionated Lignin.* ACS Sustainable Chemistry & Engineering, 2015. **3**(6): p. 1145-1154.
68. Behin, J. and N. Sadeghi, *Utilization of waste lignin to prepare controlled-slow release urea.* International Journal of Recycling of Organic Waste in Agriculture, 2016. **5**(4): p. 289-299.
69. Liu, W., et al., *From Waste to Functional Additive: Toughening Epoxy Resin with Lignin.* ACS Applied Materials & Interfaces, 2014. **6**(8): p. 5810-5817.
70. Kai, D., et al., *Sustainable and Antioxidant Lignin–Polyester Copolymers and Nanofibers for Potential Healthcare Applications.* ACS Sustainable Chemistry & Engineering, 2017. **5**(7): p. 6016-6025.

71. Buono, P., et al., *New Insights on the Chemical Modification of Lignin: Acetylation versus Silylation.* ACS Sustainable Chemistry & Engineering, 2016. **4**(10): p. 5212-5222.
72. Bernardini, J., et al., *Flexible polyurethane foams green production employing lignin or oxypropylated lignin.* European Polymer Journal, 2015. **64**: p. 147-156.
73. Xue, B.-L., et al., *Lignin-based polyurethane film reinforced with cellulose nanocrystals.* RSC Advances, 2014. **4**(68): p. 36089-36096.
74. Laurichesse, S. and L. Avérous, *Synthesis, thermal properties, rheological and mechanical behaviors of lignins-grafted-poly(ε-caprolactone).* Polymer, 2013. **54**(15): p. 3882-3890.
75. Liu, X., et al., *Preparation and characterization of Lignin-graft-poly (varepsilon-caprolactone) copolymers based on lignocellulosic butanol residue.* Int J Biol Macromol, 2015. **81**: p. 521-9.
76. Mainka, H., et al., *Lignin – an alternative precursor for sustainable and cost-effective automotive carbon fiber.* Journal of Materials Research and Technology, 2015. **4**(3): p. 283-296.
77. Fang, W., et al., *Manufacture and application of lignin-based carbon fibers (LCFs) and lignin-based carbon nanofibers (LCNFs).* Green Chemistry, 2017. **19**(8): p. 1794-1827.
78. Kadla, J.F., et al., *Lignin-based carbon fibers for composite fiber applications.* Carbon, 2002. **40**(15): p. 2913-2920.
79. Iyer, K.A. and J.M. Torkelson, *Sustainable Green Hybrids of Polyolefins and Lignin Yield Major Improvements in Mechanical Properties When Prepared via Solid-State Shear Pulverization.* ACS Sustainable Chemistry & Engineering, 2015. **3**(5): p. 959-968.
80. Liu, W.-J., H. Jiang, and H.-Q. Yu, *Thermochemical conversion of lignin to functional materials: a review and future directions.* Green Chemistry, 2015. **17**(11): p. 4888-4907.
81. Nägele, H., et al., *Arboform® - A Thermoplastic, Processable Material from Lignin and Natural Fibers*, in *Chemical Modification, Properties, and Usage of Lignin*, T.Q. Hu, Editor. 2002, Springer US: Boston, MA. p. 101-119.
82. Mohanty, A.K., M. Misra, and L.T. Drzal, *Sustainable Bio-Composites from Renewable Resources: Opportunities and Challenges in the Green Materials World.* Journal of Polymers and the Environment, 2002. **10**(1): p. 19-26.
83. Bova, T., et al., *An approach towards tailoring interfacial structures and properties of multiphase renewable thermoplastics from lignin-nitrile rubber.* Green Chemistry, 2016. **18**(20): p. 5423-5437.
84. Koning, C., et al., *Strategies for compatibilization of polymer blends.* Progress in Polymer Science, 1998. **23**(4): p. 707-757.

85. Coleman, M.M., et al., *A practical guide to polymer miscibility.* Polymer, 1990. **31**(7): p. 1187-1203.
86. Sun, Q., et al., *A study of poplar organosolv lignin after melt rheology treatment as carbon fiber precursors.* Green Chemistry, 2016. **18**(18): p. 5015-5024.
87. Charlier, L. and K. Mazeau, *Molecular Modeling of the Structural and Dynamical Properties of Secondary Plant Cell Walls: Influence of Lignin Chemistry.* The Journal of Physical Chemistry B, 2012. **116**(14): p. 4163-4174.
88. Dessbesell, L., et al., *Forest biomass supply chain optimization for a biorefinery aiming to produce high-value bio-based materials and chemicals from lignin and forestry residues: a review of literature.* Canadian Journal of Forest Research, 2016. **47**(3): p. 277-288.
89. Stewart, D., *Lignin as a base material for materials applications: Chemistry, application and economics.* Industrial Crops and Products, 2008. **27**(2): p. 202-207.
90. Thakur, V.K., et al., *Progress in Green Polymer Composites from Lignin for Multifunctional Applications: A Review.* ACS Sustainable Chemistry & Engineering, 2014. **2**(5): p. 1072-1092.
91. Laurichesse, S. and L. Avérous, *Chemical modification of lignins: Towards biobased polymers.* Progress in Polymer Science, 2014. **39**(7): p. 1266-1290.
92. McCarthy, J.L. and A. Islam, *Lignin Chemistry, Technology, and Utilization: A Brief History*, in *Lignin: Historical, Biological, and Materials Perspectives*. 1999, American Chemical Society. p. 2-99.
93. Barana, D., et al., *Influence of Lignin Features on Thermal Stability and Mechanical Properties of Natural Rubber Compounds.* ACS Sustainable Chemistry & Engineering, 2016. **4**(10): p. 5258-5267.
94. Melton, G.H., E.N. Peters, and R.K. Arisman, *2 - Engineering Thermoplastics A2 - Kutz, Myer*, in *Applied Plastics Engineering Handbook*. 2011, William Andrew Publishing: Oxford. p. 7-21.
95. Kubo, S. and J.F. Kadla, *Thermal Decomposition Study of Isolated Lignin Using Temperature Modulated TGA.* Journal of Wood Chemistry and Technology, 2008. **28**(2): p. 106-121.

CHAPTER 2
POLY(ETHYLENE OXIDE)-ASSISTED MACROMOLECULAR SELF-ASSEMBLY OF LIGNIN IN ABS MATRIX FOR SUSTAINABLE COMPOSITE APPLICATIONS

This chapter is based on the manuscript published in "ACS Sustainable Engineering and Chemistry" DOI: 10.1021/acssuschemeng.5b00509. The full list of authors includes Kokouvi Akato, Chau D. Tran, Jihua Chen, and Amit K. Naskar. Kokouvi Akato performed all experiments, processed and analyzed all data, and prepared the manuscript for submission. Chau D. Tran, Jihua Chen assisted with TEM micrographs collection. Amit K. Naskar assisted with the data analysis and editing of the manuscript.

Abstract

In this effort, we report the compatibilization of biomass-derived lignin polymer in acrylonitrile butadiene styrene (ABS) thermoplastic matrix without loss of mechanical properties via poly(ethylene oxide) (PEO)-mediated macromolecular self-assembly. ABS was blended with lignin in different concentrations, and blends with 10 wt. % PEO (relative to lignin) were prepared. The relative tensile strength improved slightly at low lignin content but diminished rapidly as the lignin content was increased. However, the inclusion of PEO as an interfacial adhesion promoter helped avoid deleterious effects. Dynamic mechanical analysis showed that PEO plasticized the hard phase and thus lowered the activation energy (E_a) for its relaxation but caused stiffening of the soft phase and increased its E_a. Microscopy revealed that incorporating lignin in ABS led to the statistical dispersion of discrete lignin domains (300−1000 nm) which, after PEO addition, were reduced to smaller interconnected particles (200–500 nm). The lignin-extended partially renewable ABS resins showed shear-thinning behavior and reduced viscosity compared to neat ABS. The preferred lignin-loaded compositions reinforced with 20 vol. % chopped carbon fibers exhibited mechanical performances (77–80 MPa) equivalent to those of reinforced ABS materials reportedly used in 3D printing applications. This approach could lower the cost of ABS while reducing its carbon footprint.

KEYWORDS: lignin, self-assembly, renewable composites, sustainable materials, Shear thinning polymer

2.1. Introduction

Thermoplastic composites are useful lightweight engineered materials. Factors such as environmental issues, conservation of resources, and reduction of energy consumption during materials processing and reuse have made recyclable thermoplastic composites consisting of renewable components and readily available biomaterials with enhanced mechanical performance highly desirable. High performance composites containing renewable materials will find immediate applications in automotive, construction, and other emerging industries.

Outstanding impact resistance, high mechanical strength, good chemical resistance, and ease of extrusion and molding are characteristics that make acrylonitrile butadiene styrene (ABS) terpolymers widely used for polymer matrix composites [1-4]. ABS composites modified with natural fiber or renewable polymers have been successful both in terms of performance and carbon emission reduction [5, 6]. Even so, the association of Plastic Manufacturers of Europe has recommended that at high fiber loading of natural fibers (>60 vol. %), such composites be used for limited roles such as automotive side panels as a result of their inferior reinforcing characteristics [7]. An efficient solution would be to use carbon fibers, instead, as the reinforcing agent. Carbon fiber at relatively smaller quantities would yield composite parts with superior mechanical properties at reduced mass and longer-term automotive fuel efficiency. Likewise, negative environmental impacts could be further minimized by using renewable carbon fibers, currently in development [8].

Ongoing research on valorization of lignin [9-11], if successful, can make sustainable biomanufacturing initiatives a reality. Lignin-based thermoplastics can either be lignin–polymer alloys [12-15], or functionalized lignin [16, 17], or copolymers of lignin [18-22]. Most polymers are not miscible with lignin, and their blends usually exhibit deteriorated mechanical properties. Lignin does not typically form a compatible blend with ABS matrix without being modified or with the assistance of a compatibilizer. It has been reported that maleic anhydride grafted hydrogenated styrene-butadiene-styrene block copolymer can enhance the compatibility of lignin in ABS [12]. Instead of using a cost-intensive functionalized derivative of hydrogenated block copolymer, we have devised a simpler solution through self-assembly of a hydrogen bonded network of lignin with polyethylene oxide (PEO) [23] in ABS matrix (Figure 1-1) for improved ductility and strength compared to lignin-only-filled ABS matrix. In this work, our goal was to exploit lignin's miscibility with PEO to enhance the compatibility between lignin and ABS, and develop a melt-extrudable, recyclable, partially renewable matrix with relatively high lignin content for sustainable composite applications. These composites meet performance goals while achieving favorable environmental impacts at low carbon fiber loadings.

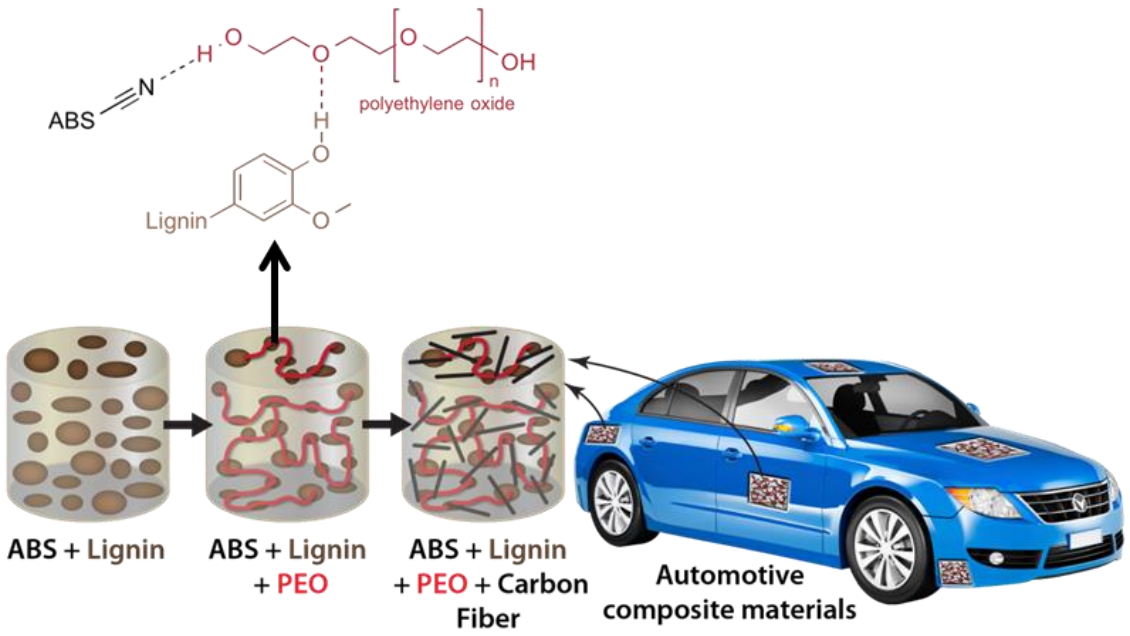

Figure 2-1. Schematic diagram of compositions of lignin-extended ABS resins and their fiber-reinforced composites created from a blend modified with poly(ethylene oxide).

2.2. Experimental section

2.2.1. Materials.

Commercial-grade Terluran GP-35 ABS was obtained from BASF. An easy-flow polymer designed for injection molding process, Terluran GP-35 has a melt volume flow rate of 3.4 cc/min at 220°C and 10 kg-force applied load. An experimental organosolv fractionated softwood Kraft lignin (pine) was dried at 80°C overnight and used. The Kraft softwood lignin was treated with methanol at room temperature to extract out the soluble fraction of lignin. The detailed method for lignin extraction and characterization is reported elsewhere [24]. The lignin melts at 150°C and flows at 160°C. High-molecular-weight (M_n = 5,000,000) PEO was obtained from Aldrich, USA.

2.2.2. Blend Preparation.

ABS/lignin blends (with 10, 20, 30 wt. % lignin) and corresponding blends with 10 wt. % PEO (relative to lignin amounts) were prepared by melt mixing at 190°C using a Brabender® polymer processing system equipped with a half-size mixer. The ABS pellets were introduced into the mixer bowls at 10 rpm and allowed to melt, followed by addition of lignin powder or lignin/PEO mixture (in the case of three-component blending) at 50 rpm. To avoid lignin degradation during prolonged melt mixing, the blends were allowed to mix for 4 min after introducing lignin into the mixing chamber. Compression molding was used to fabricate rectangular test specimens at 190°C.

2.2.3. Thermal Analysis.

Dynamic mechanical thermal analysis of the blends was performed in an RSA (TA Instruments) using a three-point bending fixture. The specimen size was 34 mm × 9.35 mm × 2.75 mm. The measurements were completed in the temperature range −100°C to 150°C and at frequencies of 0.1, 1, and 10 Hz. The heating rate was 2°C/min. Thermal degradation was evaluated by thermogravimetric analysis (TGA) using a TA Q500 from 30°C to 800°C at a heating rate of 10°C/min under nitrogen flow.

2.2.4. Tensile Testing and Morphology Analysis.

Rectangular specimens for tensile testing were prepared by compression molding. The specimens were cut to dog-bone shape and tested on a TA tensile machine at a rate of 0.001 in./s. The reported results are average data of six measurements. The tensile and cryogenically fractured surfaces of specimens were evaluated by SEM (Hitachi S4800). The surfaces were coated with a thin carbon layer before SEM imaging. To characterize blend morphology, specimens were cut at −70°C with a Leica ultramicrotome equipped with a cryochamber and a diamond knife. The thin sections were picked up on lacey carbon copper grids (Electron Microscopy Science) and then analyzed by TEM (Zeiss Libra 120) at an operating voltage of 120 kV.

2.2.5. Rheological Properties.

Melt viscosity was measured with a capillary rheometer (Instron CEASJ SR50) at 190°C, 200°C, and 210°C for neat ABS and all other blends over a range of shear rates. The L/D ratio of the 1 mm diameter die was 20.

2.3. Results and discussion

2.3.1. Tensile Properties.

Performance is important for a soft matrix and its filled derivatives. Empirically, the performance of filled materials is evaluated from the ratio of the mechanical properties [tensile strength (σ), modulus (E), elongation (ε)] of the derived compositions (c) to that of neat matrix (m). Figure 2-2 shows performance indices in terms of relative tensile strength (σ_c/σ_m), modulus (E_c/E_m), and elongation at break ($\varepsilon_c/\varepsilon_m$) of the lignin-extended ABS prepared by melt mixing at different lignin concentrations. The performance index improves slightly at low lignin content but diminishes rapidly as the lignin content is increased. Due to the poor interaction between the lignin molecules and ABS macromolecules, dispersed lignin domains coalesce at higher lignin concentrations to form large brittle inclusions. The deleterious effects of lignin loading in polyolefin matrix can be overcome by incorporating ethylene–vinyl acetate copolymer as a surfactant or an adhesion promoter [25]. In the present work, incorporation of high-molecular-weight PEO (at 10 wt. % loading of lignin content) in lignin/ABS blends has a pronounced effect on the mechanical properties and reduces the deleterious effects at high lignin loadings.

Compared with lignin molecules, the PEO has 3 orders of magnitude higher molecular weight and can act as a tie molecule between the lignin droplets in the ABS matrix through hydrogen bonding between the phenolic and aliphatic hydroxyl groups (of lignin) and ether linkages in PEO. The presence of PEO at the interface of lignin domains prevents particle coalescence and allows higher extensibility or elongation at failure. The presence or absence of PEO has no effect on the tensile modulus of any composition.

2.3.2. Morphology Analysis by SEM and TEM.

The microstructures of the lignin-loaded ABS matrices as observed on scanning electron micrographs (SEM) of cryogenically fractured and tensile failed surfaces of the compositions (displayed in Figures A-1 and A-2, respectively, of Appendix A) indicate the role of PEO in improving interfacial adhesion between the ABS matrix and lignin particles. A representative SEM image of the cryofractured surface of the molded 70/30 (ABS/lignin) composition is shown in Figure 2-3a**,** and the corresponding PEO-modified lignin formulation [i.e., 70/27/3 (ABS/lignin/PEO)] is shown in Figure 2-3b. The addition of PEO causes formation of coated lignin particles (Figure 2-3b), which improves failure stress in the ABS/lignin blends by inducing multiple crack lines and appreciable deformation of the matrix (compared to control sample).

Tensile deformation of ABS matrix leaves fibrillar structures on the failed surface, which is indicative of ductility. But incorporating lignin gradually changes the failure pattern from ductile failure (i.e., unidirectional extended fibrillar morphology containing microvoids or cavitation) to brittle failure (i.e., fast crack line propagation showing no appreciable deformation). Further incorporation of PEO in the ABS/lignin matrix, however, makes the tear paths wider with multiple non-coplanar failed surfaces (Figure A-2).

The formation of clusters of interconnected lignin domains in the presence of high-molecular-weight PEO molecules (at 10 wt. % loading of lignin) in ABS/lignin blends is evident from the transmission electron microscopy (TEM) images of the compositions (Figure 2-4). The neat ABS exhibits agglomerated irregularly shaped butadiene-containing rubbery domains in the thermoplastic matrix of polystyrene-co-acrylonitrile (Figure 2-4a). Incorporation of lignin in ABS leads to the formation of statistical dispersions of discrete 300−1000 nm sized lignin domains (Figure 2-4b). Some of the lignin domains were dropped from the microtomed specimens, leaving voids. In fact, during cryo-microtoming of thin specimens of ABS/lignin blend, a significant quantity of lignin dust was produced. This also indicates poor adhesion between the lignin and the ABS matrix. The lignin domain sizes, however, are smaller when PEO is added to the composition. Further, the micrograph shows that hydrogen-bonded lignin–PEO phase [23] is linked with well-dispersed rubbery domains in the plastic matrix (Figure 2-4c). Inclusion of lignin–PEO in the rubbery domains reduces defects caused by the stand-alone rigid lignin phase during tensile deformation [26].

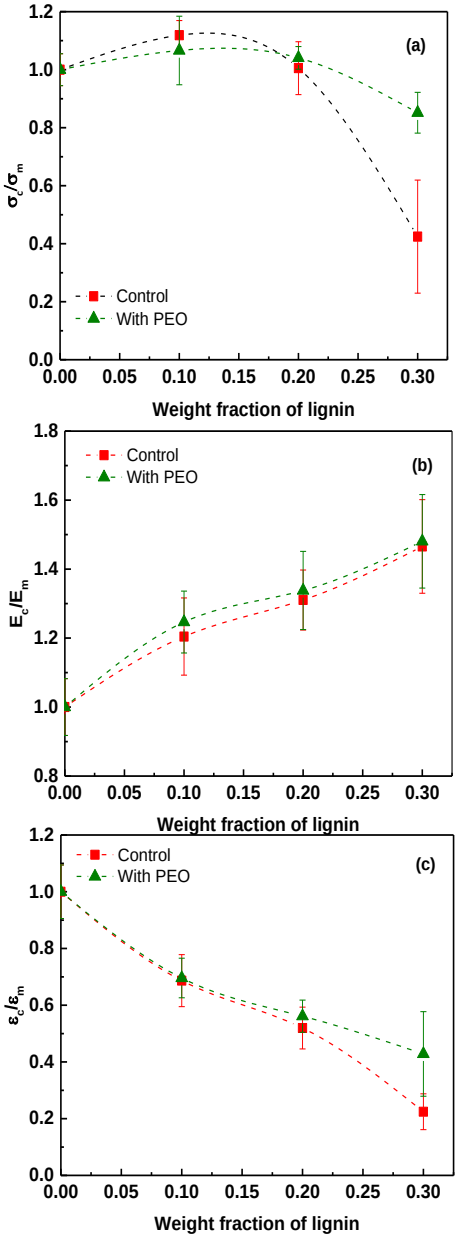

Figure 2-2. Ratios of tensile strength (a), tensile modulus (b), and ultimate elongation (c) of lignin-loaded matrices over those of neat ABS at different lignin concentrations.

In the presence of PEO, lignin domain sizes are reduced to 200–500 nm sized interconnected particles. It may be noted here that the statistical root-mean-squared end-to-end distances of PEO and ABS macromolecules are shorter than the dispersed lignin particles by at least an order of magnitude. In the absence of PEO, large neat lignin domains dispersed in ABS exhibit poor cohesive strength (due to the high brittleness of lignin oligomers) as well as poor adhesion to ABS, particularly at high lignin loadings. Thus, such a composition acts like an immiscible blend of lignin and ABS. Incorporation of PEO in such a blend allows PEO to increase the adhesion between lignin and ABS. Hydrogen bonding between (1) lignin and PEO, and (2) PEO and ABS (through interaction between nitrogen of the –CN group in ABS and the hydroxyl end group of PEO) allows improved adhesion between phases. Also, the interaction of PEO and lignin allows the formation of a ductile lignin phase which, under shear, forms smaller domains that are well adhered with ABS matrix. In other words, the interaction allows the formation of a self-assembly of lignin (in the matrix) assisted by the hydrogen bonding between PEO and the components at the interface and stabilizes lignin dispersion in the matrix. This unique morphology was further probed with dynamic mechanical analysis, and the results are discussed in a later section.

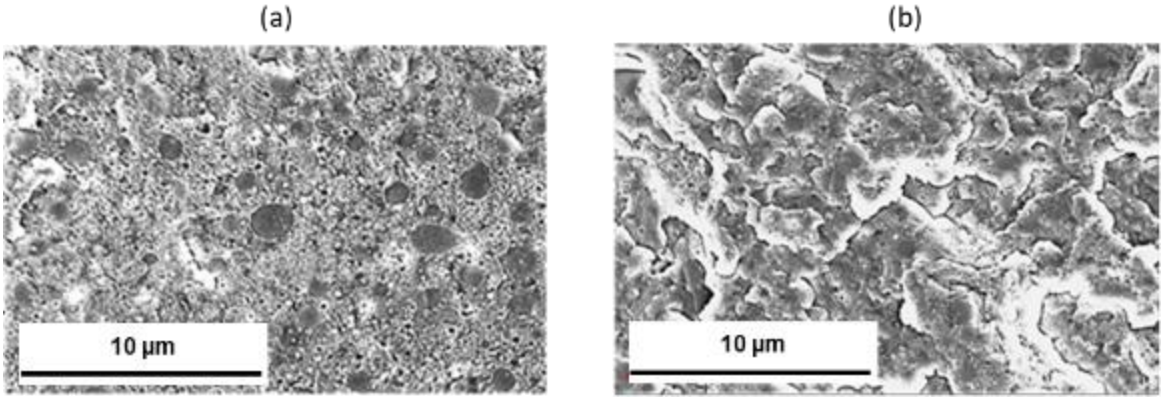

Figure 2-3. Scanning electron micrographs of the cryofractured surface of molded ABS/lignin (70/30) (a) and the corresponding performance-enhanced blend of ABS/lignin/PEO (70/27/3) (b).

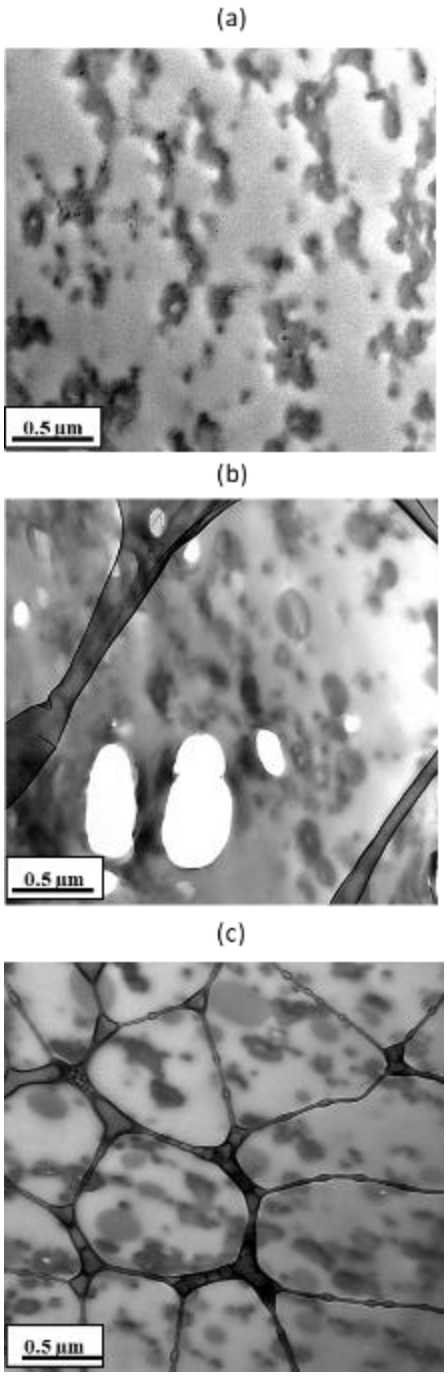

Figure 2-4. Transmission electron micrographs of neat ABS (a), ABS/lignin (70/30) (b), and ABS/lignin/PEO (70/27/3) (c) blends.

2.3.3. Capillary Rheology Study.

The plasticization effect from PEO is evident in the melt capillary rheology data of the compositions shown in Figure 2-5. As expected, all compositions exhibit power law shear thinning behavior. The low-shear viscosity plateau (η_o) decreases with incorporation of the low-molecular-weight lignin component. However, ABS/lignin compositions tend to exhibit similar viscosity at very high shear rate regions (500−1000 s^{-1}), changing the power law index (see Figure A-3). Incorporating PEO in the matrix helps to integrate lignin in the rubbery domains and ultimately in the thermoplastic matrix through self-assembly, as discussed earlier. The presence of PEO in ABS/lignin compositions lowers the matrix viscosity and enhances the melt-processability of the blends at lower temperature.

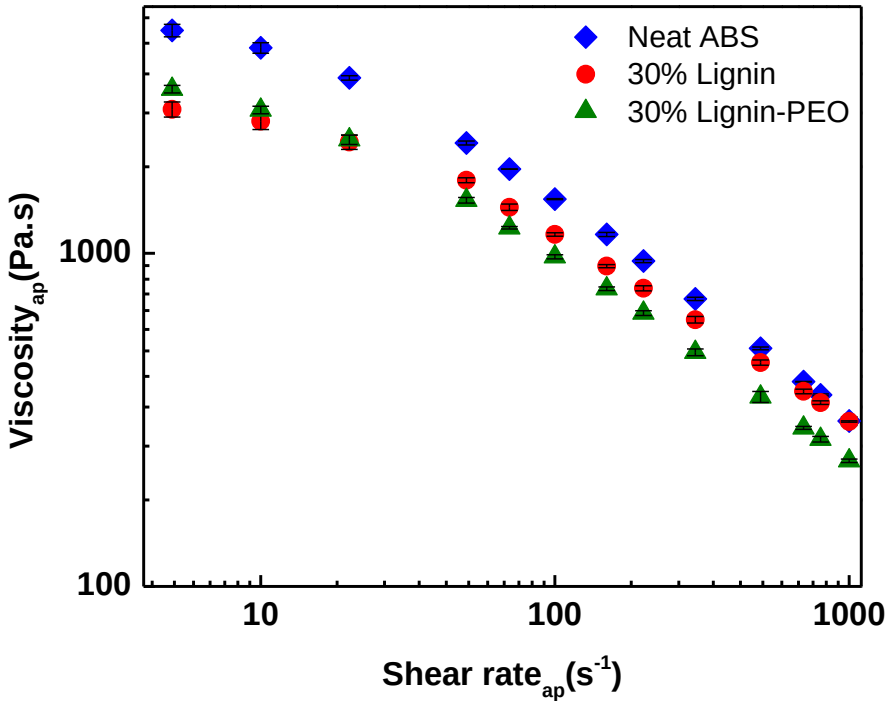

Figure 2-5. Capillary rheology data of neat ABS, its selected lignin-loaded compositions, and the corresponding PEO compatibilized formulation studied at 200°C.

2.3.4. Effect of PEO on Thermal Degradation.

Another advantage associated with using PEO is the improvement of lignin's thermal stability, through hydrogen bond formation. Lignin begins to decompose at 180°C, which is detrimental to the mixing step and processing with ABS resin at 190°C. The addition of PEO slightly elevates the temperature associated with early mass loss from the lignin phase. Early decomposition of lignin involves dehydration, which is retarded through use of PEO. Thermogravimetric analysis of neat lignin and the lignin/10 wt. % PEO mixture is shown in Figure A-4. The derivative weight curves show the degradation temperature rising from 346°C to 354°C in the presence of PEO. The decomposition temperature of PEO is higher than that of lignin, so the compounded material has a higher net degradation temperature. Thus, using PEO improves the potential recyclability of the compositions without significant thermal degradation of the lignin phase.

2.3.5. Dynamic Mechanical Analysis.

The loss tangent peaks associated with both soft and hard phases of the compositions studied at different frequencies are summarized in Table 2-1. The activation energies for relaxation of the phases were quantitatively evaluated by use of the Arrhenius equation [Eq. (1)].

$$\log f = -E_a/(2.303RT) + \log K \quad (1)$$

where *T* is the absolute temperature at which the loss maximum is observed at frequency *f*, *R* is the gas constant, *K* is an arbitrary constant, and E_a is activation energy. The temperature dependence of the loss tangent (tan δ) data was applied to the Arrhenius equation, and the activation energy for relaxation at the loss tangent was calculated for both hard and rubbery phases. Table 2-1 reveals that incorporation of lignin lowers the activation energy (E_a) associated with the relaxation of both hard and soft phases. The extent of reduction of E_a is greater at high lignin loadings. Incorporating PEO slightly increases the E_a associated with the rubbery phase and further lowers the E_a associated with the hard phase (compared to that of the corresponding ABS/lignin blends). This suggests that PEO (a soft linear macromolecule) enhances flexibility in the hard phase (consisting of styrene-acrylonitrile segments along with loaded lignin domains). Interestingly, PEO hinders flexibility in the soft rubbery segments of ABS/lignin blends due to the integration of lignin domains in the rubbery phase through the hydrogen-bonded network of PEO as described earlier.

Table 2-1 Temperatures corresponding to the loss tangent peak (T_g) at different frequencies from the dynamic mechanical analysis, and the activation energy (E_a) associated with thermal relaxation at T_g.

		Neat ABS		10% Lignin		10% Lignin–PEO		30% Lignin		30% Lignin–PEO	
	Log*f* (Hz)	T_g (°C)	E_a (KJ/mol)	T_g (°C)	E_a (KJ/mol)	T_g (°C)	E_a (KJ/mol)	T_g (°C)	E_a (KJ/mol)	T_g (°C)	E_a (KJ/mol)
Hard phase	-1	104		104		102		100		100	
	0	108	543	108	466	106	449	106	422	106	396
	1	114		114		114		116		114	
Rubbery phase	-1	-82		-84		-82		-82		-82	
	0	-80	234	-80	177	-78	182	-78	146	-78	180
	1	-76		-76		-74		-74		-74	

Representative temperature-dependent storage modulus data obtained from the dynamic mechanical analysis at 1 Hz frequency are shown in Figure 2-6. It is apparent that incorporating lignin increases the modulus at temperatures from 0 to 80°C. Plasticization occurs when PEO is added to the composition, and the moduli are slightly lowered. Loss tangent peaks for the rubbery phase and the glassy plastic phase at 1 Hz frequency are shown in Figures 2-7a-b. Rubbery domains of neat ABS show a relaxation around −80°C (Figure 2-7a). Neat ABS also show a tiny broad peak around −40°C due to relaxation of the acrylonitrile-butadiene copolymer segments present in ABS; however, such relaxation disappears when different quantities of lignin are included in the matrix. This indicates a slight degree of interaction between lignin and ABS phases, which are mostly incompatible. Further, inclusion of PEO shifts the T_g of the rubbery phase slightly (from −80°C to −78°C at 10 wt. % lignin loading), indicating that the PEO phase assists in reducing the flexibility of rubbery domains through their ability to bridge both rubbery and lignin phases (see Figure 2-1 for hypothesized interaction between phases through PEO). However, such a shift in T_g was not discernible for high (30 wt. %) lignin loadings, where T_g of the rubbery phase was already shifted to a higher temperature (−74°C).

Figure 2-7b shows the loss tangent spectra for the glassy phases of the compositions at 1 Hz frequency. The T_g of the neat ABS hard phase appears at 108°C. Inclusion of 10 wt. % lignin does not affect the T_g. However, addition of PEO in the 10 wt. % lignin lowers the T_g of the composition to 106°C. This further supports the observation that PEO interacts with the hard phase of ABS (likely the styrene-acrylonitrile copolymer segment). At 30 wt. % lignin loadings, however, there is no further reduction in the T_g of the hard phase owing to PEO use. Therefore, it must be noted that the compatibilization of the lignin and ABS by PEO is more pronounced at low to moderate lignin loadings. The plasticization effect of PEO on the overall compositions containing high lignin loading is demonstrated in the rheology data (Figure 2-5).

Therefore, on the basis of mechanical properties, TEM microscopy, rheology, and dynamic mechanical analysis, it is apparent that the ultrahigh-molecular-weight PEO assists solvent-extracted melt-processable lignin in dispersing well in both the hard and soft phases of the ABS matrix. The hydroxyl end groups of PEO can form hydrogen bonds with the nitrile group of the ABS and the hydroxyl groups of the lignin. In the same way, oxygen-containing ether groups in PEO also facilitate hydrogen bonding with hydroxyl groups in the lignin.

2.3.6. Carbon Fiber Composites.

The ABS/lignin compositions and their PEO compatibilized derivatives were also used in carbon-fiber-reinforced composite fabrication and testing. The tensile results of composites containing 20 vol. % untreated carbon fibers of the formulation ABS/lignin/PEO (70/27/3) show slightly improved mechanical properties compared to the ABS/lignin (70/30) formulation because of enhanced ductility in the matrix. The reduced viscosity of ABS/lignin/PEO also led to less breakage of carbon fibers during shear mixing through the plasticization effect of PEO. The former and the latter composite materials exhibit tensile strength of 77–80 and 68–73 MPa, respectively, with nearly equivalent tensile modulus. Such properties have the potential to qualify these composites for use as automotive parts and for manufacturing by 3D printing [1].

Even though we have demonstrated that solvent-extracted fractions from Kraft lignin can be used to extend ABS matrix, its presence stimulates a strong olfactory response. This can be detrimental for commercial adoption of the approach. Accordingly, we conducted similar experiments with organosolv (Alcell) lignin in ABS; in both the presence and absence of PEO, nearly identical trends in the mechanical properties of the compositions were observed. Details of these mechanical properties are shown in Appendix A (Figure A-5). Alcell lignins do not contain sulfur, which eliminates the unpleasant odor. Alternatively, one can use other types of lignin, such as organosolv lignin, soda pulped lignin, and lignins from biorefinery residues. All types of lignin containing hydroxyl groups and being melt-processable are expected to work in the proposed compositions.

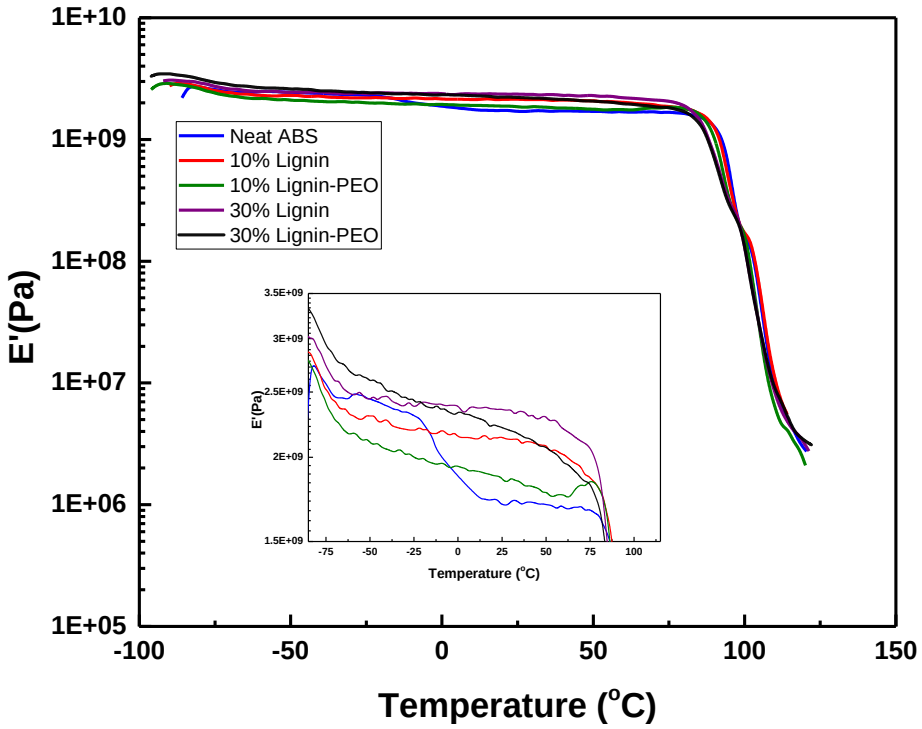

Figure 2-6. Storage modulus data for neat ABS, ABS/lignin, and ABS/ (lignin/PEO) compositions at 1 Hz frequency (inset figure show expanded storage modulus axis).

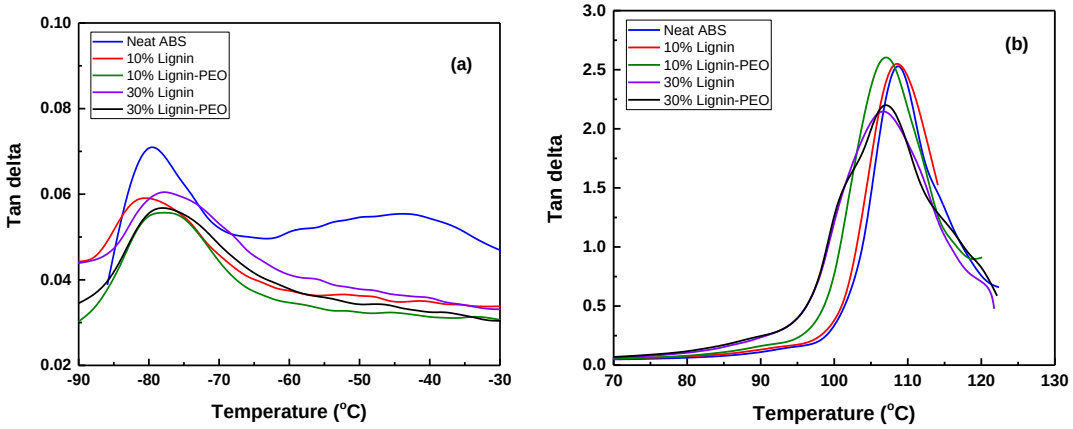

Figure 2-7. Loss tangent peak of the rubbery phase (a) and of the hard phase (b) in different ABS compositions at 1 Hz frequency.

2.4. Conclusion

We have successfully developed a path for loading a sustainable industrial co-product, lignin, to a high-performance engineering thermoplastic matrix without the usual deleterious effects on mechanical properties. A thermoplastic ABS resin containing nearly 30 wt.% lignin was formulated to exhibit properties similar to those of neat resin by incorporating 10 wt.% PEO (with respect to lignin fractions). The ABS/lignin compositions exhibited poor interfacial adhesion; however, their counterparts containing PEO showed improved adhesion of lignin in both the rubbery domains and the thermoplastic matrix as shown by microscopy. The formulations reinforced with short carbon fiber (without pretreatment) showed outstanding mechanical properties that are acceptable for automotive use.

The proposed solution of modifying industrial resin (ABS) and its composite products by incorporating a significant quantity of lignin offers to reduce the carbon footprint through the direct use of these partially renewable plastics and the production of lighter weight automotive materials for enhanced fuel economy. Therefore, the results shown here have significant potential for beneficial economic and societal impacts.

ACKNOWLEDGEMENTS

Research was sponsored by the Technology Innovation Program of ORNL, managed by UT-Battelle, LLC, for the U.S. Department of Energy. TEM (J.C. and C. D. T.) experiments were conducted at the Center for Nanophase Materials Sciences, which is a DOE Office of Science User Facility. This manuscript has been authored by UT-Battelle, LLC, under Contract No. DE-AC05-00OR22725 with the U.S. Department of Energy. The United States Government retains and the publisher, by accepting the article for publication, acknowledges that the United States Government retains a non-exclusive, paid-up, irrevocable, worldwide license to publish or reproduce the published form of this manuscript, or allow others to do so, for United States government purposes.

References

1. Tekinalp, H.L., et al., *Highly oriented carbon fiber-polymer composites via additive manufacturing.* Composites Science and Technology, 2014. **105**: p. 144-150.
2. Diez-Pascual, A.M. and D. Gascon, *Carbon Nanotube Buckypaper Reinforced Acrylonitrile-Butadiene-Styrene Composites for Electronic Applications.* ACS Applied Materials & Interfaces, 2013. **5**(22): p. 12107-12119.
3. Yang, K.M., S.H. Lee, and J.M. Oh, *Effects of viscosity ratio and compatibilizers on the morphology and mechanical properties of polycarbonate/acrylonitrile-butadiene-styrene blends.* Polymer Engineering and Science, 1999. **39**(9): p. 1667-1677.
4. Wang, W., et al., *Study on Effects of Short Glass Fiber Reinforcement on the Mechanical and Thermal Properties of PC/ABS Composites.* Journal of Applied Polymer Science, 2014. **131**(17).
5. Joshi, S.V., et al., *Are natural fiber composites environmentally superior to glass fiber reinforced composites?* Composites Part a-Applied Science and Manufacturing, 2004. **35**(3): p. 371-376.
6. Sathishkumar, T.P., et al., *Characterization of natural fiber and composites - A review.* Journal of Reinforced Plastics and Composites, 2013. **32**(19): p. 1457-1476.
7. Wotzel, K., R. Wirth, and M. Flake, *Life cycle studies on hemp fibre reinforced components and ABS for automotive parts.* Angewandte Makromolekulare Chemie, 1999. **272**: p. 121-127.
8. *Renewable, low cost carbon fiber, Summary Report from the June 4-5, 2013*. 2013.
9. Ragauskas, A.J., et al., *Lignin Valorization: Improving Lignin Processing in the Biorefinery.* Science, 2014. **344**(6185): p. 709-719.
10. Linger, J.G., et al., *Lignin valorization through integrated biological funneling and chemical catalysis.* Proceedings of the National Academy of Sciences, 2014. **111**(33): p. 12013-12018.
11. Zakzeski, J., et al., *Catalytic Lignin Valorization Process for the Production of Aromatic Chemicals and Hydrogen.* Chemsuschem, 2012. **5**(8): p. 1602-1609.
12. Song, P., et al., *Effect of Lignin Incorporation and Reactive Compatibilization on the Morphological, Rheological, and Mechanical Properties of ABS Resin.* Journal of Macromolecular Science Part B-Physics, 2012. **51**(4): p. 720-735.
13. Li, Y., J. Mlynar, and S. Sarkanen, *The first 85% kraft lignin-based thermoplastics.* Journal of Polymer Science Part B-Polymer Physics, 1997. **35**(12): p. 1899-1910.
14. Ghosh, I., R.K. Jain, and W.G. Glasser, *Multiphase materials with lignin. XV. Blends of cellulose acetate butyrate with lignin esters.* Journal of Applied Polymer Science, 1999. **74**(2): p. 448-457.
15. Li, Y. and S. Sarkanen, *Miscible blends of kraft lignin derivatives with low-T-g polymers.* Macromolecules, 2005. **38**(6): p. 2296-2306.

16. Cui, C., et al., *Toward Thermoplastic Lignin Polymers; Part II: Thermal & Polymer Characteristics of Kraft Lignin & Derivatives.* Bioresources, 2013. **8**(1): p. 864-886.
17. Wu, L.C.F. and W.G. Glasser, *Engineering Plastics from Lignin .1. Synthesis of Hydroxypropyl Lignin.* Journal of Applied Polymer Science, 1984. **29**(4): p. 1111-1123.
18. Saito, T., et al., *Turning renewable resources into value-added polymer: development of lignin-based thermoplastic.* Green Chemistry, 2012. **14**(12): p. 3295-3303.
19. Thielemans, W. and R.P. Wool, *Lignin esters for use in unsaturated thermosets: Lignin modification and solubility modeling.* Biomacromolecules, 2005. **6**(4): p. 1895-1905.
20. Hatakeyama, H.N., T. and Hatakeyama,T., *Characterization of Lignocellulosic Materials*, ed. T.Q. Hu. 2008: Blackwell Publishing Ltd.
21. Kelley, S.S., W.G. Glasser, and T.C. Ward, *Multiphase Materials with Lignin .9. Effect of Lignin Content on Interpenetrating Polymer Network Properties.* Polymer, 1989. **30**(12): p. 2265-2268.
22. Saito, T., et al., *Development of lignin-based polyurethane thermoplastics.* RSC Advances, 2013. **3**(44): p. 21832-21840.
23. Kubo, S. and J.F. Kadla, *Poly(ethylene oxide)/organosolv lignin blends: Relationship between thermal properties, chemical structure, and blend behavior.* Macromolecules, 2004. **37**(18): p. 6904-6911.
24. Saito, T., et al., *Methanol Fractionation of Softwood Kraft Lignin: Impact on the Lignin Properties.* Chemsuschem, 2014. **7**(1): p. 221-228.
25. Alexy, P., et al., *Modification of lignin-polyethylene blends with high lignin content using ethylene-vinylacetate copolymer as modifier.* Journal of Applied Polymer Science, 2004. **94**(5): p. 1855-1860.
26. Launey, M.E. and R.O. Ritchie, *On the Fracture Toughness of Advanced Materials.* Advanced Materials, 2009. **21**(20): p. 2103-2110.

Appendix A

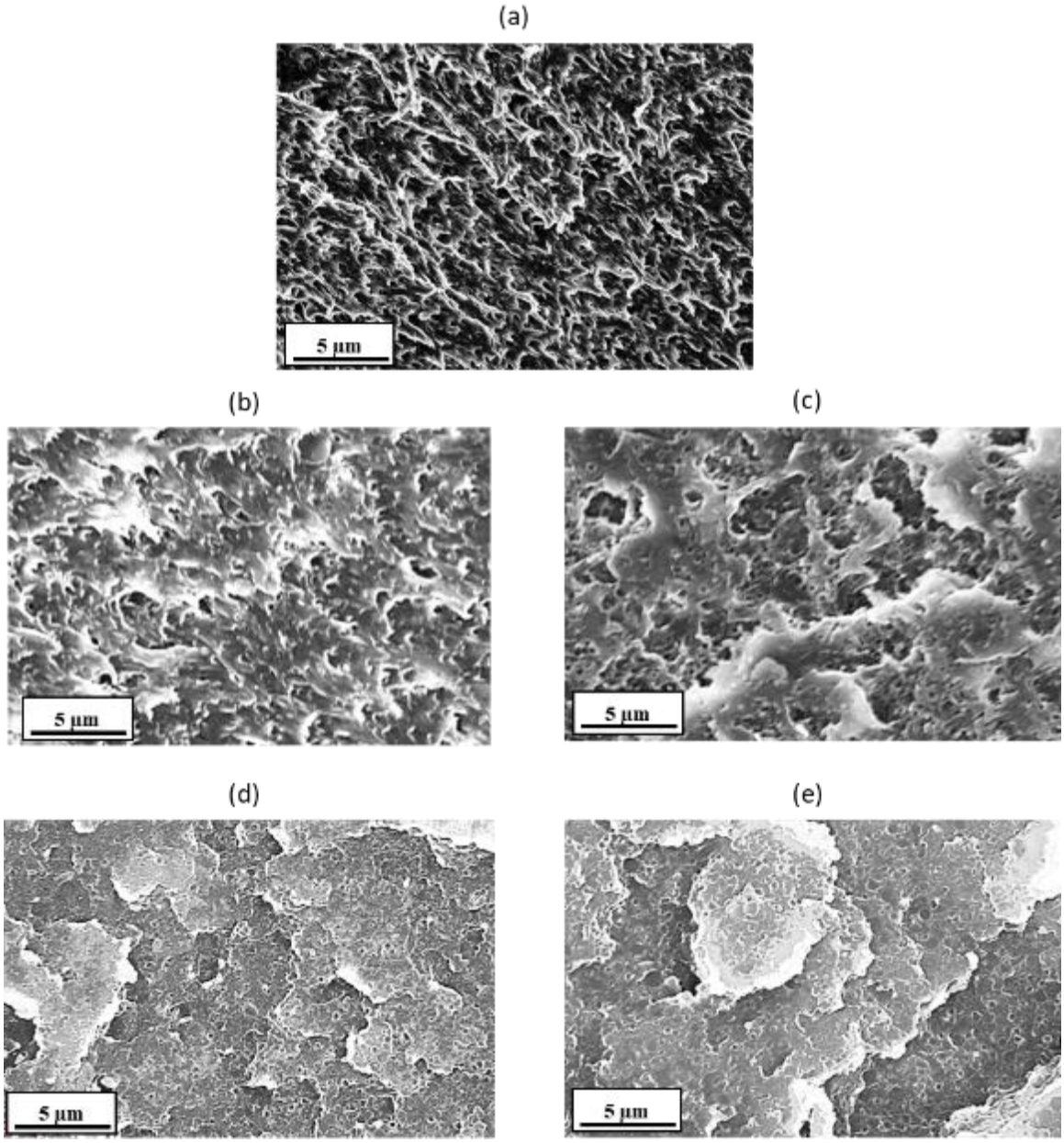

Figure A-1. Micrographs of tensile fractured surfaces; (a) neat ABS, (b) ABS/10% lignin, (c) ABS/10% lignin–PEO, (d) ABS/30% lignin, and (e) ABS/30% lignin–PEO.

.

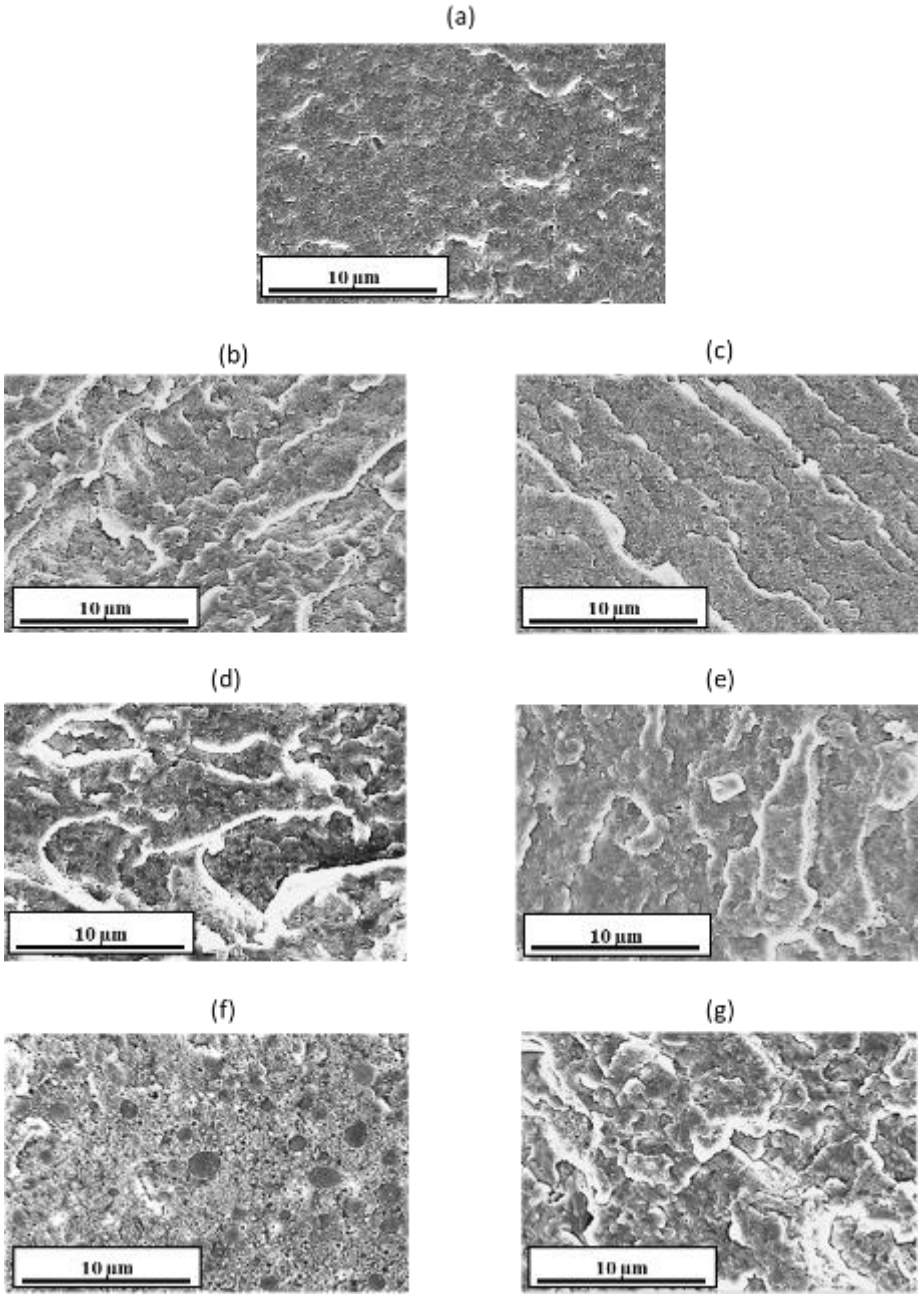

Figure A-2. Micrographs of cryofractured surfaces; (a) neat ABS, (b) ABS/10% lignin, (c) ABS/10% lignin–PEO, (d) ABS/20% lignin, (e) ABS/20% lignin–PEO, (f) ABS/30% lignin, and (g) ABS/30% lignin–PEO.

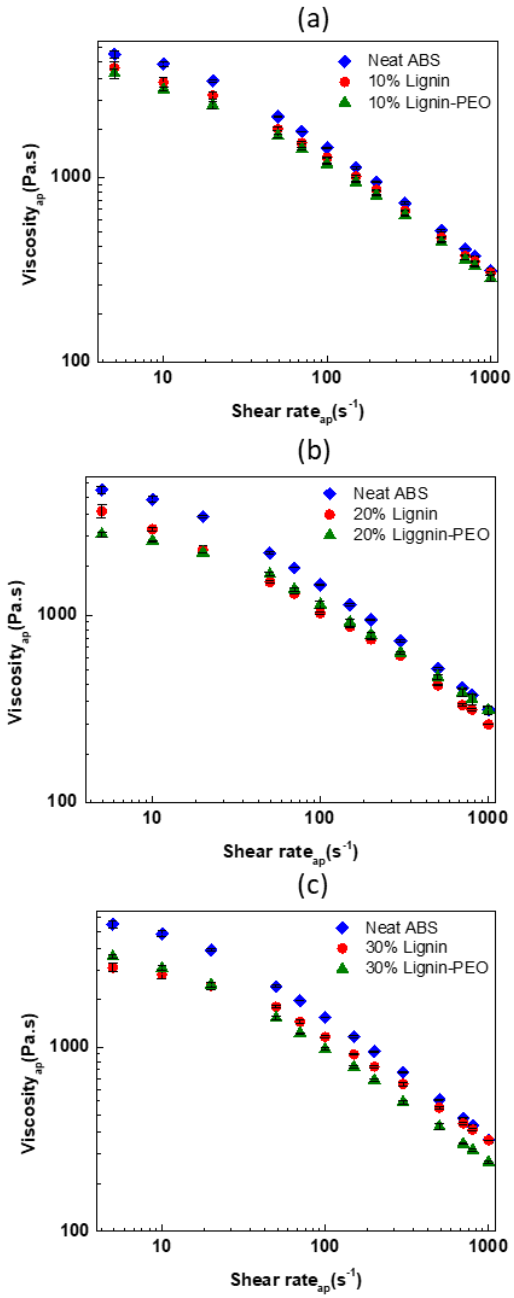

Figure A-3. Capillary rheology data of the neat ABS, its selected lignin-loaded compositions [10% (a), 20% (b), and 30% (c) lignin loadings], and corresponding PEO compatibilized formulation studied at 200°C.

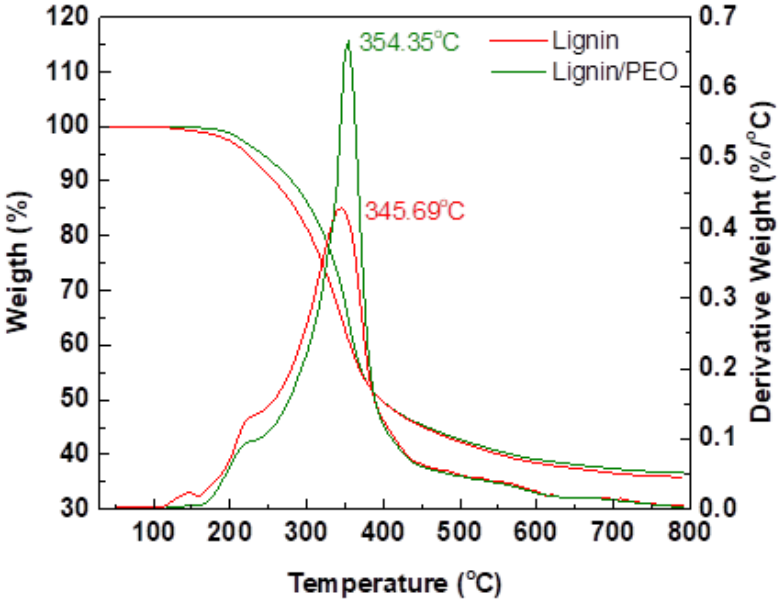

Figure A-4. Thermogravimetric analysis data of neat lignin and lignin–PEO (10 wt. % PEO) mix.

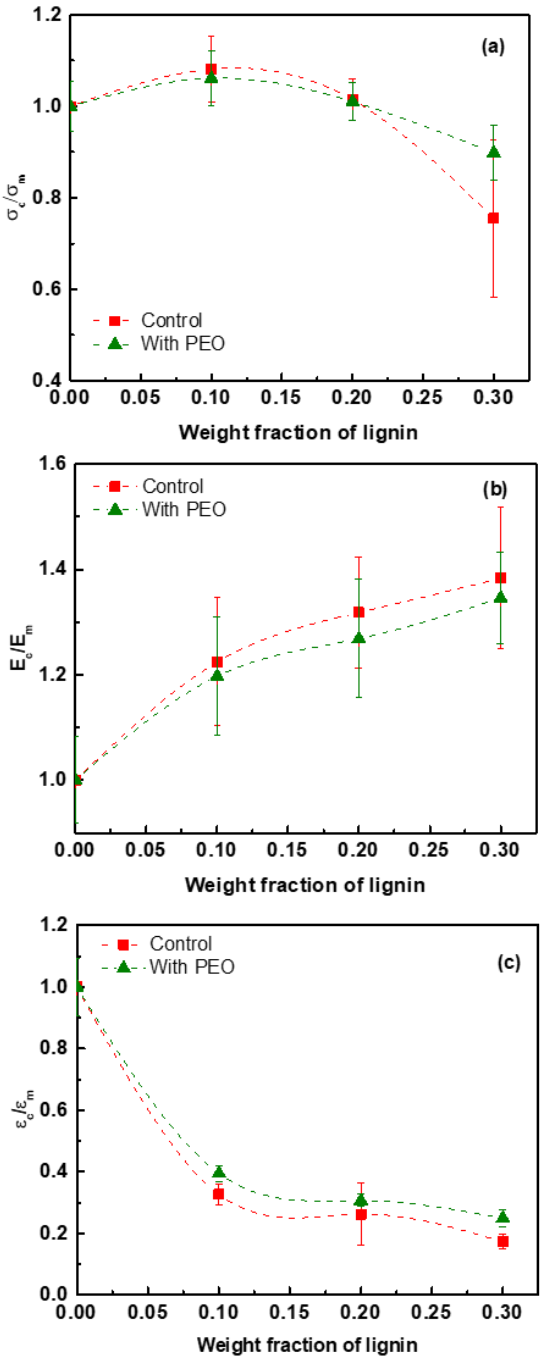

Figure A-5. Ratio of tensile strength (a), tensile modulus (b), and ultimate elongation (c) of organosolv Alcell lignin-loaded matrices over those of neat ABS at different lignin concentrations.

CHAPTER 3
RECYCLING WASTE POLYESTER VIA MODIFICATION WITH A RENEWABLE FATTY ACID FOR ENHANCED PROCESSABILITY

This chapter is based on the manuscript prepared for submission to a peer review journal. The full list of authors includes Kokouvi Akato, Ngoc A. Nguyen, David P. Harper, and Amit K. Naskar. Kokouvi Akato performed all experiments, processed and analyzed all data, and prepared the manuscript for submission. Ngoc A. Nguyen assisted with thermal characterization and rheology. David P. Harper assisted with single fiber tensile testing and editing the manuscript. Amit K. Naskar assisted with data analysis and editing of the manuscript.

Abstract

Polyethylene terephthalate (PET) waste often contains a larger amount of thermally unstable contaminants and additives that negatively impacts processing. A reduced processing temperature is desired. In this work, we report using a renewably sourced tall oil fatty acid (TOFA) as a modifier for recycled PET. To that end, PET was compounded with TOFA at different concentrations and extruded at 240°C. Phase transition behaviors characterized by thermal and dynamic mechanical analyses exhibit shifts in melting and recrystallization temperatures of PET to lower temperatures and depression of glass transition temperature from 91°C to 65°C. Addition of TOFA also creates crystal phase imperfection that slows recrystallization, an important processing parameter. Changes in morphology of plasticized PET reduces and stabilizes the melt viscosity at 240°C and 250°C. Melt-spun, undrawn continuous filaments of diameter 36-46 micrometers made from these low-melting PET exhibit 29 –38 MPa tensile strength, 2.7–2.8 GPa tensile modulus and 20-36 % elongation. These results suggest a potential path for reusing waste PET as high performance polymeric fibers.

KEYWORD: recycled PET, renewable plasticizer, crystallization rate, rheology, tall oil fatty acid

3.1. Introduction

Polyethylene terephthalate (PET) is a semi-crystalline commodity thermoplastic polyester broadly used in the packaging and apparel industries. It is estimated that 485 billion individual PET bottles were produced globally in 2016, and the number is forecasted to grow over the next 5 years [1]. Production of beverage bottles comes at a price as generated waste must be dealt with continually. Post-industrial and post-consumer PET waste often goes to landfills and creates environmental hazards because of the lack of biodegradation of PET [2]. To address the environmental issues and create potential new revenue streams for these wastes, it is logical to recycle the wastes into reusable polymer systems for a variety of end uses.

Recycling can expand spent PET to novel applications [3], but the cost to performance ratio must be reasonable. For example, the toughness can be improved by successful

modification and/or plasticization to reduce the melting point of the crystalline phase and decrease the glass temperature T_g of the amorphous phase [4]. PET can be blended with thermally unstable materials such as polyacrylonitrile (PAN), acrylonitrile butadiene styrene (ABS), poly vinyl chloride (PVC), phenolic resin, and lignin, and then to achieve success with those compositions, PET needs to be softened and melted at lower temperature. The reduction in these transition temperatures via changes in molecular dynamics require careful selection of the plasticizer. The possibility of enhanced chain mobility and depressing T_g of PET has been well studied. In fact, small amounts of codiols or long diols as comonomers were used to plasticized PET [5, 6]. Gowd used two distinct types of polyethylene glycol (PEG) and a solid-state polymerization route to plasticized PET [7]. The results showed that the T_g and crystallization rate were affected by the PEG nature. A systematic investigation of CO_2-induced crystallization of PET by Mizoguchi showed that sorbed CO_2 is in fact an effective plasticizer for PET [8]. The evaluation of the plasticizing ability of CO_2 as reported in a different study was based mostly on the mobility of the polymer segment and the reduction of T_g measured which in part is due to the high solubility of CO_2 in PET [9].

In the specific instance of choosing a plasticizer for polymer systems, renewable plasticizers are preferred as alternatives to their petroleum-based counterparts, in part because of environmental issues, renewability, and cost-effectiveness [10, 11]. Some reported renewable plasticizers include: soybean oil fatty acid methyl ester [12] and Benzyl ester of dehydrated castor oil fatty acid [13]. An example of a renewable plasticizer and polymer system was reported by Wang [14]. The work evaluated palm oil as a plasticizer for ethylene propylene diene monomer (EPDM) rubber. When added to EPDM, palm oil acts like paraffin oil, a conventional petroleum-derived plasticizer, by reducing viscosity to improve processability. PVC has been recently plasticized with novel soybean oil-based polyol ester [15]. The plasticizing effect of the polyol ester was very pronounced and effective when compared with some conventional plasticizers for PVC. Additionally, an improvement in thermal stability was reported.

The success of different renewable based plasticizers for polymeric systems addresses many environmental issues and is a path towards sustainable development. To this end, we have identified tall oil fatty acid (TOFA) as a potential renewable plasticizer for post-industrial PET resin. TOFA is a by-product of the Kraft paper making industry that uses pine trees [16]. It mainly consists of oleic acid and is cost-effective. The goal here is to use the renewable plasticizer to reduce viscosity and improve processing characteristics. This will broaden end-use applications of post-industrial PET scraps from resin manufacturers, bottle manufacturing facilities, and post-consumer wastes. Continuous fibers were also spun using the plasticized matrices to demonstrate favorable processability. Using TOFA in combination with the post-industrial PET waste gave a modified PET suitable to expand the application horizon where lower melting temperatures of PET is desired.

3.2. Experimental section

3.2.1. Materials.

Thermoplastic polyester PET was received from Eastman Chemicals USA. It is scrap from the resin manufacturing facility and supplied as white powder. Melt flow rate (MFR) measured in our laboratory was 55g/10 min (2.16Kg at 280°C). The PET was dried under vacuum at 130°C for 8 hours to avoid hydrolytic degradation during melt processing. The tall oil fatty acid (TOFA) was acquired from Westvaco Chemicals, Charleston SC. It is Westvaco L-5 Tall oil fatty acid [CAS # 61790-12-3]. The specifications of the TOFA were reported as: Acid number (min 190), rosin acids (max 5%) and color or Gardner (max 7).

3.2.2. Blending of Post-industrial Polyester and TOFA.

Dried polyester PET and TOFA were melt mixed at 240°C in a Haake MiniLab co-rotating twin-screw extruder (Thermo Scientific). TOFA was added in 3 different wt. % (10, 20 and 30). The extruder has one zone heated with screws length of 110 mm. The blends were processed at a screw rotation speed of 30 rpm. The extrudates were collected for further analysis. The extruder was then fitted with a die (0.5 mm) to produce monofilaments.

3.2.3. Blends Characterization.

The three different extrudates were named PR10, PR20 and PR30 respectively in accordance to the wt. % of TOFA added (10, 20 and 30). A Differential scanning calorimeter (DSC Q2000, TA Instruments) was used to determine the thermal characteristics of the as received PET and the plasticized PET samples. Samples with mass of approximatively 3-4 mg each were loaded in hermetic pans for measurements. A cycle of heating-cooling-heating from -50°C to 300°C at 10°C/min and an isothermal of 2 min after first heating were used. The degree of crystallization was computed from Equation 1. The melting enthalpy ΔH_m was obtained from the second heating curve. W_f is the PET weight fraction in each composition and ΔH_{100} is the theoretical fusion enthalpy of 100% crystalline PET (140 J/g) [17].

$$\chi_c = \frac{\Delta H_m}{W_f \times \Delta H_{100}} \times 100\% \quad (1)$$

The same setup of DSC was used but at different ramping rates (2, 5, 10, 20, and 30°C/min) to study the crystallization rate of as-received PET and plasticized PET resins. Dynamic mechanical thermal analysis of the blends was performed using a TA Q800 (TA Instruments) in tension mode. Monofilaments of diameters varying from 0.20 to 0.45 mm generated from each sample were used for testing. The measurements were conducted in the temperature range 30°C to 150°C and at frequencies of 1Hz and 0.01% strain. The heating rate was 3°C/min. Cryogenically fractured surfaces of extrudates were evaluated by SEM (Zeiss EVO MA 15). The samples were also analyzed by Fourier transform

infrared spectroscopy (PerkinElmer Frontier). A total of 32 scans were obtained in Attenuated Total Reflectance mode. Average spectra with 4 cm^{-1} resolution were obtained for all samples. The rheological properties were evaluated using the Discovery Hybrid rheometer (DHR-2, TA instruments). All measurements were carried out at 3 % strain, which is in the linear region as determined by a strain sweep in an inert atmosphere of nitrogen. Frequency sweeps from 100 to 1 rad/s at different temperatures were performed.

3.2.4. Fiber Melt-spinning and Characterization.

The twin screw extruder was also used to generate continuous single fibers from all three plasticized PETs with TOFA. A 200 µm spinneret was attached for fiber forming as the extrudate is forced through the orifice. A 76 mm rotating drum was used to collect continuous single fibers. Single fibers were isolated for mechanical testing. They were glued onto a paper tab using an adhesive. The tabs were mounted into a set of pneumatic grips, and the sides are cut at mid-gauge before load application. The gauge length was 25.4 mm. The tabs enable consistent and proper mounting of fiber specimens. An Instron 5943 equipped with Bluehill3 software was used for the mechanical testing at crosshead speed of 15 mm/min. The mean of 13 specimens is reported. The fibers were also characterized by DSC based on sample preparation and experimental conditions described above. SEM micrographs of the fiber lateral surface were also obtained.

3.3. Results and discussion

3.3.1. Thermal characteristics.

Polymeric materials are macromolecules with intramolecular cohesive forces among them. When heat is applied, the macromolecules become soft and flexible and easy to process. Low-molecular weight plasticizers are often added to increase the flexibility at room temperature and to improve processing. Evidence of the plasticizing effect of TOFA is shown in Figure 3-1a. DSC thermograms depict that as the amount of TOFA renewable plasticizer increases, the PET melting peak shifts toward lower temperature. Neat PET is an heterogeneous polyester with both amorphous and crystalline domains. Its thermogram shows a large endotherm with a peak temperature at ~248°C corresponding to melting of crystals. The low-molecular weight renewable plasticizer TOFA inserts its molecules between the crystalline domains of the PET allowing for softening and increased flexibility. The depression of melting temperatures T_{m1} and T_{m2} reduces the processing temperature of PET. In parallel, incorporation of TOFA shifts the recrystallization T_{rec} to lower temperatures (Figure 3-1b) because of the TOFA-induced PET chain flexibility that alters crystallization kinetics discussed in detail later.

The change in crystallization behavior was evaluated and reported in Table 3-1 using the thermodynamic melting enthalpy from the DSC thermograms in Equation 1. The neat PET ΔH_m is 48.6 J/g which is lower than 100% crystalline PET (140 J/g) thus a degree of

crystallinity of 34.7 %. The degree of crystallinity (X_C) of TOFA plasticized PET are all higher than the as-received PET except PR10. It is apparent that addition of TOFA favors segmental molecular mobility of PET which affects the crystallinity. Although the presence of TOFA increases PET crystallinity, it is obvious that the modified PET crystals are low-melting and imperfect.

The storage modulus E', related to the material stiffness, decreased with addition of plasticizer because of changes in the phase structure (Figure 3-1c). The sharp drop of E' for all samples as the temperature increases signals that glass transition events are occurring in the amorphous phase. Like most polymers, PET undergoes thermophysical transitions around its glass transition temperature T_g. T_g is known as the temperature at which binding forces between polymer chains are relaxed to initiate large-scale molecular movements. T_g is considered as an essential processing parameter as it helps to define the state of polymers at their service temperatures. Here, the T_g, as reported in Table 3-1, are the maximum peak of the loss factor Tan δ (Figure 3-1d). The as-received PET has a T_g of 91°C. As expected, addition of the renewable plasticizer decreases T_g. TOFA addition depresses PET's T_g by up to 25°C at 30 wt. % addition, which is evidence of pronounced plasticization. TOFA presence allowed the PET matrix to become less dense and facilitate motion of the PET molecular segments to start at lower temperature.

Table 3-1. Thermal and crystalline properties of neat PET and its plasticized derivatives.

Samples	T_{m1} (°C) [a]	T_{m2} (°C) [a]	ΔH_m (J/g) [a]	T_{rec} (°C)	ΔH_{rec} (J/g)	χ_c (%) [a]	(T_g) (°C) [b]
Neat PET	237.3	247.9	48.6	209.1	55.8	34.7	91
PR10	222.8	238.3	42.8	198.9	52.1	33.9	69
PR20	220.2	236.8	41.9	196.4	54.5	37.4	67
PR30	222.6	238.1	40.3	197.1	64.9	41.1	66

[a] Values obtained from second heating curve of DSC

[b] T_g reported from Tan δ peak

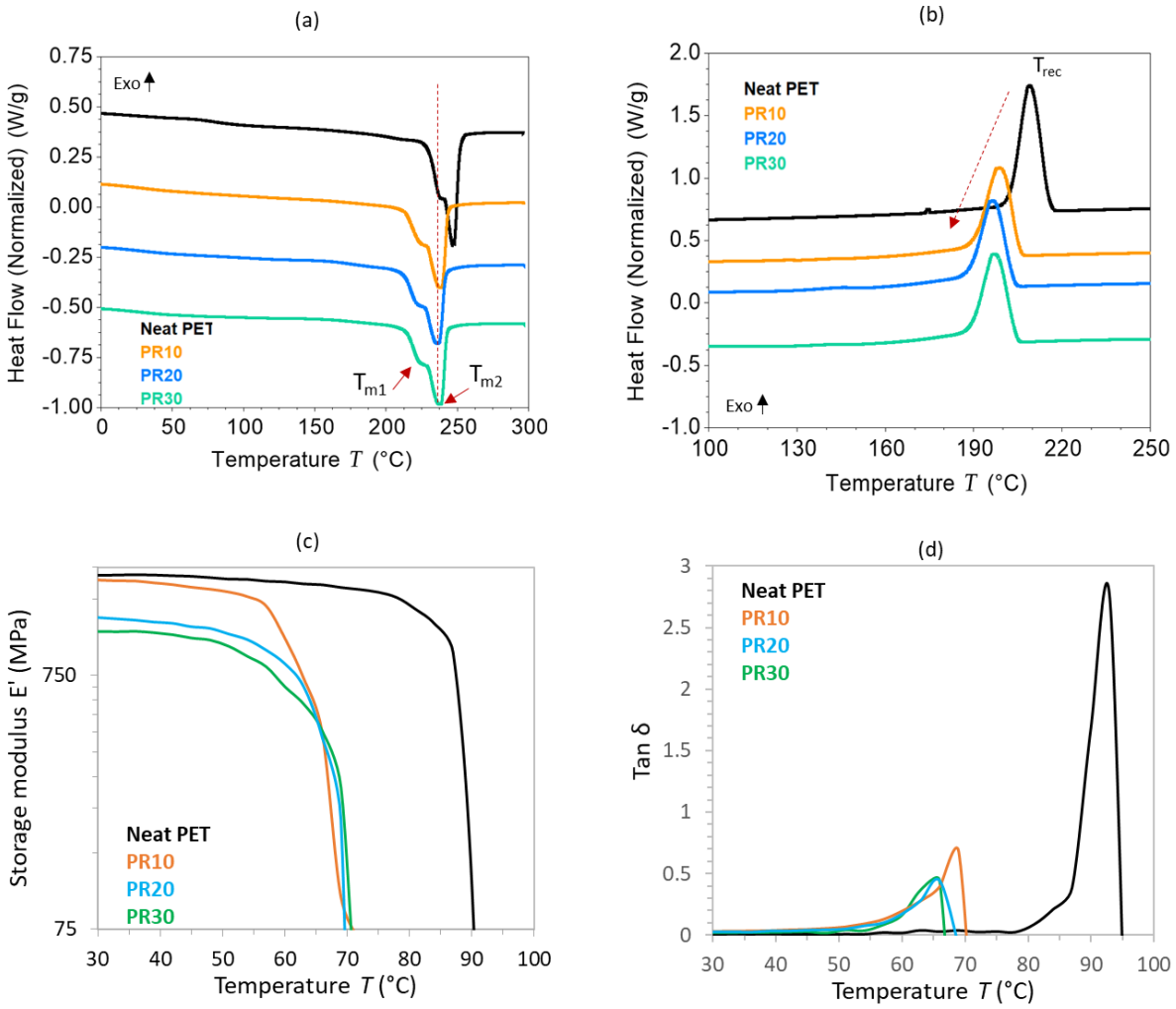

Figure 3-1. Thermal characterization of as-received recycled PET and its plasticized derivatives. (a) DSC second heating thermograms, (b) DSC cooling thermograms, (C) DMA storage modulus E’ and (d) DMA loss factor Tan δ.

3.3.2. Crystallization behavior.

The recrystallization temperatures (T_{rec}) and enthalpy (ΔH_{rec}) of neat PET decrease as the cooling rate increases (Figure 3-2). Plasticization is observed as the PET crystalizes faster than the plasticized PET resins at lower cooling rates, but the difference in T_{rec} is minimal at 30°C/min rate. T_{rec} is critical in polymer processing, especially for a semi-crystalline polymer like PET. It is measured as the solidification temperature. The fact that the neat PET and the TOFA plasticized PET display T_{rec} values close to each other at high cooling rates suggests that the crystallization mechanism is not much affected by the addition of TOFA. This is beneficial for a process like extrusion where high cooling rates are desired. ΔH_{rec} of plasticized resins diminish as the TOFA amount increases (Figure 3-2b). Nevertheless, it increases as the cooling rate increases which is different to the neat PET. Crystallization temperatures shift to lower temperatures with the addition of TOFA renewable plasticizer. Such reduction can be explained by two interconnected facts. First, TOFA addition depresses T_g and increases chain mobility, and second, TOFA addition decreases PET's melting point, which also retards crystal growth. Furthermore, the slopes of the T_{rec} vs. log cooling rate curves suggest that the excess TOFA reduces the crystallization rate because a steeper slope (neat PET) means faster crystallization compared to gentle slope (30 wt. % for example).

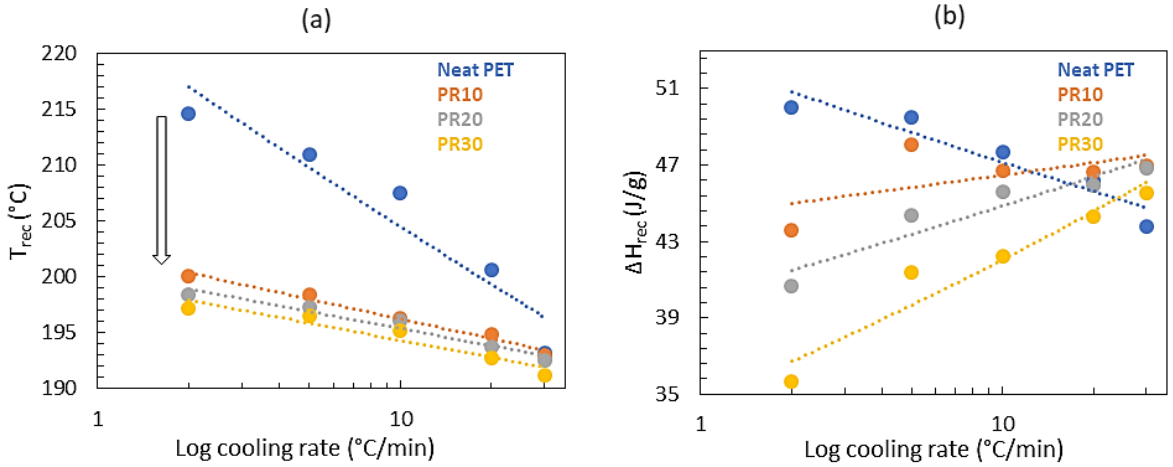

Figure 3-2. (a) Crystallization peak temperatures T_{rec} and (b) crystallization enthalpy ΔH_{rec} as a function of log cooling rate.

3.3.3. Flow characteristics.

Oscillatory frequency sweeps were used to evaluate the as-received PET and TOFA plasticized PET resins flow characteristics. The angular frequency (ω) dependence of the complex viscosity (η*) and the storage modulus (G') in the linear region have a more developed sensitivity to structural variation than the power-law region (Figure 3-3). At 240°C (Figure 3-3a), the neat PET shows a Newtonian behavior at very low frequency followed by normal shear thinning behavior where the complex viscosity starts to decrease with increasing angular frequency. The viscosity is high and decreases progressively because the data are collected in the linear region and the temperature is below the melting temperature recorded by DSC (248°C). It is anticipated that chain disentanglement and mobility limited due to lack of energy to disrupt them. The plasticized PET resins, however, show a similar decrease of viscosity with increasing frequency, but the slopes of the flow curves are sharper. Also, PR10 and PR20 show high viscosity at low frequency compared to neat PET. The effect of the plasticizer is evident for all three plasticized PET resins at 250°C (Figure 3-3b). The plasticization effect becomes more pronounced as the viscosity decreases with increasing plasticizer amount and the slopes of all the curves are steadier. The flow behavior shows that changes are occurring in the molecular structure of plasticized PET due to the addition of TOFA as a softening agent. The TOFA can interact with the PET amorphous segment and end groups through hydrogen bonding and can undergo covalent esterification reaction with hydroxyl end groups leading to changes in the structure of modified PET. Such interaction is typical for excellent plasticizers as they decrease viscosity and hence improve the processing properties of PET. The master curves at T_{ref} =240°C in Figure 3-3c shows that the storage modulus G' is increasing with increasing ω. A sharp increase in G' is observed in neat PET, but for all three plasticized PET resins, the rise is progressive. Also, all three plasticized resins have higher G' values at low frequency and G' for PR10 and PR20 continues to be higher than that of neat PET at below 10 rad/s. The master curves at T_{ref}=250°C in figure 3-3d shows that neat PET has the highest G' over the whole frequency range indicating the highest rigidity. The slopes are different, but all storage moduli increase with increasing angular frequency. The TOFA modified resins' G' values decrease with increasing plasticizer loading amounts over the entire frequency range. This suggests that the plasticizer is lubricating the PET chains, and the plasticization effect is not only favoring change in morphology and increased chain mobility but also strongly affects the moduli of the modified resins. This is a strong indication of improved processing characteristics of the modified PET.

3.3.4. Morphological evaluation.

Representative SEM micrographs of cryofractured surfaces of the as-received waste polyester and the TOFA plasticized matrices are represented in Figure 3-4. The as-

received PET surface shows a relatively smooth fracture surface with residual morphology left by the fracture path (Figure 3-4a).

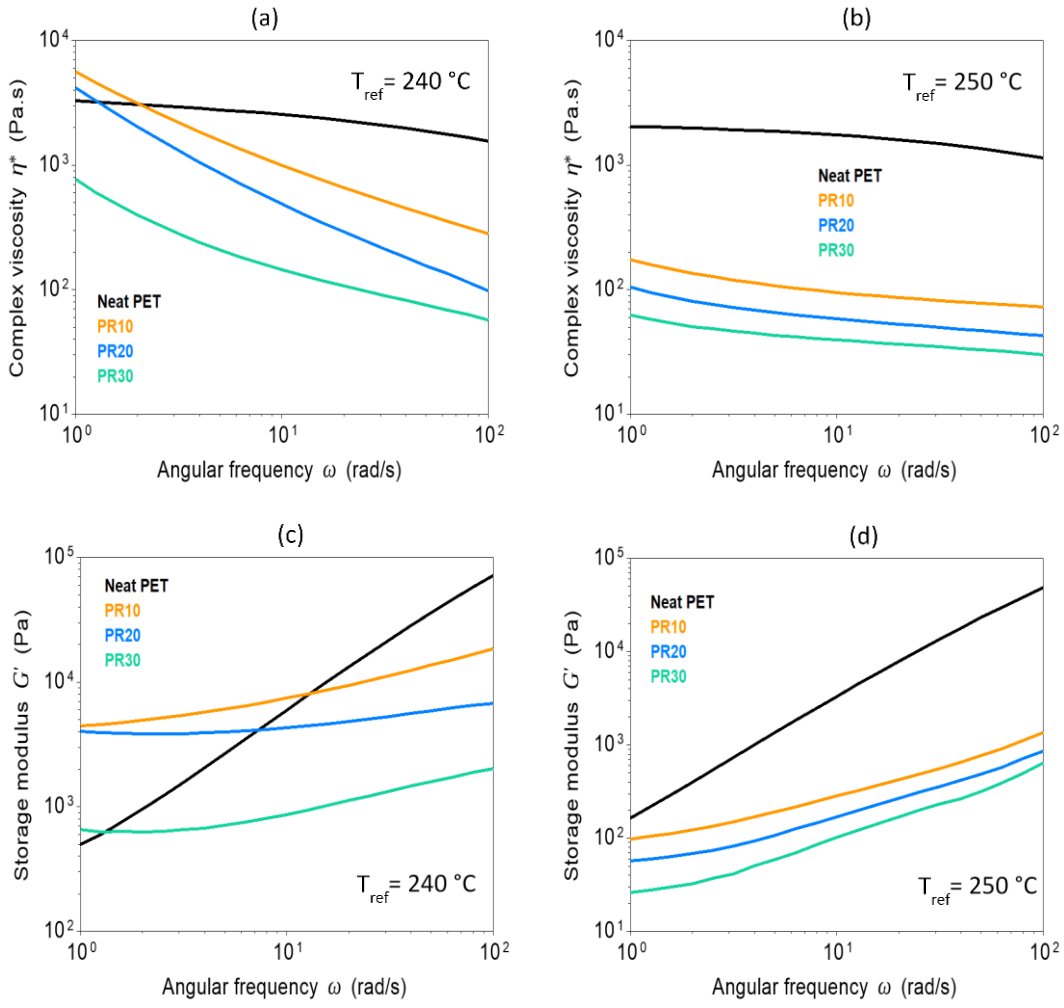

Figure 3-3. Frequency-dependent complex viscosity η* at T_{ref} = 240°C (a) and 250°C (b) and Frequency-dependent storage modulus G' at T_{ref} = 240°C (c) and 250°C (d) of recycled PET and its TOFA plasticized derivatives.

The plasticized PET samples, however, exhibit completely different topography of the fractured surface. The surfaces have cavities created by the addition of TOFA that are very well statistically dispersed and around 0.2 to 1 μm in size (Figure 3-4b, c, and d). For the 30 wt. % plasticized resin, the cavities are larger in size due to coalescence of the extra amount of TOFA during melt mixing which creates large agglomeration. The observations clearly show that the TOFA is acting as a lubricant by inserting itself in the polyester matrix and favoring chain motion and slippage of molecular constituents. This in turn introduces the thermophysical changes detected by thermal and dynamic mechanical analysis (Figure 3-1). FTIR spectra show (Appendix B, Figure B-1) that changes occurred with addition of TOFA. The insert from 1600 to 1700 cm^{-1} shows the carbonyl group (C=O) peak of both the TOFA and the PET. Addition of TOFA shifts the peak toward lower values meaning a stronger interaction between the PET and the TOFA.

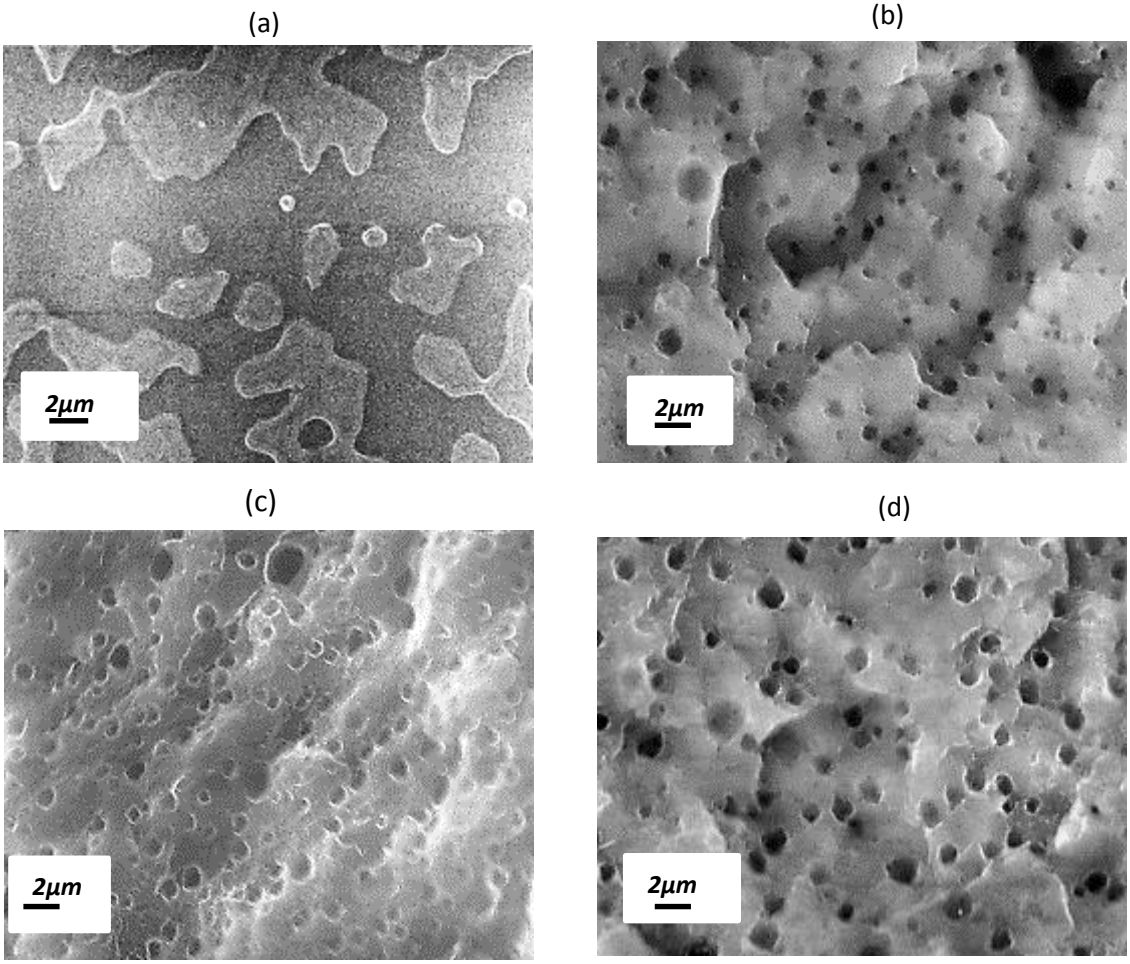

Figure 3-4. Micrographs of cryofractured surfaces; (a) neat PET, (b) PET/10% TOFA, (c) PET/20% TOFA, (d) PET/30% TOFA.

3.3.5. Properties of fibers spun from plasticized polyester resins.

The TOFA plasticized matrices were melt-spun to produce continous filaments using the benchtop extruder previously used for blending. The extruder and attached spinneret temperatures were set to 240°C and 245°C respectively for all samples, which is well below the neat PET working temperatures (~270-285°C). The 30 wt% plasticezed matrix spun the best out of all formulations. This can be explained by the pronounced effect the plasticizer has on lowering the viscosity at the spinning temperatures as shown in flow characterization (Figure 3-3). Fibers from all matrices were collected continously on a spool. The winding speed needed to be adjusted based on the material viscosity. For instance, 30 wt. % plasticized PET was collected at 130 meter/min compared to 10 wt. % plasticized matrix at 80 meter/min. These parameters will affect the mechanical performance of the fibers.

Thermal analysis by DSC (Appendix B, Figure B-2) shows interesting thermal behavior of the fibers. The first heating thermogram (Figure B-2a) shows early relaxation around 50°C for all samples that started at lower temperature for the 30 wt. % TOFA content PET fibers. The relaxation was followed by a cold crystallization around 100°C and melting behavior at 240°C. Melt-spinning process may have induced meta-order structure because of high chain alignment. In Figure B-2 b and c, the fibers behave more like their starting matrices showing recrystallization and melting peaks and similar shifts in their peak temperatures as reported in Figure 3-1 a and b.

The single fibers were isolated for tensile testing. The results are reported in Table 3-2. All fiber groups showed adequate tensile performances (tensile strength of 29-38 MPa, Tensile modulus 2.7-2.8 GPa and elongation at break of 20-36 %). It is important to recall that a limitation of our setup and the viscosity difference between the matrices made it impossible to produce the fibers using the same processing conditions, which affected the tensile properties of the fiber generated. For example, attempt was made to collect the filaments at a higher speed as possible which is critical to alignment of the polymer chains in the fibers and influences the strength of the fibers. However, PR30, which was collected at higher speed, did not have the highest tensile strenght. Defects created by large amount of TOFA could be the reason for the weaker tensile strenght. Also PR30 did not have the smallest fiber diameter. This suggests that a lower recrystallization temperature is affecting the 30 wt. % plasticized matrix overall fiber diameter. The performance of fibers displayed here could have improved if annealled at lower temperature before mechanical testing. Morphological evaluation of the fiber using SEM (Figure 3-5) shows longitudinal surface of the fibers. It is evident that the 10 wt. % TOFA plasticized PET has a small fiber diameter and very fine fibers were observed. The fibers' surfaces were not smooth and uniform as desired, which could be caused by the die capillary or temperature set up.

Table 3-2. Mechanical properties of the plasticized fibers. [1]

Composition (wt. %)		Properties			
PET	TOFA	Fiber diameter (micron)	Tensile strength (MPa)	Modulus (GPa)	Elongation (%)
90	10	36 (3.5)	38 (6.3)	2.7 (0.4)	20 (4)
80	20	46 (9.1)	29 (2.9)	2.8 (0.6)	36 (6)
70	30	42 (5.3)	32 (3.4)	2.7 (0.5)	32 (12)

[1] Standard deviations are shown in parenthesis

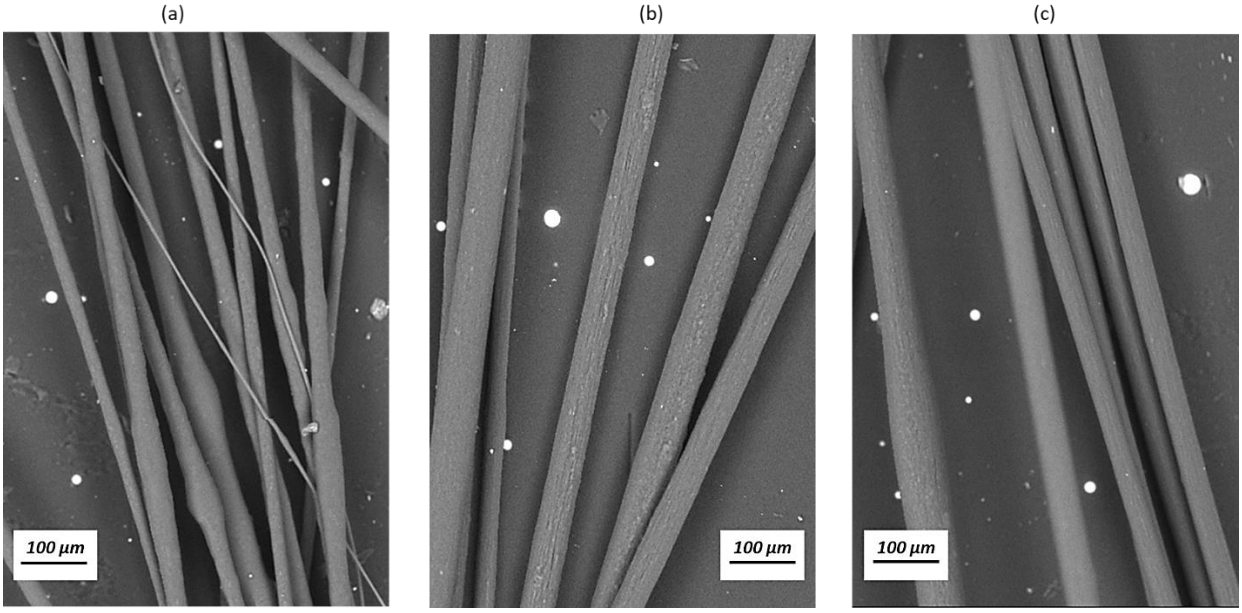

Figure 3-5. SEM micrographs of fibers from (a) Recycled PET/10 wt.% TOFA, (b) Recycled PET/20 wt.% TOFA and (c) Recycled PET/30 wt.% TOFA.

3.4. Conclusion

We have identified renewable tall oil fatty acid, a by-product of the Kraft paper making industry that uses pine trees, to plasticize polyester waste that would have ended up in landfill and caused an environmental hazard. The addition of TOFA induced changes in structure and morphology of the post-industrial PET. The melting temperature, recrystallization temperature, and T_g were shifted to lower temperatures because of increased chain mobility demonstrated by thermal and rheology analysis. The polymer blends were used to generate continuous fibers with acceptable tensile properties regardless of the processing set-up. For example, a 10 wt.% TOFA-loaded PET (the least plasticized one) could be spun into filaments with higher strength; however, these filaments made from the most plasticized compositions (20 and 30 wt.% TOFA), crystallized quickly and formed the largest diameter filaments. The developed blends obtained from manufacturing waste showed thermal and flow behaviors that can expand their end use applications and create revenue from waste materials. In summary, TOFA shows a potential as a renewable and cost-effective plasticizer for post-industrial PET wastes.

AKNOWLODGMENTS

This project is supported by the Sun Grant Initiative and by Agriculture and Food Research Initiative Competitive Grant no. 2014-38502-22598 from the USDA National Institute of Food and Agriculture and by the USDA National Institute of Food and Agriculture, Hatch project 1012359. N.A.N. acknowledges support from the U.S. Department of Energy (DOE), Office of Energy Efficiency and Renewable Energy, BioEnergy Technologies Office Program for the rheological analysis of the materials. A.K.N. acknowledges support from the Laboratory Directed Research and Development Program of Oak Ridge National Laboratory, managed by UT-Battelle, LLC, for the US Department of Energy.

References

1. Orset, C., N. Barret, and A. Lemaire, *How consumers of plastic water bottles are responding to environmental policies?* Waste Management, 2017. **61**: p. 13-27.
2. Kint, D. and S. Munoz-Guerra, *A review on the potential biodegradability of poly(ethylene terephthalate).* Polymer International, 1999. **48**(5): p. 346-352.
3. Awaja, F. and D. Pavel, *Recycling of PET.* European Polymer Journal, 2005. **41**(7): p. 1453-1477.
4. Chen, Y., Z. Lin, and S. Yang, *Plasticization and Crystallization of Poly(ethylene Terephthalate) Induced by Water.* Journal of Thermal Analysis and Calorimetry, 1998. **52**(2): p. 565-568.
5. Chen, B., L.L. Zhong, and L.X. Gu, *Thermal Properties and Chemical Changes in Blend Melt Spinning of Cellulose Acetate Butyrate and a Novel Cationic Dyeable Copolyester.* Journal of Applied Polymer Science, 2010. **116**(5): p. 2487-2495.
6. Jackson, J.B. and G.W. Longman, *The crystallization of poly(ethylene terephthalate) and related copolymers.* Polymer, 1969. **10**: p. 873-884.
7. Gowd, E.B. and C. Ramesh, *Effect of poly(ethylene glycol) on the solid-state polymerization of poly(ethylene tereplithalate).* Polymer International, 2006. **55**(3): p. 340-345.
8. Mizoguchi, K., et al., *CO2-induced crystallization of poly(ethylene terephthalate).* Polymer, 1987. **28**(8): p. 1298-1302.
9. Takada, M. and M. Ohshima, *Effect of CO2 on crystallization kinetics of poly(ethylene terephthalate).* Polymer Engineering and Science, 2003. **43**(2): p. 479-489.
10. Meier, M.A.R., J.O. Metzger, and U.S. Schubert, *Plant oil renewable resources as green alternatives in polymer science.* Chemical Society Reviews, 2007. **36**(11): p. 1788-1802.
11. Sharma, V. and P.P. Kundu, *Addition polymers from natural oils—A review.* Progress in Polymer Science, 2006. **31**(11): p. 983-1008.
12. Sander, M.M., et al., *Plasticiser effect of oleic acid polyester on polyethylene and polypropylene.* Polymer Testing, 2012. **31**(8): p. 1077-1082.
13. Mehta, B., M. Kathalewar, and A. Sabnis, *Benzyl ester of dehydrated castor oil fatty acid as plasticizer for poly(vinyl chloride).* Polymer International, 2014. **63**(8): p. 1456-1464.
14. Wang, Z., et al., *Investigation of Palm Oil as Green Plasticizer on the Processing and Mechanical Properties of Ethylene Propylene Diene Monomer Rubber.* Industrial & Engineering Chemistry Research, 2016. **55**(10): p. 2784-2789.
15. Jia, P., et al., *Green plasticizers derived from soybean oil for poly(vinyl chloride) as a renewable resource material.* Korean Journal of Chemical Engineering, 2016. **33**(3): p. 1080-1087.

16. Logan, R.L., *Tall oil fatty acids.* Journal of the American Oil Chemists' Society, 1979. **56**(11): p. 777A-779A.
17. Wunderlich B., *Thermal Analysis*. 1990: Academic Press.

Appendix B

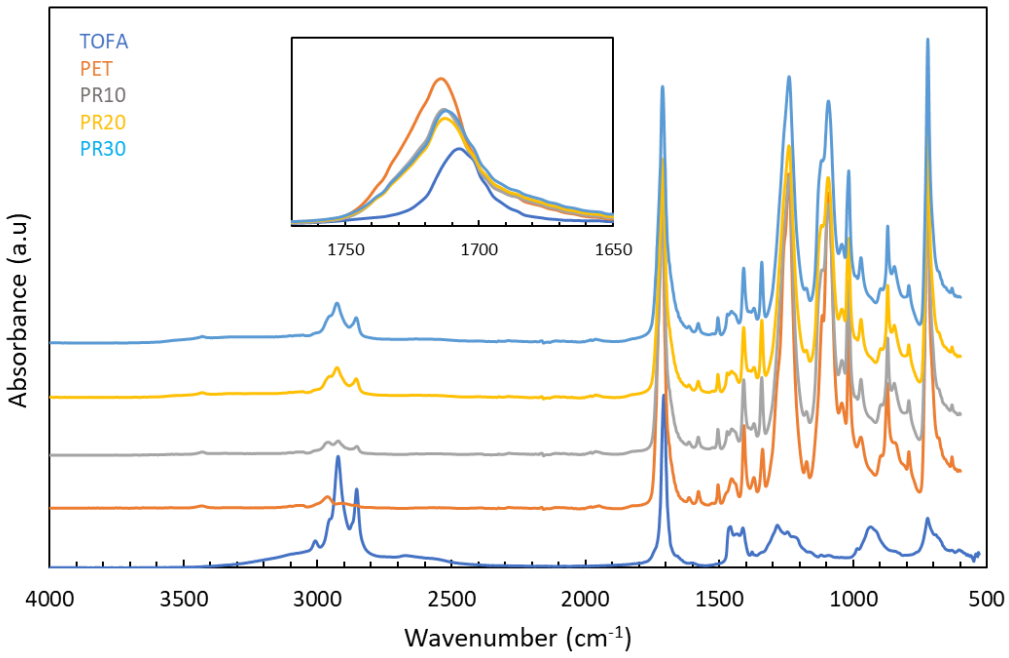

Figure B-1. FTIR spectra of TOFA, neat PET and their blends with different renewable plasticizer content (from 10 wt.% to 30 wt.%).

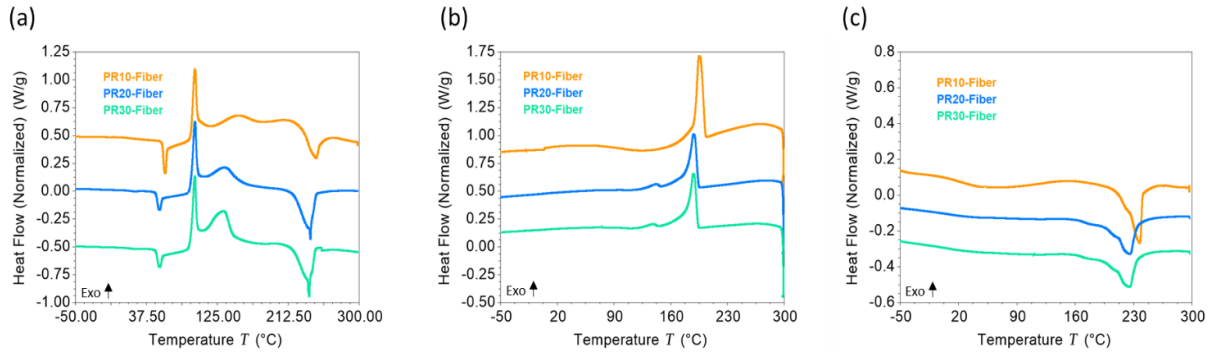

Figure B-2. DSC thermograms of the fibers spun from plasticized PET matrices. (a) The first heating cycle, (b) the consequent cooling cycle, and (c) the second heating cycle indicating similar characteristics of the bulk samples.

CHAPTER 4
CONTROLLING LIGNIN DISPERSION AND INTERFACIAL INTERACTIONS IN RECYCLED POLYESTER RENEWABLE COMPOSITES

This chapter is based on the manuscript prepared for submission to a peer review journal. The full list of authors includes Kokouvi Akato, Ngoc A. Nguyen, David P. Harper, and Amit K. Naskar. Kokouvi Akato performed all experiments, processed and analyzed all data, and prepared the manuscript for submission. Ngoc A. Nguyen assisted with thermal characterization and rheology. David P. Harper assisted with editing the manuscript. Amit K. Naskar assisted with data analysis and editing of the manuscript. Kalavathy Rajan and Stephen Chmely helped with NMR data collection.

Abstract

Brittle lignin oligomers, isolated from plant biomass, need a low-melting tough host polymer matrix to form a rigid and high-performance renewable material. In this work, we demonstrate controlling lignin phase dispersion and interfacial interactions in softened recycled polyethylene terephthalate (PET), a polyester matrix, using a simple melt-blending technique. To avoid lignin degradation and devolatilization during amalgamation, it was thermally treated. Tall oil fatty acid was used to enable PET processability at low enough temperature to accommodate lignin without charring. Chemical analysis reveals reduction of aliphatic hydroxyl content from 2 mmol/g to 1.63 mmol/g and an increase of total phenolic hydroxyl moieties from 5.86 to 6.64 mmol/g, and cleavage of β-O-4 ether linkages due to thermal treatment. Structural transformation of lignin macromolecules during heat treatment was further confirmed by an increase in molar mass and improved thermal stability. Interfacial interactions between lignin and PET were assessed from mechanical properties and thermal analyses. Thermal treatment not only helps to improve the stability of lignin but also reduces dispersed lignin domains via favored interfacial interactions with PET matrix.

KEYWORDS: renewable polymer, recycled PET, thermal treatment of lignin, interfacial interactions

4.1. Introduction

Conservation of petrochemicals and utilization of wastes and renewable materials are essential to avoid industrial pollution [1]. Proposed reliable solutions include usage of materials made from renewable sources and development of value-added products from wastes [2]. In this perspective we propose intermingling of post-consumer polyethylene terephthalate (PET) waste and lignin, currently considered as waste or cheap power source, to produce a new class of sustainable polymeric materials. This creates a win-win solution by adding value to renewable resources, spent and recycled materials, and curtailing environmental concerns.

PET is a semi-crystalline thermoplastic polyester broadly used in packaging industries. Wastes generated during manufacturing and consumption of PET are detrimental to the

environment because PET lacks biodegradability [3]. Thus, recycling these wastes is desired for environmental protection and to generate additional revenue streams. Recycled waste PET is used in construction, packaging, and composite applications. For example, recycled PET is used readily in structural concrete reinforcement, where crack control and enhancement of ductility are valuable [4, 5]. Recycled PET is also used to develop new materials through blending with other polymers [6-9]. Most blends are immiscible at molecular levels due to unfavorable interfacial tension between the components and often require the addition of a compatibilizer.

Blends of PET and lignin were evaluated as an alternate route in the efforts of lignin valorization to derive thermoplastic/lignin alloys [10-16]. Unfortunately, only moderate interactions and a downward trend of the tensile strength as a function of the amount of lignin loading were observed. Therefore, in most cases, lignin was modified to introduce functional moieties that favor strong interactions between the components. Typically, properly tailored interfacial interactions, either by chemical route or by addition of compatibilizer, drastically improve the dispersion of fine homogenous lignin domains that is valuable for performance enhancement of the blends. In that regard, esterification is often used as a lignin modification route [17, 18]. The additional step increases cost and creates a need for chemical disposal, which constitutes an inherent disadvantage for the new polyester-lignin blends for industrial adoption.

Most of the above reports on PET-lignin blends claim full miscibility, partial miscibility or total immiscibility between lignin and the host matrix with widespread variations in structures and properties based on microscopy, differential scanning calorimetry (DSC), and Fourier transformed infrared (FTIR) spectroscopy. Yet very little information is available on process engineering of the blends. Due to the high melting temperature (~260°C) of PET, choosing appropriate blending temperatures for PET/lignin blends is important to avoid lignin degradation during mechanical blending. Jeong [14] reported mixing temperature of 170°C for blends of lignin and synthetic polymers including PET, which is nearly impossible in the case of PET. Temperature setup as high as 265°C were used elsewhere [10]. In general, the rheology of the blend components impacts processing and phase behavior of the resulting PET/lignin blends.

The scope of this study lies within usage of melt-based blending techniques to develop partially renewable polymer blends of post-manufacturing PET waste and an organosolv lignin, a low-priced natural polymer obtained from biomass without chemical modification. In general, normal processing temperatures (270°C to 280°C) of post-manufacturing PET are deemed detrimental for lignin amalgamation. For this reason, lignin can be thermally treated to remove low molecular weight volatile materials and improve its heat resistance during blending. It also helps to avoid devolatilization that negatively impacts the blend morphology (by creating porosity) and properties. Based on our previous experience (Chapter 3), a renewable plasticizer (Tall oil fatty acid - TOFA) at 10 wt. % relative to PET was added to help soften PET chains and to reduce its melting temperatures. TOFA is

another co-product of paper industry and plant-derivatives used here in combination with the recycled PET and lignin for preparation of lignin thermoplastic alloys that are malleable and reprocessable. Combining thermal treatment with plasticizing permits appropriate choices in mixing temperature, to control dispersion of lignin, and associated promotion of interfacial adhesion that are necessary to create higher performance sustainable composites of lignin. In summary, this study involves adept characterization of lignin, its structural transformation during thermal treatment followed by an assessment of interfacial interactions of lignin in PET matrix, and subsequent correlation to morphology and mechanical properties of partially renewable PET/lignin blends.

4.2. Experimental section

4.2.1 Materials.

Thermoplastic polyester PET was received from Eastman Chemical USA. It is scrap from the resin manufacturing facility and supplied as white ground plastic. Melt flow rate (MFR) measured in our laboratory is 55g/10 min at 280°C at 2.16Kg applied force. The PET was dried under vacuum at 130°C for 12 hours to avoid hydrolytic degradation during melt processing. Organosolv hardwood lignin (L) was provided by Lignol Innovations, Canada. The lignin melts fully at 147°C and flows at 163°C (Fisher Scientific melting point tester). The lignin was dried at 60°C for 8 hours. The tall oil fatty acid (TOFA) was acquired from Westvaco Chemicals, Charleston SC. It is a Westvaco L-5 Tall oil fatty acid. The specifications of the TOFA were reported as: Acid number (min 190), rosin acids (max 5%) and color or Gardner (max 7).

4.2.2. Lignin thermal treatment and characterization.

The lignin (L) was thermally treated in a vacuum oven at 200°C for 60 minutes to improve its thermal stability. The thermally treated lignin is identified as L_{HT}. Both as-received L and L_{HT}, were characterized using Gel permeation chromatography (GPC) to evaluate molecular weight and molecular weight distribution (see Appendix C). Functional features were characterized and quantified by ^{31}P NMR and 2D $^{1}H–^{13}C$ HSQC NMR spectroscopy using preparation and analysis methods previously reported [19-21]. Thermogravimetric analysis was used to study thermal stability of the lignin in a nitrogen atmosphere from 100°C to 800°C at 10°C/min after a drying step at 100°C for 20 min.

4.2.3. Blend preparation.

Blends of recycled PET and lignin at 10, 20 and 30 wt. % lignin loading of both as-received lignin (L) and thermally treated lignin (L_{HT}) were prepared respectively, with 10 wt.% of renewable plasticizer relative to the PET weight at 240°C. A Haake MiniLab co-rotating twin extruder (Thermo Scientific) with screw length of 110 mm was used at screw rotation speed of 30 rpm. In a different setup, the extruder was fitted with a die to generate monofilament of 0.20 to 0.40 mm diameter. The partially renewable blends are identified

as PET_{PL}/10L, where 10 wt.% L was added and PET_{PL}/30L_{HT}, where 30 wt. % L_{HT} were added respectively. All neat PET filaments used in this study were generated at 280°C and used as reference.

4.2.4. Thermal analysis.

A differential scanning calorimeter (DSC Q2000, TA Instruments) was used to determine the thermal transitions of the control PET and its lignin-derived blends. Samples with mass of approximatively 3-4 mg each were loaded in hermetic pans for measurements. A cycle of heating-cooling-heating from -50°C to 300°C at 10°C/min and an isothermal of 2 min after first heating were used. Thermal decomposition of the blends was evaluated using thermogravimetric analyzer (TGA Q50, TA Instruments) under oxidative atmosphere from 100°C to 600°C at 20°C/min after a short drying step.

4.2.5. Scanning electron microscopy and morphology analysis.

A Zeiss EVO MA 15 electron scanning microscope was used to obtain micrographs of the cryo-fractured surfaces of the blends. The samples were kept in 1M NaOH solution for 20 min at 80°C after cryofracture before SEM analysis to remove lignin phases from the surface. Washed and dried samples were coated with gold to avoid charging when images were collected. Images were collected at an operating voltage of 20 KV.

4.2.6 Tensile and dynamic mechanical testing.

Monofilaments of control PET and its lignin-derived blends were tested using an Instron 5943 equipped with Bluehill3 software and pneumatic side action grip. The crosshead speed was to 15mm/min and the filaments cross-sectional diameters were used for calculation of cross-sectional area and applied stress. Dynamic mechanical analysis (DMA) measurements were carried out on the monofilaments (diameter 0.20 - 0.40 mm depending on the sample) at 0.1% strain rate, discrete frequencies of 1, 10, and 100Hz, and between 30°C and 150°C temperature window scanned at 3°C/min.

4.2.7 Rheological evaluation.

The rheological properties were analyzed using the Discovery Hybrid rheometer (DHR-2, TA instruments). All measurements were carried in the linear regions at 3% strain in nitrogen atmosphere. Frequency sweeps from 100 to 1 rad/s at different temperatures were used to generate master curves at 240°C and 250°C reference temperatures.

4.3. Results and discussion

4.3.1. Lignin structural transformation.

Lignin has gained valuable importance recently in preparation of a new class of renewable thermoplastic elastomeric materials [22, 23]. Lignin is an excellent renewable feedstock for manufacturing of environment-friendly materials because of its multifunctional nature

and associated chemistries. Here, lignin was thermally treated at 200°C under vacuum for 60 minutes to avoid thermal decomposition during blending with recycled PET. Detailed insight into the microstructural transformation induced by thermal treatment is important for the final properties of the manufactured blends. ^{31}P NMR and 2D HSQC NMR were used to identify and quantify the chemical group profiles of both the as-received and thermally treated lignins.

Phosphorylation of OH groups in lignin allows quantification of different OH moieties of lignin by ^{31}P NMR analysis. The ^{31}P NMR spectra with chemical shifts and microstructural assignments are shown in Figure 4-1, whereas the amount of OH groups determined from the spectra is summarized in Table 4-1. Thermal treatment decreased the aliphatic OH content of lignin. L has the higher amount of aliphatic hydroxyl (2.01 mmol/g) compared to L_{HT} (1.63 mmol/g). This indicates that during thermal treatment, structural transformation of lignin starts with dehydration which eliminates the side chain OH groups [24]. The total amount of phenolic OH increased after thermal treatment, however, the carboxylic group content remained the same. L is an organosolv-extracted hardwood lignin and is expected to have phenolic syringyl (S-OH) and guaiacyl (G-OH) with little to no p-hydroxyphenol (H-OH) [19, 25]. The results are in accordance as these two groups are higher than the H-OH groups. However, thermal treatment introduced an increase of S-OH, G-OH, and H-OH groups. For L_{HT}, the condensed and noncondensed phenol content increased as well. Possible cleavage of β-O-4 linkage associated with S and G occurred during heat treatment.

Two regions of the 2D HSQC NMR spectra analyzed are shown in Figure 4-2. Cross peak assignments and corresponding inter-unit linkages are available in Figure C-1 and Table C-1 (Appendix C). The regions possess similarities between the spectra except for a few signals. The cross peaks corresponding to C_α-H_α in β-O-4' substructures δ_C/δ_H 71.9/4.9 and C_β-H_β in β-aryl ether (β-O-4) substructures δ_C/δ_H 86.3/4.15 in syryngyl units were significantly reduced or disappeared after thermal treatment. The C_5-H_5 and C_6-H_6 in guaiacyl units were also reduced. This indicates that β-O-4' and β-O-4 aryl ether bonds cleaved during at the thermal treatment and confirms the ^{31}P NMR results discussed above. The β-O-4 linkages are easily altered by heat [26] as discussed. The expectation is that ether radicals and phenolic radicals will result from these cleavages and react among themselves to initiate crosslinking reactions (condensation) or remain available for further interactions during melt blending of lignin with the engineered polyester. However, phenolic hydroxyls are free radical scavengers and are susceptible to find these radicals for reactions among the lignin. The possibility of condensation reactions occurring among the lignin free radicals generated during thermal treatment explains the increase of S-OH, G-OH, and H-OH groups after thermal treatment in L_{HT}.

Molecular mass and its distribution for both lignins obtained by GPC indicate the effect of thermal treatment at 200°C on structural transformation of lignin. GPC results show increase in Mn, Mw and Mw/Mn after thermal treatment. L was found to have M_n = 890,

M_w = 1486, and M_w/M_n = 1.67, while L_{HT} had M_n = 1103, M_w = 1924, and M_w/M_n = 1.75. The increased of average molecular weight is the result of condensation reactions that occurred during thermal treatment. Evidence of the reactions are found in products features detected by ^{31}P NMR and 2D HSQC NMR. Thermal behaviors analysis by DSC agrees with these findings as glass transition temperature of lignin increased from 86°C to 97°C after thermal treatment (Appendix C Figure C-2). The degree of crosslinking was mild; otherwise, pronounced crosslinking would have enlarged the macromolecules to higher range. For example, L_{HT} would have had higher molecular weight and reduced viscosity. The fact that L_{HT} still flows at ~ 165°C is an evidence of mild crosslinking. This also suggests that oxidation was avoided in vacuum. A treatment duration of 60 minutes should have been enough to advance the condensation reactions when conducted in an oxidative atmosphere [27].

Thermal treatment improved thermal stability of the lignin through removal of volatiles, dehydration, crosslinking in aromatic structures and increasing the degree of condensation [24]. As-received lignin started to degrade at 185°C. Thermal treatment shifted the onset of degradation to higher temperatures to accommodate melt mixing with PET at 240°C. TGA thermograms of L and L_{HT} are shown in Figure C-3 (Appendix C). Weight reduction temperatures recorded at 5% weight loss was 247°C for L compared to 265°C for L_{HT}. The derivative weight thermogram of as-received lignin has a shoulder from 143°C to 258°C that disappeared after thermal treatment by removing low molecular weight volatiles and cleaving thermal liable ether bonds. Overall, thermal treatment under vacuum only changed lignin structure slightly to improve its thermal stability. This avoids significant oxidative degradation reactions that are detrimental to keeping the lignin malleable. In addition, the soak time of 60 minutes was good enough to generate lignin that is thermally stable and malleable for amalgamation in engineered polymer matrices.

Table 4-1. Functional groups of the L lignin and thermally treated lignin (L_{HT}) as determined by the quantitative ^{31}P NMR method (mmol/g).

		syringyl OH		guaiacyl OH				
Samples	aliphatic OH	C[a]	NC[b]	C[a]	NC[b]	p-hydroxy phenol OH	total phenolic OH	Carboxylic group
L	2.01	0.39	2.46	0.80	1.79	0.42	5.86	0.45
L_{HT}	1.63	0.35	2.73	0.96	2.04	0.56	6.64	0.46

[a] Condensed. [b] Noncondensed

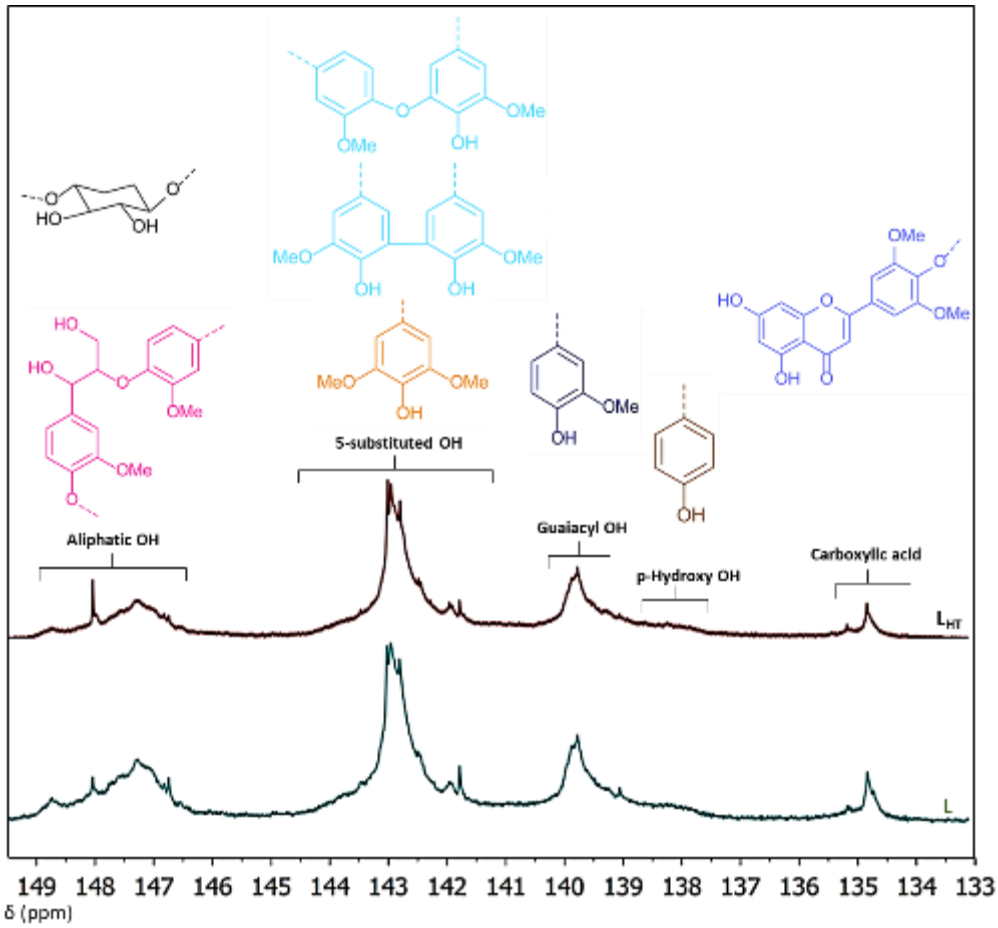

Figure 4-1. Functional groups identified by quantitative ^{31}P NMR measurements after phosphorylation of lignins L and L_{HT}.

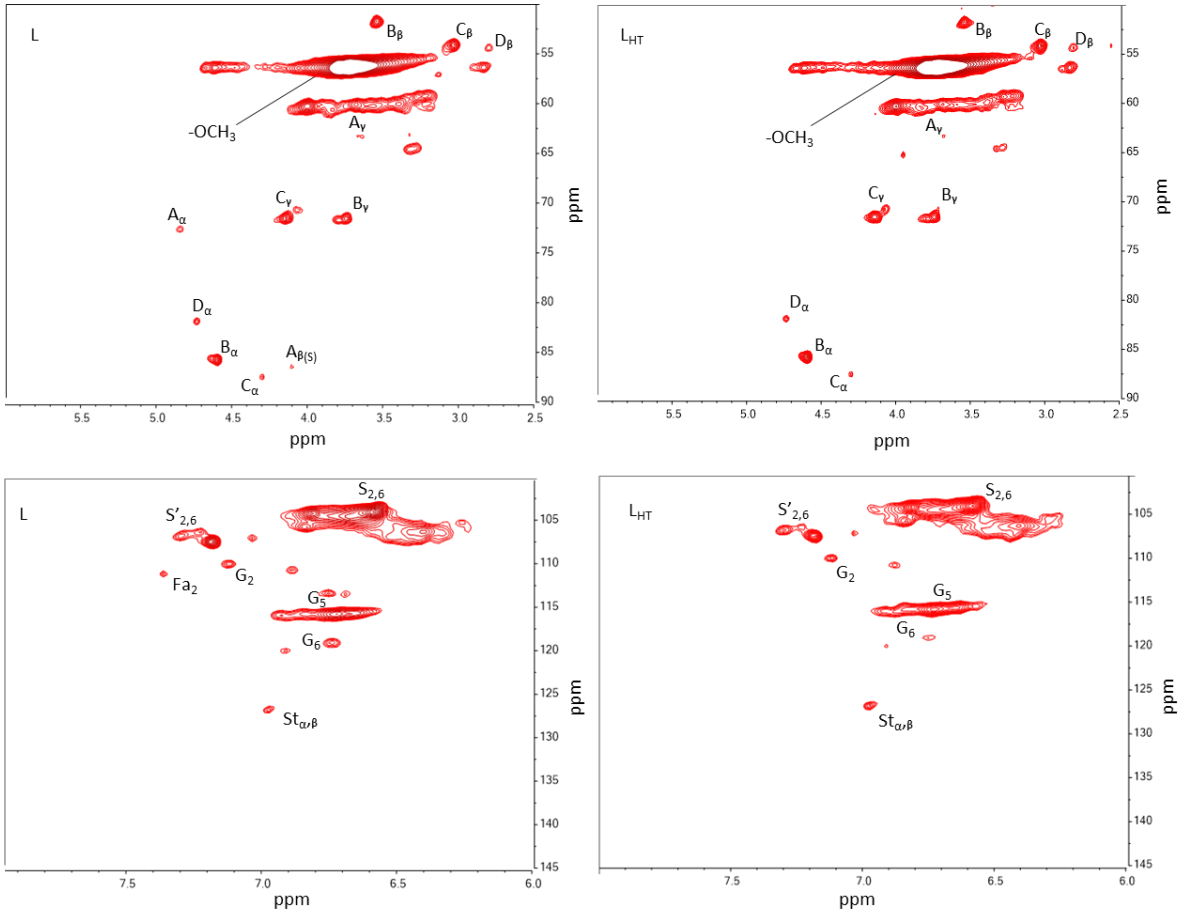

Figure 4-2. Two-dimensional 2D NMR heteronuclear single quantum coherence (HSQC) spectra of both L and L_{HT} lignins. The top two images are the aliphatic oxygenated side chain region (δ_C/δ_H 90-150/2.5-6) and the bottom two images represent the aromatic/unsaturated region (δ_C/δ_H 90-150/5-8).

4.3.2. Thermal and morphological properties of the compositions.

Thermal transition temperatures, calorimetric values, and degree of crystallinity computed from cooling and second heating of DSC thermograms are shown in Appendix C (Table C-3). The results suggest that addition of TOFA plasticizer reduces the melting temperature of the neat PET. The melting temperature of PET shifted from 247°C to 239°C in presence of 10 wt.% TOFA. Plasticizers are small molecular weight materials that are added to help soften the rigid amorphous phase of polymer. It enhances segmental mobility by depressing the glass transition temperature (T_g) of the amorphous phase of the host polymers. The effect of the plasticizer on recrystallization during cooling is observed as the recrystallization temperature shifts from 208°C to 202°C.

Addition of lignins (L and L_{HT}) in all compositions further reduces the melting temperatures and decreases the heat of fusion. This is evidence for reduction in crystallite sizes in PET with incorporation of lignin in the blends. Also, the difference between the behavior of L series alloys compared to L_{HT} series alloys suggests variance in the degree of interactions between the lignins and PET. In theory, the addition of oligomeric lignin increases the free volume in the PET matrix which led to the plasticization effect. Additionally, lignin addition shifts the recrystallization temperature (T_{rec}) of PET to lower temperatures. Shift of T_{rec} and ΔH_{rec} suggests that lignin is decelerating the recrystallization and crystal growth during cooling. Conclusions from these results show that interactions exist between both lignins and PET. These interactions could be the hydrogen bonding and π electron interactions. The degree of crystallinity (χ_c) was computed using Equation S1 (Appendix C) and first heating curve calorimetric values. Increasing lignin content increases χ_c in the L series but it decreases with increases in the L_{HT} content. It implies that different degrees of interactions occur between the PET and the as-received lignin versus the PET and the thermally treated lignin.

Microscopic analysis of cryo-fractured surfaces of the blends (Figure 4-3) shows that the morphologies depend on the nature of lignin at 30 wt. % lignin contents in the blends. The samples were etched in 1 M solution of NaOH to dissolve lignin from the cryofractured surface before SEM imaging. In Figure 4-3a, the blend of PET and as-received lignin (L) appears as less concentrated but larger lignin droplets in PET matrix. Lignin droplet sizes vary from 1 to 2 micrometers. However, the thermally treated lignin-derived PET blend shows formation of homogenously dispersed cavities after removal of lignin macromolecules (0.2 to 2 micrometer). Controlling lignin-lignin intermolecular interaction through thermal treatment by decreasing aliphatic hydroxyl helps avoid coalescence of the lignin phase during mixing in the engineered polyester matrix. It has been reported that controlling microstructure and dispersion of lignin in thermoplastic blends is important for improved performance [28].

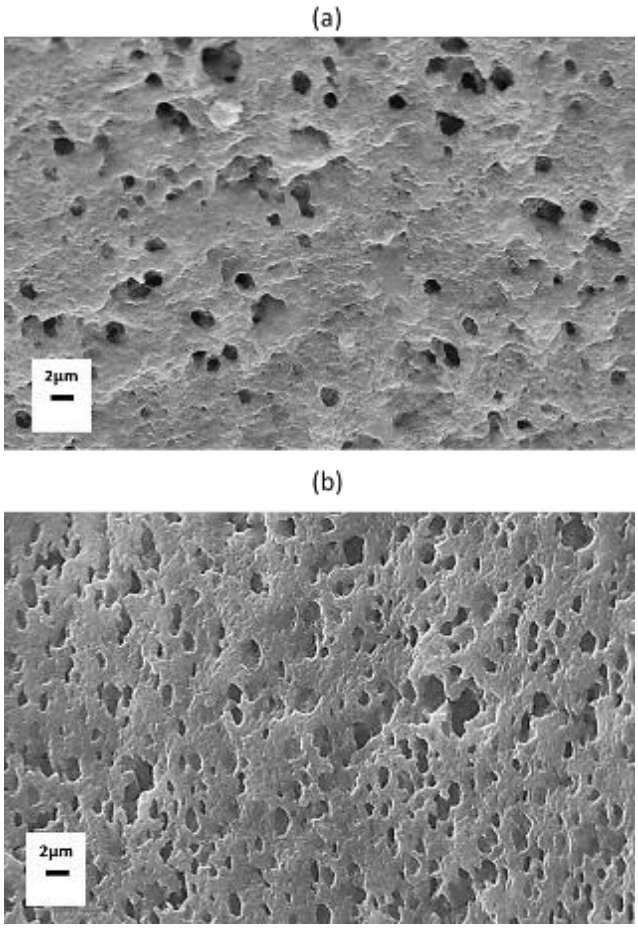

Figure 4-3. Scanning electron micrographs of cryo-fractured and NaOH etched surfaces of PET_{PL}/30L (a) and PET_{PL}/$30L_{HT}$ (b) blends.

4.3.3. Interfacial interactions-performance relationships.

Mechanical properties. Amalgamation of lignin in thermoplastics often reduces tensile strength. This is primarily because the lignin forms large domains in thermoplastic matrices causing defect centers. However, lignin was reported to impart rigidity and stiffness in some systems [22]. Improving overall performance of the blends relies on the level of interactions between the lignin and the host polymer molecules. Figure 4-4a illustrates the relationship between the tensile strength presented as a ratio of tensile strength of the lignin-derived composites over the tensile strength of the matrix (σ_c/σ_m) as a function of weight fraction of lignin in the blends. The (σ_c/σ_m) diminishes with increasing lignin amount. Obviously, weak interactions between the PET and lignin generate large lignin domains in the blends (Figure 4-3a) that affect performance of the blends negatively. Also, there is a possibility of thermal degradation of lignin during mixing at 240°C leading to inferior performance. In this study, we find that the thermal pre-treatment

improves lignin stability and helps to improve lignin dispersion in the PET matrix and, thus, the mechanical properties. Although thermal treatment increases the molar mass of L_{HT}, mechanical shear during blending helps to break the aggregates of lignin macromolecules into finer droplets compared to the system consisting of original lignin, L. Complete performance indices of tensile modulus (E_C/E_m), elongation ($\varepsilon_c/\varepsilon_m$) and ($\sigma_c/\sigma_m$) are shown in Appendix C (Figure C-4). The addition of lignin increased the modulus as expected in filled materials due to the natural rigidity of lignin macromolecules, however, elongation was reduced because of the inherent brittleness of the added lignin. Nonetheless, low lignin-loaded compositions show slightly improved performance of the PET matrix combined with L_{HT} compared to its control counterparts.

The composition dependence of the mechanical properties somehow limits our ability to draw a definitive conclusion on the interactions in each blend. We observe, however, that better interactions exist between the L_{HT} and the PET compared to L blends. Nevertheless, the results of L series imply that some level of interactions is also occurring between L and PET, possibly competing hydrogen bonding between the lignin OH and PET end groups (ester and ethylene groups) and π-π interaction between aromatic groups of lignin and PET.

Figure 4-4b shows natural logarithm of reduced tensile strength as a function of volume fraction of lignin. The reduced tensile strength is described by Equation (1) [29]. The plot is used for quantitative estimation of interaction using the composition dependence of strength model. The model relates the interfacial interactions, structure and the mechanical properties of the blends. It is expressed to reflect the effect of volume fraction (φ) of the dispersed component, and the load bearing capacity of the dispersed lignin constituent (B), which is dependent on interfacial adhesion [30, 31].

$$\sigma_{Tred} = \sigma_T \frac{1+2.5\varphi}{1-\varphi} = \sigma_{T0} \exp(B\varphi) \quad (1)$$

Where σ_{Tred} is the reduced tensile strength of the blend, σ_T and σ_{T0} are the tensile strength of the blends and the matrix, respectively.

The results are summarized in Table 4-2. It reveals that parameter B, which is the slope of the linear correlation applied to the data, increased from 0.79 to 1.21 when the thermally treated lignin L_{HT} was used instead of L highlighting divergent interfacial adhesion. Thermal treatment was beneficial to improve thermal stability, control lignin-lignin intermolecular interactions and to control lignin-PET interaction likely through a combination of hydrogen bonding and π electron interactions that is clearly different in the composites based on as-received lignin (L). Calculated tensile stress of the matrix (σ_{T0}) for both cases (L and L_{HT} series) agrees well with the measured value.

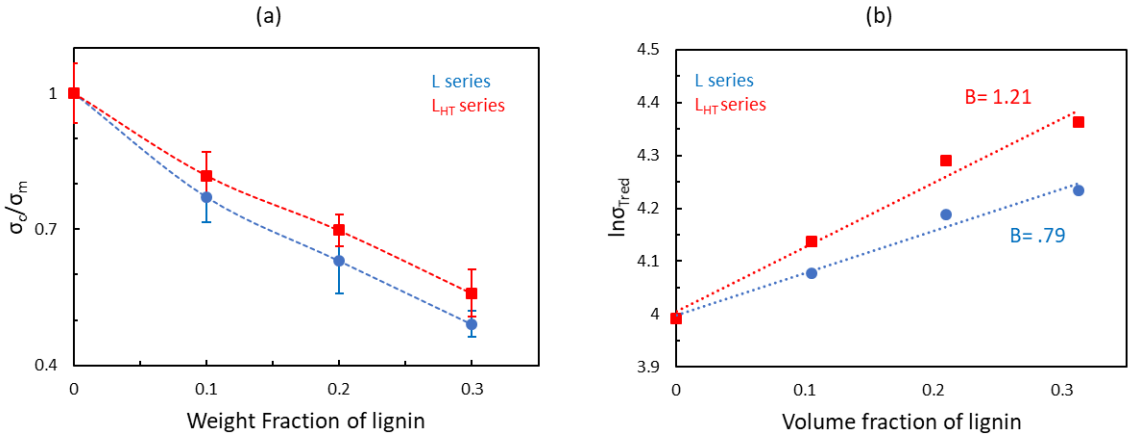

Figure 4-4. Ratios of tensile strength of lignin-loaded matrices over those of neat PET at different lignin weight fraction (a), and the natural logarithm of reduced tensile strength as a function of volume fraction of lignin (b).

Table 4-2. Quantitative estimation of interactions computed from mechanical properties of the blends.

Lignin		σ_{T0} (MPa)			
	Treatment	Measured	Calculated [b]	B	R^2
L	As-received	54.19 (3.58) [a]	54.46	0.79	0.978
L_{HT}	Heat treated		54.91	1.21	0.981

[a] standard deviation is shown in parenthesis.
[b] Computed from the y-intercept of $\ln\sigma_{Tred}$ vs. volume fraction of lignin plots.

Dynamic mechanical analysis. Loss tangent (tan δ) peaks for PET and its lignin-based alloys at 10 Hz frequency are shown in Figure 4-5. Neat PET shows a narrow tan δ peak representative of its glass transition temperature T_g at 101°C. This shift is likely attributed to the presence of TOFA at 10 wt. % of PET in each blend. The tan δ peaks became broader in the presence of lignin in PET matrix and increase in lignin content increases the T_g. When lignin L is used, moderate interactions with PET matrix are expected. The T_g is 86°C for a 10 wt.% lignin loading in plasticized PET; use of L_{HT} makes better dispersion and interactions with PET matrix and thus, a slight increase in T_g is observed (89°C). Similar observations were made in the case of higher lignin loading (30 wt.%) in blends.

The loss tangent data represents the energy dissipated by the materials under cyclic load. Application of the Arrhenius equation to the loss factor (tan δ) peak temperature as a function of frequency data provides quantitative evaluation for the relaxation behavior of PET phase in the blends. In this instance, the Arrhenius equation can be expressed in the following form:

$$\log f = \frac{-E_a}{(2.303RT)} + \log K \qquad (2)$$

here *T* is the absolute temperature at which the loss maximum is observed at frequency *f*, *R* is the gas constant, *K* is an arbitrary constant, and E_a is activation energy associated with glassy to rubber transition or relaxation. Table 4-3 shows computed E_a data for neat PET (479 KJ/mol). Addition of TOFA reduced the activation energy in PET. However, the thermally treated lignin alloys have higher E_a compared to the as-received lignin compositions in TOFA plasticized PET; although, the increase in E_a becomes marginal at high L_{HT} content in the blend. Two phenomena are occurring simultaneously. First, the plasticizer is helping to depress T_g while rigid lignin hinders segmental motion of PET. Treated lignin L_{HT} has a higher degree of interaction with PET matrix and thus restrains the flexibility of the PET phase. At high L_{HT} loading, however, the advantageous effect of improved dispersion on relaxation of PET matrix diminishes.

4.3.4. Processing engineering and degradation parameters of partially renewable blends.

PET is a semi-crystalline polymer. Its normal processing temperatures is between 270°C to 280°C. Amalgamation of lignin with PET requires manipulating the PET thermal behavior to prevent degradation of lignin. Our approach to address this involves using a renewable plasticizer to soften PET matrix. In practice, low molecular weight plasticizers are often added to increase the flexibility at room temperature and to improve processing. All blends studied in this report were mixed at 240°C, a processing of PET that was enabled by the addition of plasticizer.

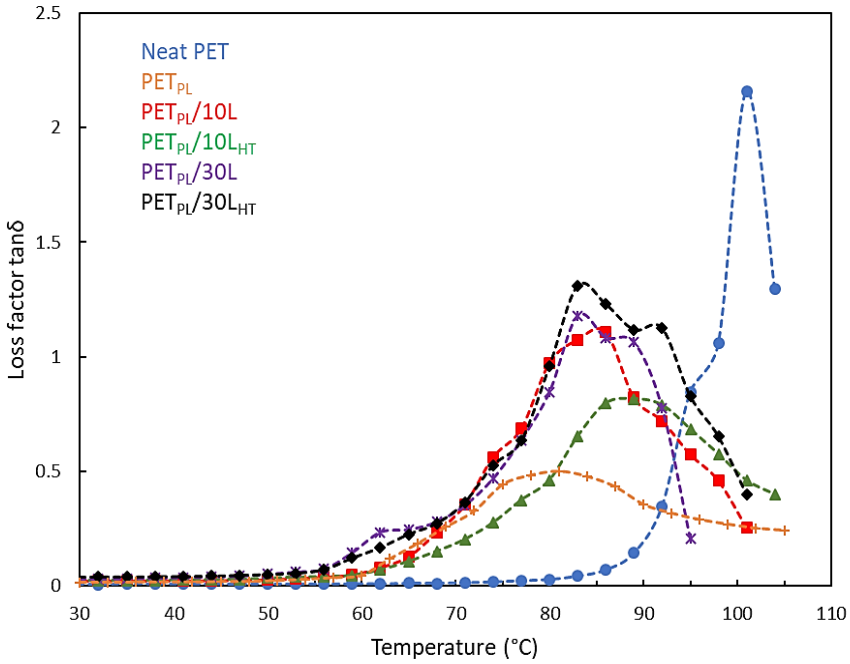

Figure 4-5. Loss tangent peak of PET, plasticized PET and its derived blends with L and LHT at in different compositions at 10 Hz frequency.

Table 4-3. Temperatures corresponding to the loss tangent peak (T_g) at different frequencies from the dynamic mechanical analysis, and the activation energy (E_a) associated with thermal relaxation at T_g.

	Neat PET		PET_{PL}		$PET_{PL}/10L$		$PET_{PL}/10L_{HT}$		$PET_{PL}/30L$		$PET_{PL}/30L_{HT}$	
log *f* (Hz)	T_g (°C)	E_a (KJ/mol)	T_g (°C)	E_a (KJ/mol)	T_g (°C)	E_a (KJ/mol)	T_g (°C)	E_a (KJ/mol)	T_g (°C)	E_a (KJ/mol)	T_g (°C)	E_a (KJ/mol)
0	92		70		71		74		80		83	
1	101	404	81	270	86	180	89	200	98	195	101	198
2	104		87		98		98		104		107	

In thermoplastic matrix-lignin systems, compatibility and dispersion of lignin are desired for enhanced mechanical properties [32]. Often, partial or full miscibility help improve the properties of the blends. Our results show some level of affinity between the L lignin and PET. However, such interactions are improved when L_{HT} is used. Miscibility could have been increased by raising the melt-mixing temperature, but that approach would degrade the lignin, cause its charring and subsequent phase separation during shear mixing. Viscous heating is another cause of lignin degradation during melt-mixing. Thus, rheological behaviors of the components and the blends are important. Ultimately, the process depends on the molecular structures of the components. Therefore, differences in lignin molecular structure are expected to affect rheological behaviors of the resulting polymer blends.

Influence of lignin molar structure on flow characteristics of the PET blends is illustrated in Figure 4-6. The angular frequency (ω) dependence of the complex viscosity (η*) and the storage modulus (G') were used to study flow characteristics of neat PET, its plasticized blend at 10 wt. % plasticizer amount (PET_{PL}), and its lignin derived blends at high-lignin-loading (30 wt. %) at reference temperatures of 240°C and 250°C. Plasticization outcome is clear as the viscosity decreased at both temperatures with increasing frequency. The materials stiffness at 240°C is higher compared to its stiffness at 250°C (Figure 4-6c and d). Addition of lignin further decreases the viscosity and the storage modulus at both reference temperatures, suggesting a role of viscous oligomeric lignin on plasticization of the PET. Interestingly, the blend with thermally treated lignin ($PET_{PL}/30L_{HT}$) has higher viscosity and storage modulus than the as-received lignin blend ($PET_{PL}/30L$). As discussed earlier, this is due to the homogenous dispersion of L_{HT} in PET (as shown by microscopy), and possible enhanced interfacial interactions through combination of hydrogen bonding and π-π interaction of lignin with PET chains and restrained chain disentanglement along with retardation of segmental relaxation (in accordance to DMA data around the glass transition temperature T_g of the blends).

Thermogravimetric analysis was used to evaluate thermal degradation behavior of the blends in oxidative atmosphere. Mass loss data collected at 20°C/min scanning rate are shown in Figure C-5 in Appendix C. The results are summarized in Table 4-4. Addition of lignin reduces the temperature corresponding to 5% mass loss (T_i) and the onset temperature (T_d) but increases the derivative weight peak temperature. Addition of lignin improves net degradation of the blends and confirms the effect of thermal treatment of lignin on the thermal stability of the blends. L_{HT} blend is marginally more stable at higher temperatures than the L blend. Additionally, mass at 500°C increased with the addition of lignin showing the protective effect of lignin at higher temperatures.

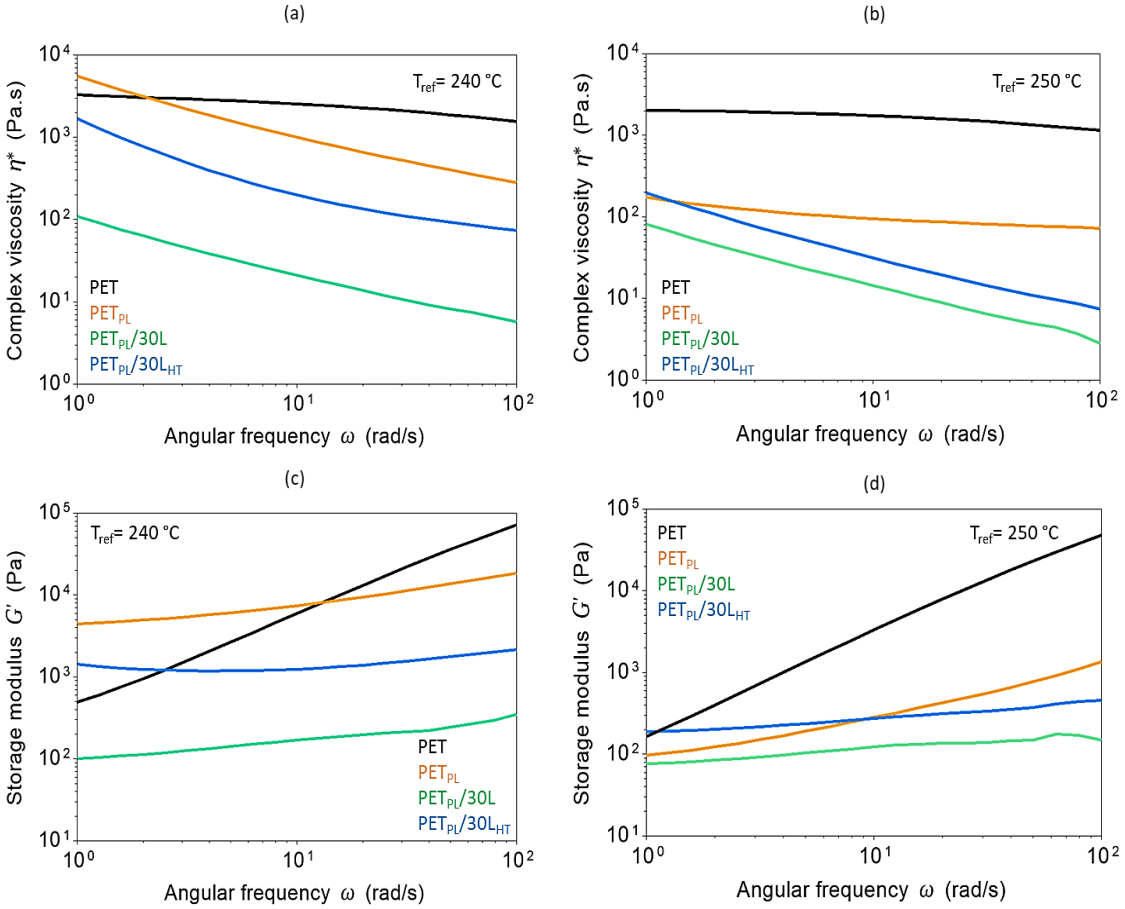

Figure 4-6. Frequency-dependent complex viscosity (η*) at Tref = 240°C (a) and 250°C (b) and Frequency-dependent storage modulus (G') at Tref = 240°C (c) and 250°C (d) of recycled PET, its plasticized resin (PET_{PL}), and its lignin-derived blends (PET_{PL}/30L and PET_{PL}/30L_{HT}).

Table 4-4. Thermal degradation parameters of neat PET, PET_{PL}/30L and PET_{PL}/30 L_{HT}.

	PET	PET_{PL}/30L	PET_{PL}/30L_{HT}
5% weight loss Temp. T_i (°C)	391	290	303
Onset temperature Td (°C)	400	388	390
DTG peak temperature (°C)	436	438	440
Mass at 300°C (%)	99.9	93.9	95.3
Mass at 500°C (%)	14.3	27.1	27.6

4.4. Conclusion

We have successfully demonstrated that lignin dispersion and interfacial interaction can be controlled in recycled PET/lignin alloys through thermal pretreatment of lignin. The addition of renewable plasticizer at 10 wt.% relative to PET helped to soften PET below it normal processing temperature to avoid further degradation of lignin during mixing. Thermal treatment of lignin decreases the aliphatic hydroxyl group, minimizes lignin-lignin intermolecular interactions and improves lignin thermal stability. Relative tensile failure stress of lignin-PET alloys with respect to that of the PET matrix (σ_c/σ_m) improves by 15% (from 0.49 to 0.56) by thermal pretreatment of lignin for the composition with 30 wt. % lignin. Computed interfacial interaction of the dispersed lignin with the PET matrix improves significantly from 0.79 to 1.21 when thermally pretreated lignin is used. This clearly shows that combined interactions (hydrogen bonding and π electron interactions) are enhanced after heat treatment of lignin. Dynamic mechanical analysis and rheology study confirm balanced interactions between the PET and heat-treated lignin as oligomeric lignin is known to enhance chain disentanglement (shear thinning) and restrain segmental motion resulting increased T_g. Our formulations use lignin, a low-cost renewable resource, post-industrial PET waste destined for landfills, and renewable plasticizer TOFA, a low-priced byproduct from pulping industries to develop a renewable alloy with well dispersed lignin domain and moderate mechanical performance. This work highlights development of renewable thermoplastics based on lignin and sustainable industrial waste PET, offering a path for high-volume utilization of lignin in a value-added form.

ACKNOWLEDGMENTS

This project is supported by the Sun Grant Initiative and by Agriculture and Food Research Initiative Competitive Grant no. 2014-38502-22598 from the USDA National Institute of Food and Agriculture and by the USDA National Institute of Food and Agriculture, Hatch project 1012359. N.A.N. acknowledges support from the U.S. Department of Energy (DOE), Office of Energy Efficiency and Renewable Energy, BioEnergy Technologies Office Program for the rheological analysis of the materials. A.K.N. acknowledges support from the Laboratory Directed Research and Development Program of Oak Ridge National Laboratory, managed by UT-Battelle, LLC, for the US Department of Energy.

References

1. Yearley, S., *Environmental Social Science and the Distinction between Resource Use and Industrial Pollution: Reflections on an International Comparative Study.* Ambiente & Sociedade, 2005. **8**: p. 11-26.
2. Koltun, P., *Materials and Sustainable Development.* Progress in Natural Science: Materials International, 2010. **20**: p. 16-29.
3. Mohsin, M.A., T. Abdulrehman, and Y. Haik, *Reactive Extrusion of Polyethylene Terephthalate Waste and Investigation of Its Thermal and Mechanical Properties after Treatment.* International Journal of Chemical Engineering, 2017. **2017**: p. 10.
4. Ochi, T., S. Okubo, and K. Fukui, *Development of Recycled PET Fiber and its Application as Concrete-Reinforcing Fiber.* Cement and Concrete Composites, 2007. **29**(6): p. 448-455.
5. Dehghan, Z. and A. Modarres, *Evaluating the Fatigue Properties of Hot Mix Asphalt Reinforced by Recycled PET Fibers Using 4-point Bending Test.* Construction and Building Materials, 2017. **139**: p. 384-393.
6. Pawlak, A., et al., *Recycling of Postconsumer Poly(ethylene terephthalate) and High-Density Polyethylene by Compatibilized Blending.* Journal of Applied Polymer Science, 2002. **86**(6): p. 1473-1485.
7. Burillo, G., et al., *Compatibilization of Recycled and Virgin PET with Radiation-oxidized HDPE.* Radiation Physics and Chemistry, 2002. **63**(3): p. 241-244.
8. Taghavi, S.K., H. Shahrajabian, and H.M. Hosseini, *Detailed Comparison of Compatibilizers MAPE and SEBS-g-MA on the Mechanical/thermal Properties, and Morphology in Ternary Blend of Recycled PET/HDPE/MAPE and Recycled PET/HDPE/SEBS-g-MA.* Journal of Elastomers & Plastics, 2018. **50**(1): p. 13-35.
9. Fang, C., et al., *Effect of Multi-Walled Carbon Nanotubes on the Physical Properties and Crystallisation of Recycled PET/TPU Composites.* RSC Advances, 2018. **8**(16): p. 8920-8928.
10. Kadla, J.F. and S. Kubo, *Lignin-based Polymer Blends: Analysis of Intermolecular Interactions in Lignin–Synthetic Polymer Blends.* Composites Part A: Applied Science and Manufacturing, 2004. **35**(3): p. 395-400.
11. Kubo, S. and J.F. Kadla, *Lignin-based Carbon Fibers: Effect of Synthetic Polymer Blending on Fiber Properties.* Journal of Polymers and the Environment, 2005. **13**(2): p. 97-105.
12. Canetti, M. and F. Bertini, *Supermolecular Structure and Thermal Properties of Poly(ethylene terephthalate)/Lignin Composites.* Composites Science and Technology, 2007. **67**(15): p. 3151-3157.
13. Chaudhari, A., J.D. Ekhe, and S. Deo, *Non-isothermal Crystallization Behavior of Lignin-Filled Polyethylene Terepthalate (PET).* International Journal of Polymer Analysis and Characterization, 2006. **11**(3): p. 197-207.

14. Jeong, H., et al., *Use of Acetylated Softwood Kraft Lignin as Filler in Synthetic Polymers.* Fibers and Polymers, 2012. **13**(10): p. 1310-1318.
15. Kim, S., et al., *Potential of a Bio-disintegrable Polymer Blend using Alkyl-chain-Modified Lignin.* Fibers and Polymers, 2015. **16**(4): p. 744-751.
16. Agafitei, G.E., et al., *Polyester/lignosulfonate Blends with Enhanced Properties.* Die Angewandte Makromolekulare Chemie, 1999. **267**(1): p. 44-51.
17. Monteil-Rivera, F. and L. Paquet, *Solvent-Free Catalyst-Free Microwave-Assisted Acylation of Lignin.* Industrial Crops and Products, 2015. **65**: p. 446-453.
18. Maldhure, A.V., A.R. Chaudhari, and J.D. Ekhe, *Thermal and Structural Studies of Polypropylene Blended with Esterified Industrial Waste Lignin.* Journal of Thermal Analysis and Calorimetry, 2011. **103**(2): p. 625-632.
19. Balakshin, M. and E. Capanema, *On the Quantification of Lignin Hydroxyl Groups With 31P and 13C NMR Spectroscopy.* Journal of Wood Chemistry and Technology, 2015. **35**(3): p. 220-237.
20. Guerra, A., et al., *Comparative Evaluation of Three Lignin Isolation Protocols for Various Wood Species.* Journal of Agricultural and Food Chemistry, 2006. **54**(26): p. 9696-9705.
21. Hosseinaei, O., et al., *Role of Physicochemical Structure of Organosolv Hardwood and Herbaceous Lignins on Carbon Fiber Performance.* ACS Sustainable Chemistry & Engineering, 2016. **4**(10): p. 5785-5798.
22. Tran, C.D., et al., *A New Class of Renewable Thermoplastics with Extraordinary Performance from Nanostructured Lignin-Elastomers.* Advanced Functional Materials, 2016. **26**(16): p. 2677-2685.
23. Bova, T., et al., *An Approach Towards Tailoring Interfacial Structures and Properties of Multiphase Renewable Thermoplastics from Lignin-Nitrile Rubber.* Green Chemistry, 2016. **18**(20): p. 5423-5437.
24. Kim, J.-Y., et al., *Investigation of Structural Modification and Thermal Characteristics of Lignin after Heat Treatment.* International Journal of Biological Macromolecules, 2014. **66**: p. 57-65.
25. Constant, S., et al., *New Insights into the Structure and Composition of Technical Lignins: a Comparative Characterisation Study.* Green Chemistry, 2016. **18**(9): p. 2651-2665.
26. Zhang, Y., et al., *Heat Treatment of Industrial Alkaline Lignin and its Potential Application as an Adhesive for Green Wood–Lignin Composites.* ACS Sustainable Chemistry & Engineering, 2017. **5**(8): p. 7269-7277.
27. Kadla, J.F., et al., *Lignin-based Carbon Fibers for Composite Fiber Applications.* Carbon, 2002. **40**(15): p. 2913-2920.
28. Pouteau, C., et al., *Lignin–Polymer Blends: Evaluation of Compatibility by Image Analysis.* Comptes Rendus Biologies, 2004. **327**(9): p. 935-943.

29. Turcsanyi, B., B. Pukanszky, and F. Tudos, *Composition Dependence of Tensile Yield Stress in Filled Polymers.* Journal of Materials Science Letters, 1988. **7**(2): p. 160-162.
30. Fekete, E., B. Pukánszky, and Z. Peredy, *Mutual Correlations between Parameters Characterizing the Miscibility, Structure and Mechanical Properties of Polymer Blends.* Die Angewandte Makromolekulare Chemie, 1992. **199**(1): p. 87-101.
31. Szabó, G., et al., *Competitive Interactions in Aromatic Polymer/Lignosulfonate Blends.* ACS Sustainable Chemistry & Engineering, 2017. **5**(1): p. 410-419.
32. Akato, K., et al., *Poly(ethylene oxide)-Assisted Macromolecular Self-Assembly of Lignin in ABS Matrix for Sustainable Composite Applications.* Acs Sustainable Chemistry & Engineering, 2015. **3**(12): p. 3070-3076.

Appendix C

Detailed GPC Analysis

GPC was performed for both L and L_{HT} lignins using a Tosoh EcoSEC gel permeation chromatography (GPC) system with a refractive index (RI) detector equipped with a flow reference cell. Prior to measurements, lignin was dissolved in THF at a concentration of 1 mg/mL and filtered using a 0.22 µm membrane. The instrument and reference cell flow rates were set to 0.35 mL/min and the analysis was performed at 40 °C. Sample injections of 10 µL were separated using two consecutive Tosoh TSKgel SuperMultiporeHZ-M analytical columns (4.6 mm I.D., 150 mm length, 5 µm particle size) and a TSKgel SuperMultiporeHZ-M guard column using a total run time of 15 min. Evaluation of the number-average molecular weight (M_n), weight-average molecular weight (M_w) and their ratio (PDI) was complete using in-house polystyrene standard curves in the range of 600-7.5×10^6 Da.

^{31}PMNR

Table C-1 *Assignment of hydroxyl groups peaks in ^{31}P NMR spectroscopy.*

Sample name/ mmol per g lignin	Assignments, δ (ppm)
Aliphatic OH	150-146
S-OH condensed	144.5-143.5
S-OH non-condensed	143.5-142.25
G-OH condensed	142.25-141
G-OH non-condensed	141-138.5
H-OH	138.5-136.5
COOH	136-133.5

2D $^{1}H-^{13}C$ HSQC NMR

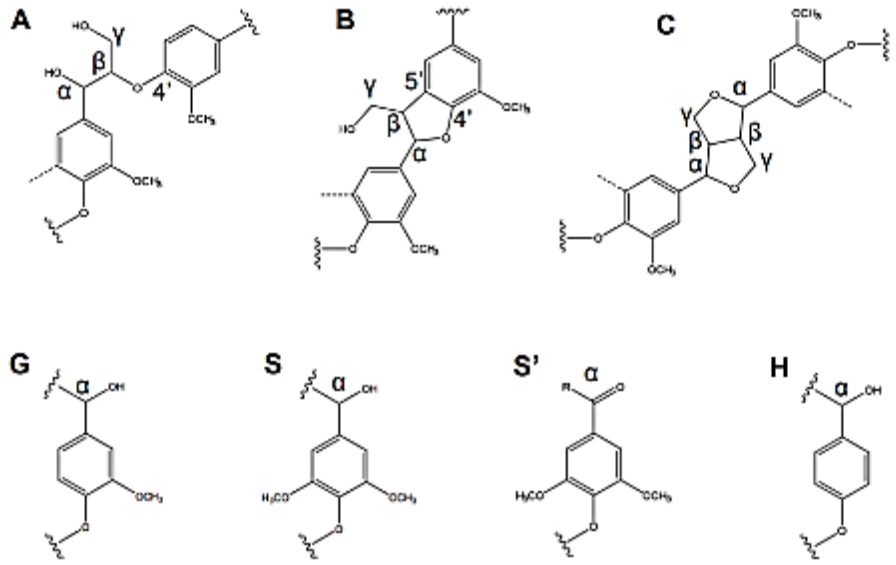

Figure C-1. Lignin substructures detected by 2D HSQC NMR. (A) β-O-4'; (B) β-5' (phenylcoumaran structure); (C) β-β' (resinol structures); (G) guaiacylpropane unit; (S) syringyl propane unit; (S') syringyl propane unit with carbonyl at Cα; (H) p-hydroxyphenolpropane unit [1].

Table C-2. ^{13}C and ^{1}H assignments of the lignin signals in 2D HSQC spectra [2].

Label	δC/δH (ppm)	Assignment
B_β	53.1/3.4	C_β−H_β in phenylcoumaran substructures (B)
C_β	53.5/3.1	C_β−H_β in β−β′ resinol substructures (C)
−OCH3	55.6/3.73	C−H in methoxyls
A_γ	59.4/3.4 and 3.7	C_γ−H_γ in γ− hydroxylated β-O- 4′ substructures (A)
I_γ	61/4.1	C_γ−H_γ in cinnamyl alcohol end-groups (I)
B_γ	63.4/3.6	C_γ−H_γ in phenylcoumaran substructures (B)
Hk_γ	67.5/4.2	C_γ−H_γ in Hibbert ketone structuresb
C_γ	71.2/4.2	C_γ−H_γ in β−β′ resinol substructures (C)[b]
A_α	71.9/4.9	C_α−H_α in β-O-4′ substructures (A)
X_2	73/3.1	C_2−H_2 in xylan substructures (X)
X_3	74/3.3	C_3−H_3 in xylan substructures (X)
X_4	75.7/3.5	C_4−H_4 in xylan substructures (X)
A_β	80.4/4.5, 84.4/4.4 and 85.6/4.2	C_β−H_β in β-O-4’ substructures (A)
$A_{ox}\beta$	83/5.2	C_β−H_β in α-oxidized β-O-4′ substructures (Aox)
C_α	85.5/4.6	C_α−H_α in β−β′ resinol substructures (C)
B_α	87.7/5.5	C_α−H_α in phenylcoumaran substructures (B)
T_8	94.4/6.6	C_8−H_8 in tricin units (T)
T_6	99.5/66.2	C_6−H_6 in tricin units (T)
$T_{2,6}$	104.5/7.4	C_2−H_2 and C6-H6 in tricin units (T)
$S_{2,6}$	104.2/6.7	C_2−H_2 and C6−H6 in syringyl units (S)
T_3	107/7.2	C_3−H_3 in tricin units (T)
$S'_{2,6}$	107.4/7.4	C_2−H_2 and C6−H6 in syringyl units with α oxidization(S’)
G_2	110.2/6.9	C_2−H_2 in guaiacyl units (G)
Fa_2	111.5/7.3	C_2−H_2 in ferulate (Fa)
G_5/G_6	115/6.7 and 119.7/6.8	C_5−H_5 and C6−H6 in guaiacyl units (G)
Fa_6	123.1/7.1	C_6−H_6 in ferulate (Fa)
HMF	123.6/7.5	C_3− H_3 in 5-O-substituted furfurals -like units
$St_{\alpha,\beta}$	126.6/6.9	C_α−H_α and C_β−H_β in stilbene structures (St)
$H_{2,6}$	128.2/7.2	$C_{2,6}$−$H_{2,6}$ in p-hydroxyphenyl units (H)
I_α	130.6/6.3	C_α−H_α in cinnamyl alcohol end-groups (I)
$Pca_{2,6}$	130.1/7.5	C_2−H_2 and C_6−H_6 in p-coumarate (Pca)
$Pb_{2,6}$	131.6/7.7	C_2−H_2 and C_6−H_6 in p-benzoate (Pb)
HMF	179/9.6	C_α−H_α in 5-O-substituted furfurals -like units

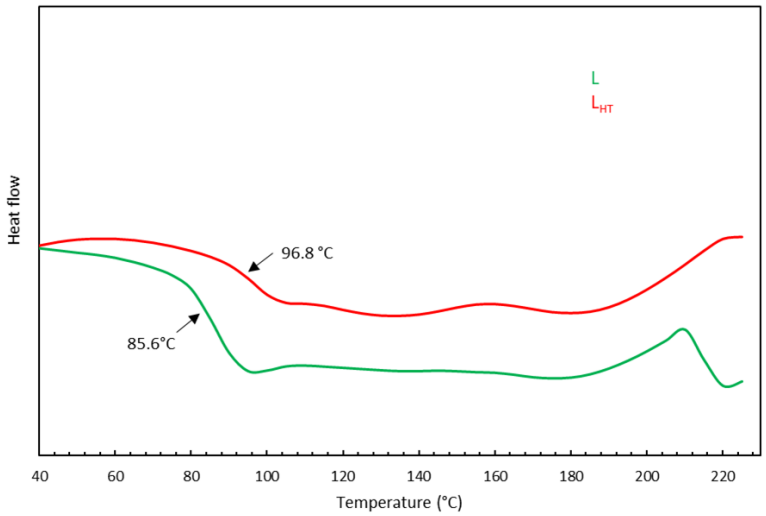

Figure C-2 DSC thermograms of L and L_{HT} in nitrogen atmosphere showing the glass transition temperatures T_g.

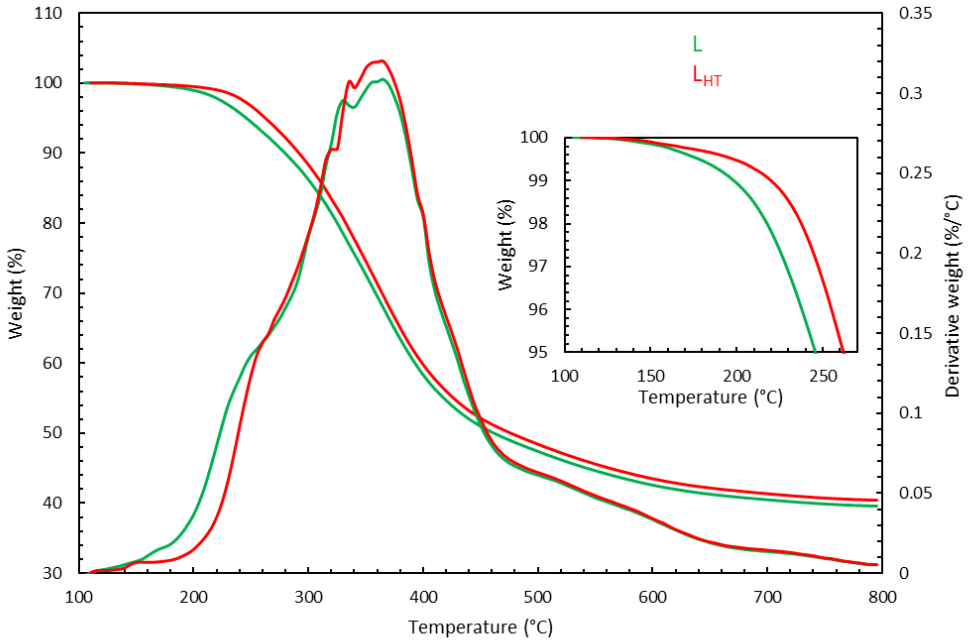

Figure C-3. TGA and derivative weight thermograms of L and L_{HT} in nitrogen atmosphere showing the effect of thermal treatment on lignin thermal stability.

Table C-3 Thermal behavior temperatures, calorimetric values, and degree of crystallinity of PET and it lignin derived blends.

Samples	T_m (°C) [a]	ΔH_m (J/g) [a]	T_{rec} (°C)	ΔH_{rec} (J/g)	X_c (%) [b]
PET	247	46	208	53	57
PET_{PL}	239	41	202	49	23
PET_{PL}/10L	237	33	209	44	23
PET_{PL}/20L	232	32	203	39	31
PET_{PL}/30L	229	29	198	33	30
PET_{PL}/$10L_{HT}$	236	36	208	41	30
PET_{PL}/$20L_{HT}$	233	29	203	38	23
PET_{PL}/$30L_{HT}$	231	24	199	32	20

[a] Values obtained from second heating curves [b] Computed using first heating curves

The degree of crystallinity (χ_c) was computed using the first heating curves information and applying the following equation.

$$\chi_c = \frac{\Delta H_m}{W_f \times \Delta H_{100}} \times 100\% \quad \text{(S1)}$$

where ΔH_m is the melting enthalpy from the first heating curve, W_f is the PET weight fraction in each composition and ΔH_{100} is the theoretical fusion enthalpy of 100% crystalline PET (140 J/g) [3]

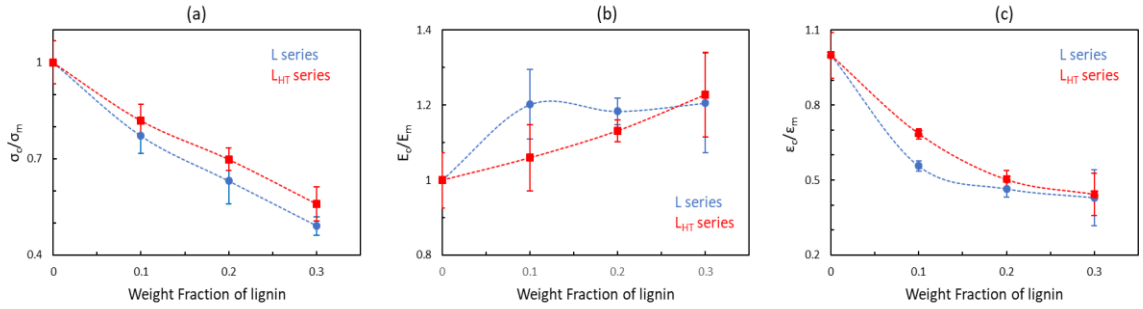

Figure C-4. Ratios of tensile strength (a), tensile modulus (b), and ultimate elongation (c) of lignin-loaded matrices over those of neat PET at different lignin concentrations.

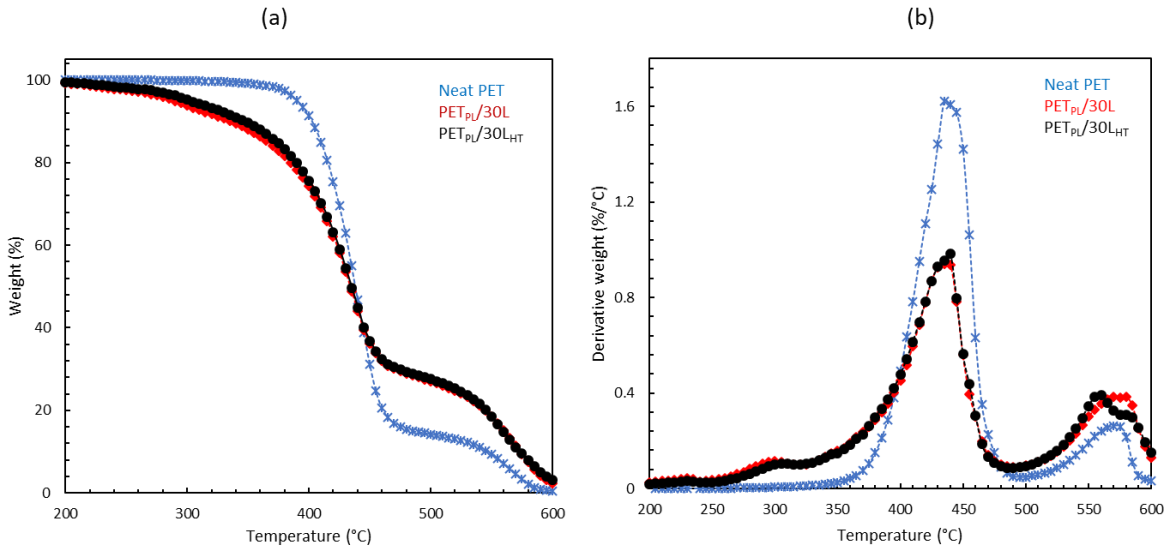

Figure C-5. Thermal decomposition of PET and it lignin derived blends at 30 wt.% lignin contents in oxidative atmosphere at 20°C/min.

1. Nguyen, N.A., et al., *An Acrylonitrile–Butadiene–Lignin Renewable Skin with Programmable and Switchable Electrical Conductivity for Stress/Strain-Sensing Applications.* Macromolecules, 2018. **51**(1): p. 115-127.
2. Constant, S., et al., *New insights into the structure and composition of technical lignins: a comparative characterisation study.* Green Chemistry, 2016. **18**(9): p. 2651-2665.
3. Blaine, R.L., *Thermal Applications Note. TN048 Polymer Heats of Fusion, TA Instruments New Castle, DE.*

CHAPTER 5
INFLUENCE OF LIGNIN FUNCTIONALITIES ON INTERMOLECULAR INTERACTIONS IN POLYLACTIC ACID BLENDS

This chapter is based on the manuscript prepared for submission to a peer review journal. The full list of authors includes Kokouvi Akato, Ngoc A. Nguyen, Kalavathy Rajan, Stephen Chmely, David P. Harper, and Amit K. Naskar. Kokouvi Akato performed all experiments, processed and analyzed all data, and prepared the manuscript for submission. Ngoc A. Nguyen assisted with thermal characterization. Kalavathy Rajan and Stephen Chmely helped with NMR data collection and analysis. David P. Harper assisted with DMA and editing the manuscript. Amit K. Naskar assisted with data analysis, writing and editing of the manuscript.

Abstract

Lignin structure is highly dependent on its botanical source and isolation methodology. Selecting an appropriate lignin structure and functionality for a preferred host matrix remains a significant challenge in designing thermoplastic-lignin alloys with superior performance. Properties of the blends strongly depend on the interactions between the components. Herein, we aim to understand the effect of source-dependent complex lignin structure on the molecular interactions and relaxation dynamics in a biodegradable polyester, polylactic acid (PLA) matrix. Three lignins isolated from oak, pine, and wheat exhibit their signature chemical profiles and compositions. The results show that the lignins are different in term of molar mass, purity, thermal stability and composition. Their PLA-derived blends' properties correlate to the lignin features. Hardwood lignin, with the highest purity and the lowest aliphatic hydroxyl content, when blended with PLA at 30 wt.% lignin exhibits tensile strength of 43 MPa and stain at break of 5%, a respective net retention of 67% and 74% of neat PLA performance. The performance deteriorates significantly when thermally least stable wheat straw lignin was used with PLA for thermal shear mixing. Dynamic mechanical analysis showed that the glass transition behavior and activation energy E_a of the blend are mostly dependent on the T_g of the used lignin.

KEYWORDS: lignin chemistry, PLA, thermal stability, chain dynamics, renewable polymer blends

5.1. Introduction

New value-added polymeric materials are being formulated from blends of renewable-sourced lignin and existing thermoplastics (either biodegradable or not) to compete with petroleum-derivative counterparts. It is envisaged that the renewable plastics would replace fossil fuel-derived materials in all application fields [1]. Desired amalgamation of lignin in the blend formulations has so far been a challenge as most systems show diminishing trend in tensile properties as function of lignin loading due to lack of compatibility and poor dispersion [2].

To overcome the drawback, fundamental researches has been focused on modifying the lignin-polymer interface through chemical alteration [3] or assistance of compatibilizers [4, 5] to promote interchain interactions and thus to improve adhesion and dispersion. The extra step is cost-intensive and creates chemical wastes. In parallel, low-loading of lignin is often used (less than 20 wt. %) in the systems [6]. Lignin is known as a renewable, low-cost by-product of pulp and biofuel production. High-volume loading of lignin is desired to widen the commercials applications of the new blends and surge widespread valorization of lignin, which is still considered as a waste or cheap source for power for the industries that extract it.

The most significant problem that hampers tailoring new class thermoplastic-lignin materials is related to lack of homogeneity in accessible (industrial or technical) lignins and the complexity of lignin chemistry. Lignin is a “class” or “group” of polyaromatic molecules with functionalities that differ by biomass source and isolation method [7, 8]. An example of lignin’s variability was highlighted in a recent study where the severity of fractionation changed the architectural and physicochemical properties of lignin from the same botanical source [9]. In parallel, lignin’s complex chemical structure is also a significant bottleneck in the preparation of polymer/lignin blends; additionally, it is difficult to predict the properties of the blends. Structural units found in various lignin botanical sources are shown in Figure 5-1. For instance, the p-coumaryl alcohol, which is low in hardwood and softwood lignin, is chiefly present in lignin from herbaceous crops, such as straws and grasses. Softwood lignin from gymnosperms, is almost exclusively comprised of coniferyl alcohol, and hardwood lignin from angiosperms is made of varying ratios of both coniferyl and sinapyl alcohol. Adding to this variation and complexity, functional units such as hydroxyl, methoxyl and carbonyl, arrangement balances lignin’s polarity [10]. Therefore, understanding the functional group profile from each biomass species or introduced by the separation method is critical for industrialization of new thermoplastic-lignin materials.

Success in development of new polymeric materials that are cost-effective and readily accessible to all industries, not only relies on lignin chemistry but also on choice of polymer host matrices. The goal is to develop thermoplastics for rigid applications. Soft rubber matrix [11-13], acrylonitrile butadiene styrene (ABS) [5], polyethylene [14, 15], and polystyrene [16] have all been extensively evaluated in that regard. Polyamides and polyesters were reported to be more compatible with lignin because they can have hydrogen bonding with lignin hydroxyl groups [6]. This motivates us to choose polylactic acid (PLA) for this study as PLA is a polyester derived from renewable resources. PLA use in industrial applications has grown recently as it is easy to process, full biodegradable and biocompatible, and possesses a combination of high tensile strength and modulus [17]. Numerous studies of PLA/lignin blends have been reported. The results were mixed as some researchers claimed immiscibility [18, 19] while other reported homogenous single-phase blends [20]. Technical lignins used in these reports

are Kraft softwood that was methanol fractionated, Indulin AT pine Kraft lignin, and cellulolytic enzyme lignin. It is evident that the results were affected by the variability of

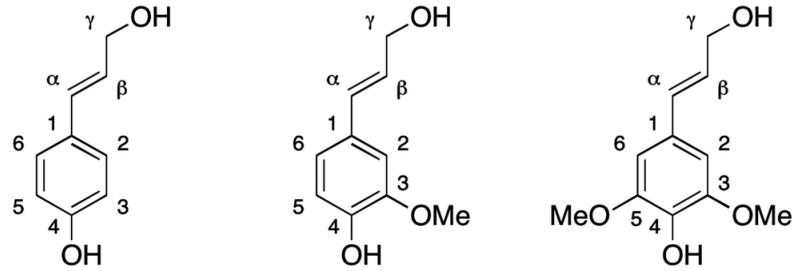

Figure 5-1 . Phenylpropanoid monomers of lignin: p-coumaryl (H-type), coniferyl (G-type), and sinapyl (S-type) alcohols [11].

the lignin and likelihood that each has distinct chemical functionality that participates in the molecular interactions with the host matrix. Lignin functional groups were mentioned or discussed in these systems but barely investigated in detail and quantified.

The goal of this work was to study the molecular interactions in blends of PLA and three technical lignins from different botanical sources and means of extraction. To meet this goal blends at high-lignin-loading (30 wt. %) were prepared to understand lignin's chemical profiles and their effect on the proprieties of the blends. Organosolv lignin from hardwood (OLH), methanol fractionated Kraft softwood lignin (MKS) and methanol fractionated organic acid fractionated wheat straw lignin (MOW) were used in this study. These fractionated lignins are also melt processable. The functional groups composition was characterized by ^{31}P and 2D $^{1}H-^{13}C$ heteronuclear single quantum coherence (HSQC) NMR for each lignin. The results help to elucidate structural features of each lignin and the potential of molecular interaction with the PLA matrix.

5.2. Experimental section

5.2.1. Materials.

General purpose PLA 4043D was obtained from NatureWork LLC, USA. It has a melt flow rate of 6g/10 min at 210 °C at 2.16 kg applied force. Its relative viscosity measured at 1.0 g/dL in chloroform at 30°C is 4. The PLA was dried in vacuum at 80°C for 4 hours. Experimental Alcell hardwood lignin (OLH) produced by organosolv extraction was used. Experimental grades of Kraft softwood lignin and organic acid pulped wheat straw lignin were further modified with methanol fractionation in this study [21]. Only the methanol soluble fractions of the Kraft softwood lignin (MKS) and the organic wheat straw lignin (MOW) were used. The lignins were dried at 60°C overnight under vacuum before blending with PLA.

5.2.2 Lignin characterization.

All three lignins (OLH, MKS, and MOW) were characterized using Gel permeation chromatography (GPC) to evaluate molecular weight and molecular weight distribution. Small fractions of the lignin were dissolved in THF for the analysis. Details of the analysis are reported in Appendix D. Functional groups were characterized and quantified by ^{31}P and 2D $^{1}H-^{13}C$ HSQC NMR spectroscopy using preparation and analysis methods previously reported [9, 22, 23]. The degree of lignin purity was obtained as the sum of acid soluble lignin constituent and Klason lignin which represent the acid-insoluble content. The detail of this procedure is reported somewhere else.[24].

5.2.3 Blend preparation and compression molding.

PLA and each technical lignin were melt-mixed at 30 wt. % lignin loading at 180°C. A Haake MiniLab co-rotating twin extruder (Thermo Scientific) with screw length of 110 mm was used at screw rotation speed of 30 rpm. The extrudates were compression molded in rectangular mold using a Carver Hydraulic press at 180°C. Predetermined amount of the extrudate was placed in a rectangular mold and pressed for 5 minutes before cooling at 10°C/minute.

5.2.4. Thermal analyses.

A Differential scanning calorimeter (DSC Q2000, TA Instruments) was used to determine the thermal properties of the samples. Samples with mass of approximatively 3-4 mg each were loaded in hermetically sealed pans for measurements. A cycle of heating-cooling-heating from -80°C to 300°C at 10°C/min and an isothermal of 2 min after first heating were used. Thermogravimetry was used to study degradation of the lignin under oxidative atmosphere from room temperature to 800°C after a short drying step. Dynamic mechanical thermal analysis of the blends was performed in an Pyris Diamond DMA (Perkin Elmer) using a three-point bending fixture at 2°C/min and amplitude set to 10 micrometers. The specimen size was 34 mm × 9.35 mm × 2.75 mm.

5.2.5. Tensile testing and morphology analysis.

Rectangular specimens for tensile testing were prepared by compression molding. The specimens were cut to dog-bone shape based on ASTM D 638 type V and tested on an Instron 5567 coupled with Bluehill software. The strain rate was 1 mm/min. The reported results are average data of six measurements. The tensile and cryogenically fractured surfaces of the specimens were evaluated by Zeiss EVO MA 15 scanning electron microscope. The surfaces were coated with a thin gold layer before SEM imaging and images were acquired at 20 KV.

5.3. Results and discussion

5.3.1. Survey of lignins variability.

The characteristics of the organosolv hardwood lignin (OLH) and the two-alcohol fractionated lignins (MKS, and MOW) are reported in Table 5-1. The results show distinctive architectural and physicochemical properties that are direct consequences of the pulping method and wood species. For example, OLH produced from organosolv pulping process without addition of catalyst, has the highest purity between the three lignins. Extraction method is known to significantly alter the chemical structure of lignin mainly due to the differential degrees of cleavage of β-O-4 linkages present in lignin [25, 26]. It is suggested that lignin purity, structural features, thermal behavior, and molar mass distribution are valuable for choosing a lignin suitable for melt-blending with thermoplastics, in this case PLA. 2D ^{1}H-^{13}C heteronuclear single quantum coherence (HSQC) has been used recently to elucidate ether linkages units and aromatic substructures that are helpful for evaluation of processability and degradability of lignin. 2D NMR spectra of the lignins used in this present work are shown in Figure 5-2. The spectra were divided into two regions: an aliphatic oxygenated side chain region (δ_C/δ_H 50-90/2.5-6) and an aromatic region (δ_C/δ_H 90-145/6-8). Peaks assignments and substructures are summarized in Appendix D (Table D-2 and Figure D-3). The purity of the lignin was all higher than 97% except MOW due to the presence of low molecular weight insoluble moieties such as sugars. The aliphatic hydroxyl and carboxylic acid contents in MOW are significantly higher than the other samples. Their values were 3.19 mmol/g and 1.47 mmol/g, respectively.

5.3.2 Thermal stability.

Thermal stability of lignin is very important for incorporation in thermoplastics to avoid lignin charring during blend preparation. Additionally, lignin must exhibit melt-processability or malleability for efficient dispersion in a blend. In Figure 5-3, there is a slight weight loss for all lignins up to 180°C due to slow evaporation of moistures or residual solvents. Decomposition of lignin starts with dehydration which eliminates the side chain OH groups. The main mass loss starts at 200°C with MOW dropping at faster rate with a large shoulder. This can be reconciled with the abundance of aliphatic groups and carboxylic acids in MOW and potential sugars. It is reported that early decomposition in lignin is due to decay of aliphatic groups, carboxylic acids, and volatilization of low-molecular weight phenols [27, 28].

2D HSQC NMR spectra reveal difference in chemical features of all three lignins (Figure 5-2). The results are in accordance to the lignin biomass sources as the hardwood lignin OLH is expected to have abundant S G groups. For example, S units are observed at cross-peaks corresponding to $C_{2,6}$-$H_{2,6}$ correlations in C_α-oxidized S' units at δ_C/δ_H 107.4/7.4 ($S'_{2,6}$) and $C_{2,6}$-$H_{2,6}$ correlations in S units at δ_C/δ_H 104.2/6.7 ($S_{2,6}$). The G units are observed at cross-peaks corresponding to C_2-H_2 correlations in guaiacyl units at δ_C/δ_H

110.2/6.9 (G_2); C_5-H_5 correlations at δ_C/δ_H 115/6.7 (G_5) and C_6-H_6 correlations at δ_C/δ_H 119.7/6.8 (G_6), respectively. Softwood lignin MKS has G units mainly and wheat straw lignin MOW has cross-peaks corresponding to S and G and H units. MOW has signature units such as $C_{2,6}$-$H_{2,6}$ correlations in p-coumarate acid at δ_C/δ_H 130.1/7.5 ($PCA_{2,6}$) and at δ_C/δ_H 128.2/7.2 (PCA_α) that are not present in the other two lignins. The spectra reveal substantial number of methylene-bridged subunits connected via β-O-4, β-β, β-5 and other linkages that are bridged in the α, β, and γ sites. Quick reduction of mass for MOW at ~ 200°C can be associated with the H unit (δ_C/δ_H 130.1/7.5) representing esterified hydroxymethyl groups decomposition. The MOW could have a higher content of less thermally stable compounds, which explain its broad first derivative (DTG) thermogram peak. Above 300°C, decomposition is marked by fragmentation of interunit linkages, condensation of aromatic rings and charring. Additionally, MKS has large amount of G unit (Figure 5-2d) that are susceptible to condense during thermal degradation [27]. That explains the high peak DTG thermogram at 378°C. In all three lignins, MOW is the least stable followed by MKS and OLH.

Table 5-1. Isolation method, content in hydroxyl groups quantified by ^{31}P NMR, Average molar mass indexes measured by GPC of the lignins used for blending with PLA.

		Hardwood (OLH)	Softwood (MKS)	Wheat straw (MOW)
Isolation method		Organosolv process	Kraft process /Solvation in MeOH [a]	Organic acid process/solvation in MeOH [a]
Purity (%)		98.3	97.2	84.1
T_g (°C) [b]		86	97	81
T_{flow} (°C) [c]		163	176	
^{31}P NMR (mmol g^{-1})				
Aliphatic -OH		2	2.85	3.19
S-OH	C	0.39	0.89	0.58
	NC	2.46	0.69	0.92
G-OH	C	0.8	1.41	0.41
	NC	1.79	3.68	1.58
H-OH		0.42	0.45	0.58
Total phenolic-OH		5.86	7.12	4.07
Total -OH group		7.86	9.97	7.26
Carboxylic acids		0.45	1.05	1.47
GPC indexes (g mol^{-1})				
M_n		890	810	972
M_w		1486	1082	1236
PDI		1.67	1.34	1.27
ash content (%)		0.3	0.3	0.3

[a] Solvation in methanol processed in our laboratory [b] T_g computed by DSC measurements
[c] Measured from melting point tester

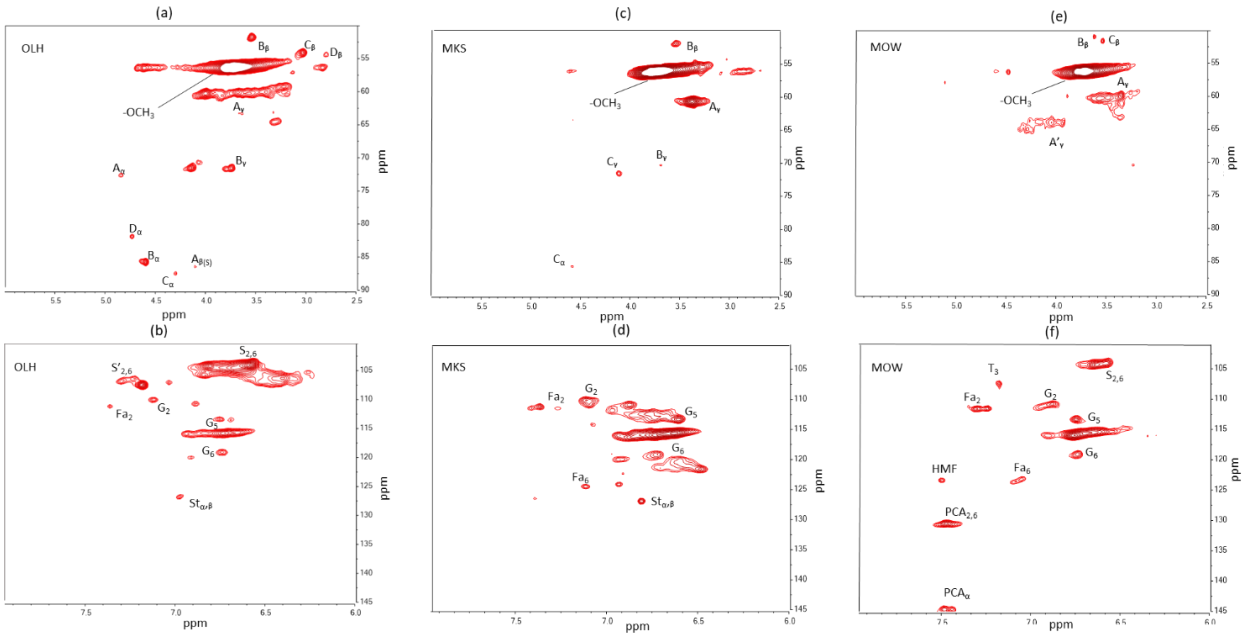

Figure 5-2. Oxygenated Aliphatic side chain (δ_C/δ_H = 50-90/2.5-6) and aromatic (δ_C/δ_H = 100-145/6-8) regions of 2D NMR heteronuclear single quantum coherence HSQC spectra of OLH, MKS, MOW lignins.

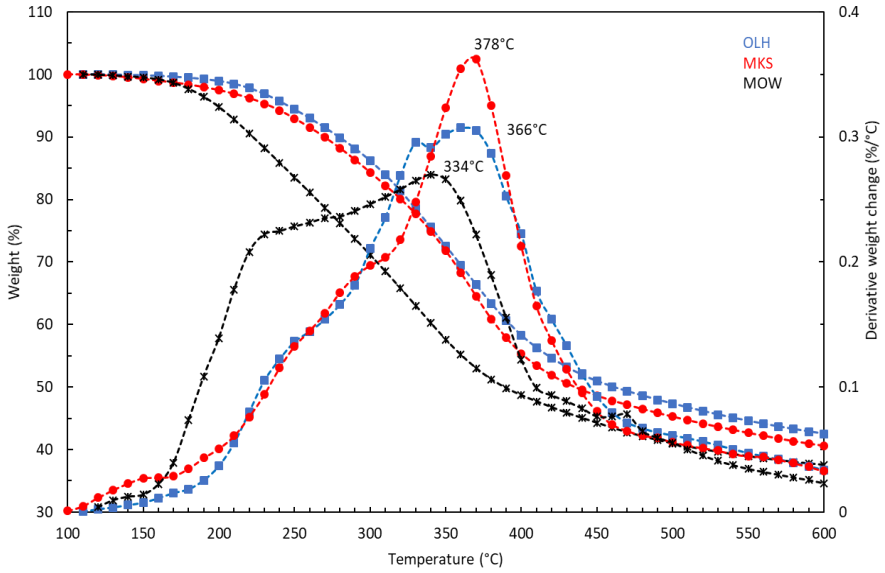

Figure 5-3. TGA and derivative weight change (DTG) thermograms in nitrogen atmosphere of OLH, MKS, MOW lignins.

The data in Appendix D (Figure D-4) show TGA and first derivative (DTG) thermograms of PLA, each lignin and their blends. PLA has the highest degradation temperature. Addition of lignin reduced the degradation temperature. As expected PLA-MOW was the least thermally stable. Weight reduction temperatures recorded at 5% weight loss ($T_{5\%}$) were: PLA 320°C, PLA-OLH 300°C, PLA-MKS 303°C, and PLA-MOW 280°C. $T_{5\%}$ was higher for PLA-MKS blend due to the high phenolic OH content (MKS > OLH > MOW) compared to the other two PLA-lignin blends. This demonstrates the thermal stabilization attributes of MKS due to the scavenging nature of abundant phenolic groups.

As discussed earlier, abundance of aliphatic OH and carboxylic acids and their early decomposition products lead to unstable MOW lignin. During melt-blending, MOW released volatiles due to the high impurity content and created large pores throughout the extrudates. Thermal degradation of the blends can be correlated to hydrogen bonding interactions between the PLA and each lignin. Superior interaction through hydrogen bonding and fine dispersion of lignin domain could help with thermal stabilization. For example, Kraft lignin has been reported to improve thermal stability of PLA. In that scope, blend containing acetylated lignin exhibited enhanced interfacial bonding due to reduction of hydroxyl groups during esterification. The overall thermal stability of the PLA and acetylated lignin was better that the unmodified lignin blend [29]. Surprisingly, PLA-MOW showed the opposite, and this is mainly due to purity issue and thermal instability of the MOW. MOW has the lowest total phenolic-OH (4.07 $mmol.g^{-1}$) and total-OH group (7.26 $mmol.g^{-1}$) content between all 3 lignins.

5.3.3. Mechanical properties.

Amalgamation of lignin in thermoplastic often results in poor mechanical properties. This is due to poor dispersion and poor interaction between the lignin and the host matrix. Tensile properties of PLA were measured as, tensile strength = 63 MPa, tensile modulus = 1.1 GPa, and elongation = 6.9, which decreased with lignin addition in all cases (Figure 5-4). The tensile modulus does not change significantly with addition of lignin and is not shown in Figure 5-2, (values are reported in Appendix D Tables D-3). Failure strength decreases with addition of lignin at 30 wt. % but the PLA-OLH blend show better property followed by PLA-MKS, and PLA-MOW, which has the least failure strength (24 MPa). Lignin features, quantitatively shown in Table 5-1 and associated degradation and porosity in the composition appears to be responsible for the reduction of the tensile properties.

OLH has higher polydispersity index PDI = 1.67. Number average molecular weights in three lignin are comparable; however, M_w value follows the following trend: OLH > MOW > MKS. We can conclude that MeOH solvation process extracts soluble low-molecular weight fractions present in MKS and MOW and these 100% MeOH soluble fractions and are of difference sizes compared to the original lignins. Same observations of low molecular weight were reported by Saito [21]. The effect of molecular weight is expected to be minimal as all three lignins have M_n in the same range. Solubility of lignin in THF, solvent used for GPC, is limited which could have affected our results. Recommendation suggests that acetylated lignin dissolves entirely in THF and will provide results that represent the complete molar mass distribution profile of the samples. For these reason, the reduction in mechanical properties cannot be correlated with the molar mass distribution. Nonetheless, use of low molecular weight lignin is important for its effective dispersion in PLA matrix.

Mechanical properties can, however, be reconciled with the aliphatic hydroxyl group content. Tensile strength and elongation decreased with increasing aliphatic OH. The ^{31}P NMR spectra of the lignin are shown in figure D-2 (Appendix D). From table 5-1, OLH has the lowest amount of OH (2 mmol g^{-1}) compared to the other lignins and it has better mechanical properties in all the PLA-lignin blends. Aliphatic -OH groups are known for thermal dehydration and thus its minimal presence helps to avoid lignin degradation during melt-mixing. A comparison of the ratio of phenolic OH to aliphatic OH obtained by ^{31}P NMR (Table 5-1), indicates highest ratio for OLH. Additionally, phenolic ether linkages remain thermally stable although it gets involved with thermal stabilization reactions. Nonetheless, the higher aliphatic OH in MOW can be correlated to poor mechanical properties of its blend with PLA. Also, high content of aliphatic OH translates to strong lignin-lignin intermolecular interactions which makes MOW unstable, difficult to disperse. Lignin intermolecular interactions compete with PLA and MOW interactions and strongly affect the blend properties. The lignin-lignin intermolecular hydrogen bonding needs to be

controlled to enhance the interfacial interactions between PLA and leading to fine dispersion of lignin phase and production of blends without deteriorating performances.
Microscopy analysis of tensile fracture surfaces reveals that overall the lignins were well dispersed throughout the blends creating a single-phase material through hydrogen bonding of lignin OH and PLA ester group (Figure 5-5). However, there is evidence of random areas that contained large lignin agglomeration (Appendix D Figure D-5) that could have affected mechanical performance of the blends. The size of the aggregates varies from 1 to 30 microns depending on the lignin. This agglomeration is due to poor mixing, and the fact that short mixing time was preferred to avoid lignin degradation. OLH blend exhibit the largest lignin agglomerations. Mechanical shear during melt-blending may have helped to break the lignin macromolecules down; hence, smaller particles were observed for MOW in comparison to PLA-OLH and PLA-MKS blends. SEM reveals that MOW particles are on the surface as the other two lignin particles are embedded in the matrices.
Porosity in PLA-MOW are also believed to affect the mechanical properties. MOW was found to have the highest carboxylic acid content (MOW > MKS > OLH) and its blend has large pores from volatile degassing. During compression molding, volatiles evolved from decarboxylation of carboxylic acids and units associated with H group representing esterified hydroxymethyl groups decomposition as confirmed in TGA results (large shoulder of DTG starting around ~ 170°C). This effectively forms a foam structure in the PLA-MOW blends that further degrades material strength. Residual sugar can also be suspected for such low temperature unstable characteristic.

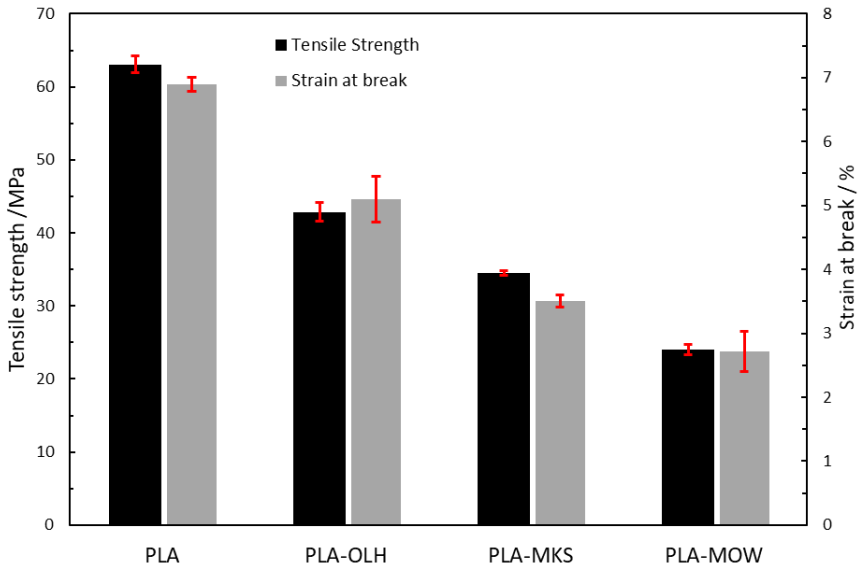

Figure 5-4. Bar chart shows the tensile strength and elongation at break of PLA and its lignin derived blends.

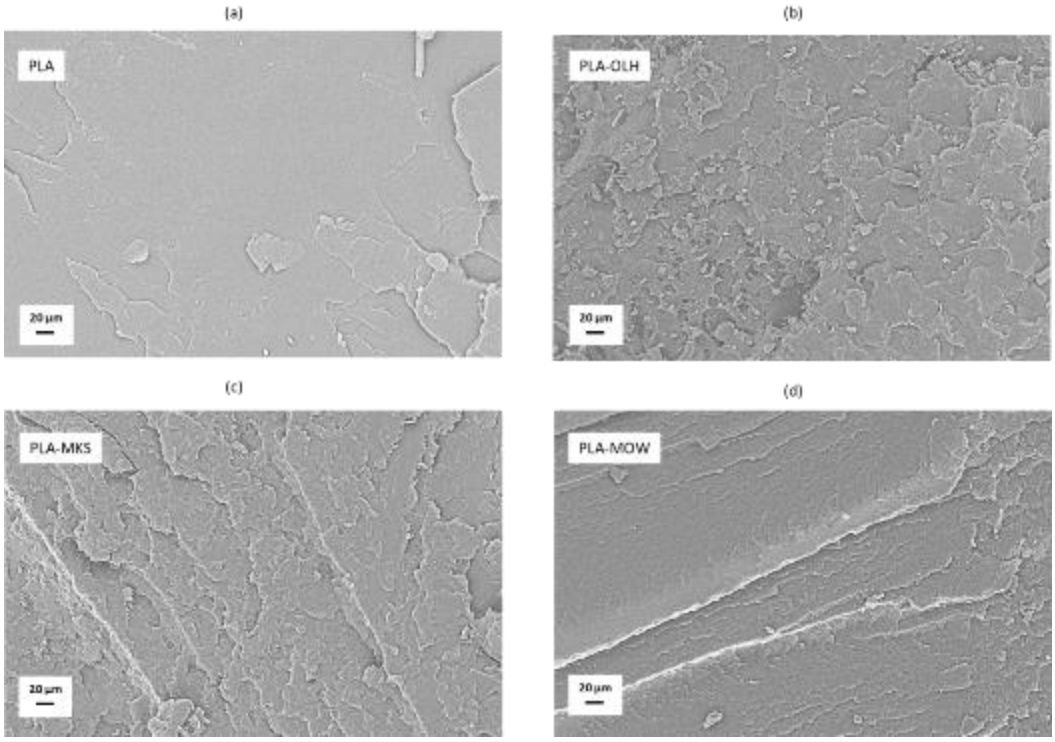

Figure 5-5. Micrographs of tensile fractured surfaces the samples. (a) PLA, (b)PLA-OLH, (c) PLA-MKS and (d) PLA-MOW showing the samples fracture pattern and single-phase blends.

5.3.4. Glass transition behavior and activation energy for thermal relaxation.

Glass transition temperature T_g is a very important parameter in processing of materials. From Table 5-1, MOW had the lowest glass transition determined by DSC (81°C). T_g of the as-received lignin was found to 172°C [12]. Methanol fractionation reduced T_g of lignin that were methanol extracted (MKS and MOW). High glass transition temperature in the as-received lignin is due to condensed rigid phenolic moieties and strong lignin-lignin intermolecular interactions. Same observation was made for MKS as the methanol soluble fraction MKS has T_g =97°C. MKS is found to have the highest condensed S and G units in the lignin which explains the high T_g observed even after fractionation.
In thermoplastic/lignin blend, glass transition temperatures are profoundly influenced by polymer-lignin interactions. Figure 5-6 depicts the loss factor (tan δ) as a function of temperature. Addition of lignin shifts T_g (peak maximum) to lower temperature but only one T_g was observed for all 3 lignins blends suggesting intermolecular hydrogen bonding between PLA ester and lignin OH potentially lead to coupling of motion at the molecular level which lead to single T_g and lone segmental (α) relaxation. Neat PLA T_g was found to be 66°C, however, it decreased to 59°C with addition of MOW. The storage modulus E and loss modulus E" as function of temperature are shown in Appendix D (Figure D-6). The modulus at low temperature is high for PLA-OLH compared to other blends. PLA-MOW has the lowest modulus. In fact, attempt to anneal the blends at 80°C in vacuum before DMA measurements shows foaming of PLA-MOW. The sample was needed to be pressed again. As discussed earlier MOW has low molecular weight thermally unstable moieties that were volatilizing at temperatures just above T_g of the matrix.
The loss factor data was linearly fitted with the following Arrhenius equation to evaluate the activation energy E_a associated with the α-relaxation in the blends using the absolute temperature (*T)* at which the loss maximum is observed at frequency (*f)*, the gas constant (*R)*, and an arbitrary constant (*K*).

$$\log f = \frac{-E_a}{(2.303RT)} + \log K \qquad (1)$$

Results in Table 5-2 show that the activation energy is dependent of the lignin used for the blend. Depending on the lignin type, E_a either increased or decreased. PLA-OLH has the lower activation energy for relaxation compared to neat PLA suggesting plasticization effect. PLA-MOW has comparable activation energy to that of neat PLA. Surprisingly, PLA-MKS show an increase of E_a and had the highest T_g. MKS lignin may be hindering chain mobility around T_g thus increase in E_a. MKS has high noncondensed G units in the lignin which indicate less steric hindrance around the phenolic hydroxyl and higher reactivity. This could suggest that it can interact and couple with PLA chains and reduce mobility around T_g.

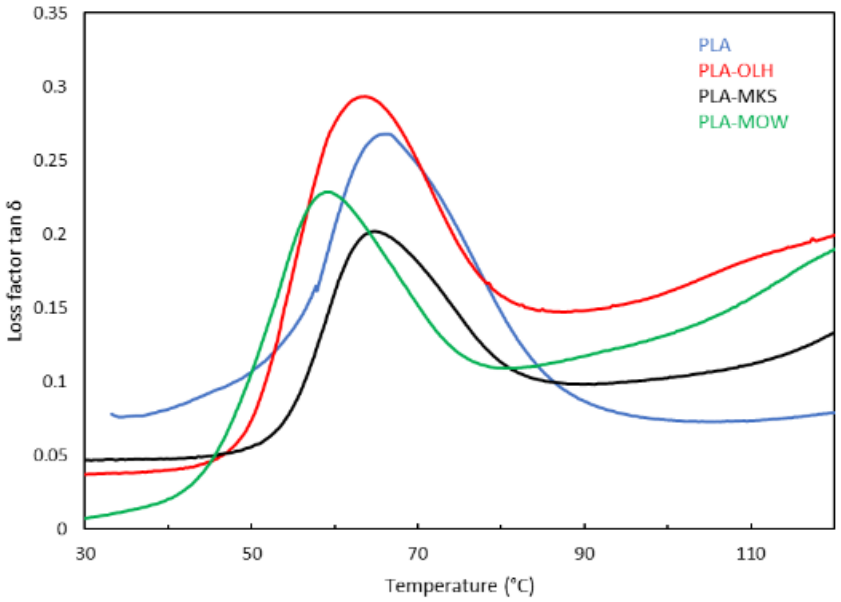

Figure 5-6.The loss factor tan δ of PLA and its lignin derived blends at 1 Hz in the α-relaxation region.

*T*able D-2. Temperatures corresponding to the loss tangent peak (T_g) at different frequencies from the dynamic mechanical analysis, and the activation energy (E_a) associated with thermal relaxation at T_g.

	PLA		PLA-OLH		PLA-MKS		PLA_MOW	
log *f*	T_g (°C)	E_a (KJ/mol)	T_g (°C)	E_a (KJ/mol)	T_g (°C)	E_a (KJ/mol)	T_g (°C)	E_a (KJ/mol)
1.3	72.1		69.2		70.8		64.9	
1.0	70.3		68.0		69.0		63.4	
0.6	68.8	499	66.5	478	67.2	520	61.3	495.0
0.3	67.2		64.9		66.0		60.4	
0.0	66.4		63.7		64.7		59.4	

5.4. Conclusion

We studied the interactions of three technical lignins with polylactic acid (PLA) matrix. First, lignin molecular weight and softening points were normalized by adopting alcohol-based fractionation of soluble lignin stream from two technical sources. Aliphatic and carboxylic acid groups decomposition affect thermal stability of the PLA-lignin blends. Mechanical properties were reduced from neat PLA. PLA-MOW had the lowest properties due to foam structures it developed during compression molding from decomposition of carboxylic acid and H units around the mixing temperatures. Microscopy analysis revealed that PLA and the lignins developed single-phase blends through hydrogen bonding, but random areas of large lignin agglomeration were observed due to poor mixing and short mixing time. These areas reduced mechanical properties of the blends as well. Other characteristics such as purity, foaming due to thermally unstable low molecular weight content created defects that affected the properties of the blends. This study can help to establish a library of available lignin and work with lignin manufacturers to deliver homogeneous consistent lignin for thermoplastic-lignin development toward lignin valorization.

ACKNOWLEDGMENTS

This project is supported by the Sun Grant Initiative and by Agriculture and Food Research Initiative Competitive Grant no. 2014-38502-22598 from the USDA National Institute of Food and Agriculture and by the USDA National Institute of Food and Agriculture, Hatch project 1012359. N.A.N. and A.K.N. acknowledges support from the U.S. Department of Energy (DOE), Office of Energy Efficiency and Renewable Energy, BioEnergy Technologies Office Program for the rheological analysis of the materials.

References

1. Dessbesell, L., et al., *Forest Biomass Supply chain Optimization for a Biorefinery Aiming to Produce High-Value Bio-Based Materials and Chemicals from Lignin and Forestry Residues: a Review of Literature.* Canadian Journal of Forest Research, 2016. **47**(3): p. 277-288.
2. Wu, W., et al., *Lignin Valorization: Two Hybrid Biochemical Routes for the Conversion of Polymeric Lignin into Value-added Chemicals.* Scientific Reports, 2017. **7**(1): p. 8420.
3. Laurichesse, S. and L. Avérous, *Chemical modification of lignins: Towards biobased polymers.* Progress in Polymer Science, 2014. **39**(7): p. 1266-1290.
4. Sailaja, R.R.N., *Low Density Polyethylene and Grafted Lignin Polyblends using Epoxy-Functionalized Compatibilizer: Mechanical and Thermal Properties.* Polymer International, 2005. **54**(12): p. 1589-1598.
5. Akato, K., et al., *Poly(ethylene oxide)-Assisted Macromolecular Self-Assembly of Lignin in ABS Matrix for Sustainable Composite Applications.* ACS Sustainable Chemistry & Engineering, 2015. **3**(12): p. 3070-3076.
6. Pouteau, C., et al., *Lignin–Polymer Blends: Evaluation of Compatibility by Image Analysis.* Comptes Rendus Biologies, 2004. **327**(9): p. 935-943.
7. Obst, J.R. and T.K. Kirk, *Isolation of Lignin*, in *Methods in Enzymology*. 1988, Academic Press. p. 3-12.
8. Hosseinaei, O., et al., *Improving Processing and Performance of Pure Lignin Carbon Fibers through Hardwood and Herbaceous Lignin Blends.* International Journal of Molecular Sciences, 2017. **18**(7).
9. Hosseinaei, O., et al., *Role of Physicochemical Structure of Organosolv Hardwood and Herbaceous Lignins on Carbon Fiber Performance.* ACS Sustainable Chemistry & Engineering, 2016. **4**(10): p. 5785-5798.
10. Feldman, D. and D. Banu, *Interactions in poly(vinyl chloride)–lignin blends.* Journal of Adhesion Science and Technology, 2003. **17**(15): p. 2065-2083.
11. Bova, T., et al., *An Approach Towards Tailoring Interfacial Structures and Properties of Multiphase Renewable Thermoplastics from Lignin-Nitrile Rubber.* Green Chemistry, 2016. **18**(20): p. 5423-5437.
12. Tran, C.D., et al., *A New Class of Renewable Thermoplastics with Extraordinary Performance from Nanostructured Lignin-Elastomers.* Advanced Functional Materials, 2016. **26**(16): p. 2677-2685.
13. Barana, D., et al., *Influence of Lignin Features on Thermal Stability and Mechanical Properties of Natural Rubber Compounds.* ACS Sustainable Chemistry & Engineering, 2016. **4**(10): p. 5258-5267.
14. Dehne, L., et al., *Influence of Lignin Source and Esterification on Properties of Lignin-Polyethylene Blends.* Industrial Crops and Products, 2016. **86**: p. 320-328.

15. Maldhure, A.V. and J.D. Ekhe, *Effect of Modifications of Lignin on Thermal, Structural, and Mechanical Properties of Polypropylene/Modified Lignin Blends.* Journal of Thermoplastic Composite Materials, 2015. **30**(5): p. 625-645.
16. Reza Barzegari, M., et al., *Mechanical and Rheological Behavior of Highly Filled Polystyrene with Lignin.* Polymer Composites, 2012. **33**(3): p. 353-361.
17. Jamshidian, M., et al., *Poly-Lactic Acid: Production, Applications, Nanocomposites, and Release Studies.* Comprehensive Reviews in Food Science and Food Safety, 2010. **9**(5): p. 552-571.
18. Chen, R., et al., *Biobased Ternary Blends of Lignin, Poly(Lactic Acid), and Poly(Butylene Adipate-co-Terephthalate): The Effect of Lignin Heterogeneity on Blend Morphology and Compatibility.* Journal of Polymers and the Environment, 2014. **22**(4): p. 439-448.
19. Rahman, M.A., et al., *Biocomposites Based on Lignin and Plasticized Poly(L-lactic acid).* Journal of Applied Polymer Science, 2013. **129**(1): p. 202-214.
20. Ouyang, W., et al., *Poly(Lactic Acid) Blended with Cellulolytic Enzyme Lignin: Mechanical and Thermal Properties and Morphology Evaluation.* Journal of Polymers and the Environment, 2012. **20**(1): p. 1-9.
21. Saito, T., et al., *Methanol Fractionation of Softwood Kraft Lignin: Impact on the Lignin Properties.* ChemSusChem, 2014. **7**(1): p. 221-228.
22. Guerra, A., et al., *Comparative Evaluation of Three Lignin Isolation Protocols for Various Wood Species.* Journal of Agricultural and Food Chemistry, 2006. **54**(26): p. 9696-9705.
23. Balakshin, M. and E. Capanema, *On the Quantification of Lignin Hydroxyl Groups With 31P and 13C NMR Spectroscopy.* Journal of Wood Chemistry and Technology, 2015. **35**(3): p. 220-237.
24. Sluiter A., *Determination of Structural Carbohydrates and Lignin in Biomass Laboratory Analytical Procedure (LAP) : issue date, 4/25/2008*, Editor. 2008, National Renewable Energy Laboratory: Golden, Colo.
25. Bouxin, F.P., et al., *Catalytic Depolymerisation of Isolated Lignins to Fine Chemicals using a Pt/alumina Catalyst: Part 1-Impact of the Lignin Structure.* Green Chemistry, 2015. **17**(2): p. 1235-1242.
26. Constant, S., et al., *Reactive Organosolv Lignin Extraction from Wheat Straw: Influence of Lewis Acid Catalysts on Structural and Chemical Properties of Lignins.* Industrial Crops and Products, 2015. **65**: p. 180-189.
27. Jakab, E., et al., *Thermogravimetry/Mass Spectrometry Study of Six lignins Within the Scope of an International Round Robin Test.* Journal of Analytical and Applied Pyrolysis, 1995. **35**(2): p. 167-179.
28. Brodin, I., E. Sjöholm, and G. Gellerstedt, *The Behavior of Kraft Lignin during Thermal Treatment.* Journal of Analytical and Applied Pyrolysis, 2010. **87**(1): p. 70-77.

29. Gosselink, R.J.A., et al., *Analytical Protocols for Characterisation of Sulphur-Free Lignin.* Industrial Crops and Products, 2004. **19**(3): p. 271-281.

Appendix D

Detailed GPC Analysis

GPC was performed on all 3 lignins using a Tosoh EcoSEC gel permeation chromatography (GPC) system with a refractive index (RI) detector equipped with a flow reference cell. Prior to measurements, lignin was dissolved in THF at a concentration of 1 mg/mL and filtered using a 0.22 µm membrane. The instrument and reference cell flow rates were set to 0.35 mL/min and the analysis was performed at 40 °C. Sample injections of 10 µL were separated using two consecutive Tosoh TSKgel SuperMultiporeHZ-M analytical columns (4.6 mm I.D., 150 mm length, 5 µm particle size) and a TSKgel SuperMultiporeHZ-M guard column using a total run time of 15 min. Evaluation of the number-average molecular weight (M_n), weight-average molecular weight (M_w) and their ratio (PDI) was complete using in-house polystyrene standard curves in the range of 600-7.5×10^6 Da.

Table D-1. The extraction method, biomass type, melting temperature (T_m) and flow temperature (T_{flow}) determined by hot stage.

Sample ID	Extraction and biomass	T_m (°C)	T_{flow} (°C)
OLH	Organosolv Hardwood mix	157	163
MKS	Kraft Softwood pine/ MeOH extraction	168	176
MOW	Organic acid Wheat straw/ MeOH solvation	111	121

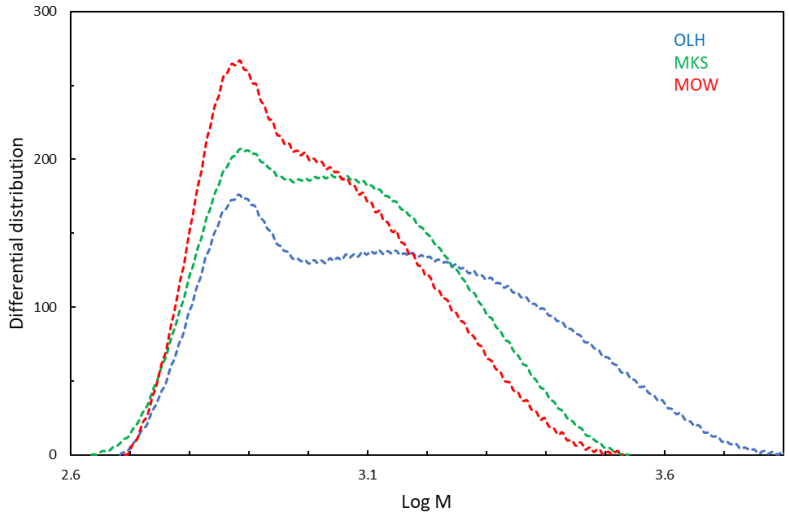

Figure D-1. Molecular weight distribution OLH, MKS and MOW dissolved in THF.

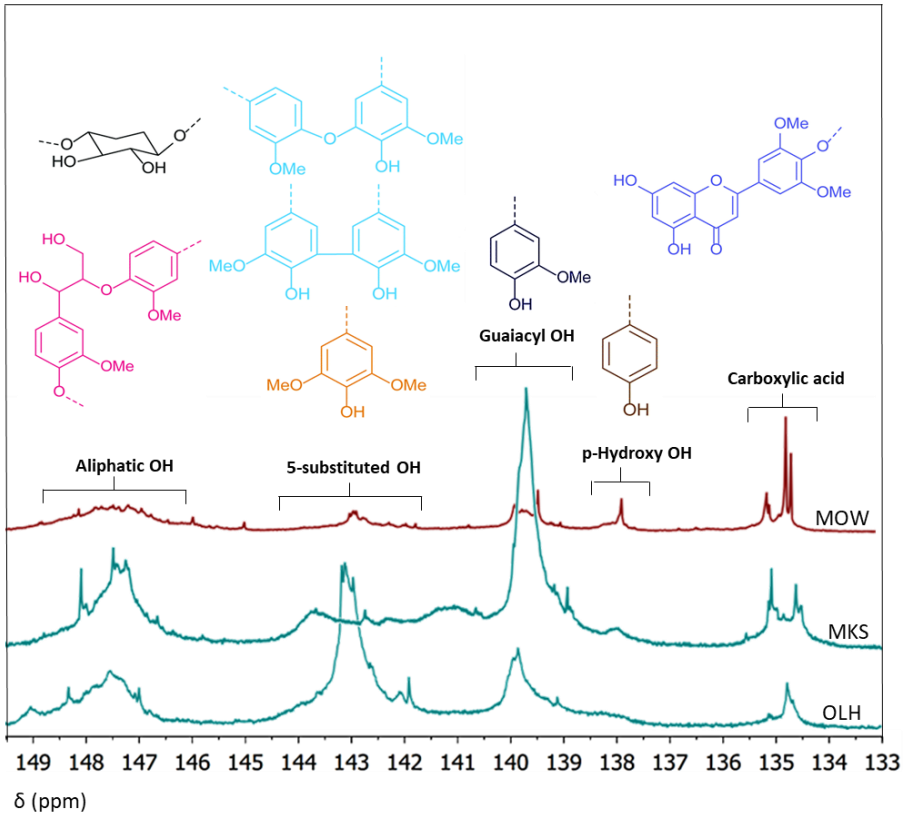

Figure D-2. Functional groups identified by quantitative ^{31}P NMR measurements after phosphorylation the lignins studied.

Table D-2. ^{13}C and ^{1}H assignments of the lignin signals in 2D HSQC spectra.

Label	δC/δH (ppm)	Assignment
B_β	53.1/3.4	C_β−H_β in phenylcoumaran substructures (B)
C_β	53.5/3.1	C_β−H_β in β−β′ resinol substructures (C)
−OCH3	55.6/3.73	C−H in methoxyls
A_γ	59.4/3.4 and 3.7	C_γ−H_γ in γ− hydroxylated β-O- 4′ substructures (A)
I_γ	61/4.1	C_γ−H_γ in cinnamyl alcohol end-groups (I)
B_γ	63.4/3.6	C_γ−H_γ in phenylcoumaran substructures (B)
Hk_γ	67.5/4.2	C_γ−H_γ in Hibbert ketone structuresb
C_γ	71.2/4.2	C_γ−H_γ in β−β′ resinol substructures (C)[b]
A_α	71.9/4.9	C_α−H_α in β-O-4′ substructures (A)
X_2	73/3.1	C_2−H_2 in xylan substructures (X)
X_3	74/3.3	C_3−H_3 in xylan substructures (X)
X_4	75.7/3.5	C_4−H_4 in xylan substructures (X)
A_β	80.4/4.5, 84.4/4.4 and 85.6/4.2	C_β−H_β in β-O-4’ substructures (A)
$A_{ox}\beta$	83/5.2	C_β−H_β in α-oxidized β-O-4′ substructures (Aox)
C_α	85.5/4.6	C_α−H_α in β−β′ resinol substructures (C)
B_α	87.7/5.5	C_α−H_α in phenylcoumaran substructures (B)
T_8	94.4/6.6	C_8−H_8 in tricin units (T)
T_6	99.5/66.2	C_6−H_6 in tricin units (T)
$T_{2,6}$	104.5/7.4	C_2−H_2 and C6-H6 in tricin units (T)
$S_{2,6}$	104.2/6.7	C_2−H_2 and C6−H6 in syringyl units (S)
T_3	107/7.2	C_3−H_3 in tricin units (T)
$S'_{2,6}$	107.4/7.4	C_2−H_2 and C6−H6 in syringyl units with α oxidization(S’)
G_2	110.2/6.9	C_2−H_2 in guaiacyl units (G)
Fa_2	111.5/7.3	C_2−H_2 in ferulate (Fa)
G_5/G_6	115/6.7 and 119.7/6.8	C_5−H_5 and C6−H6 in guaiacyl units (G)
Fa_6	123.1/7.1	C_6−H_6 in ferulate (Fa)
HMF	123.6/7.5	C_3− H_3 in 5-O-substituted furfurals -like units
$St_{\alpha,\beta}$	126.6/6.9	C_α−H_α and C_β−H_β in stilbene structures (St)
$H_{2,6}$	128.2/7.2	$C_{2,6}$−$H_{2,6}$ in p-hydroxyphenyl units (H)
I_α	130.6/6.3	C_α−H_α in cinnamyl alcohol end-groups (I)
$Pca_{2,6}$	130.1/7.5	C_2−H_2 and C_6−H_6 in p-coumarate (Pca)
$Pb_{2,6}$	131.6/7.7	C_2−H_2 and C_6−H_6 in p-benzoate (Pb)
HMF	179/9.6	C_α−H_α in 5-O-substituted furfurals -like units

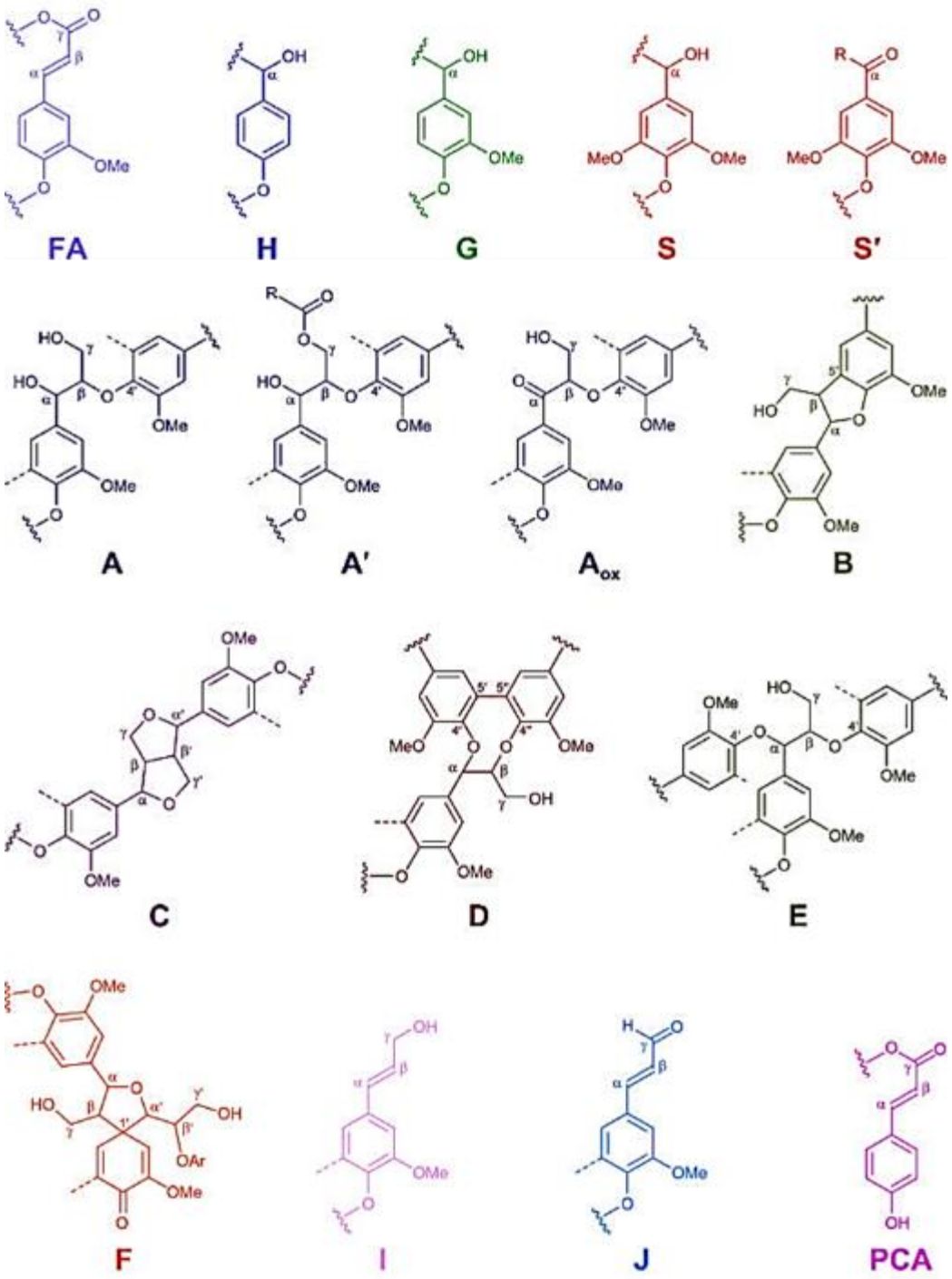

Figure D-3. Major lignin substructures detected by 2D HSQC NMR.

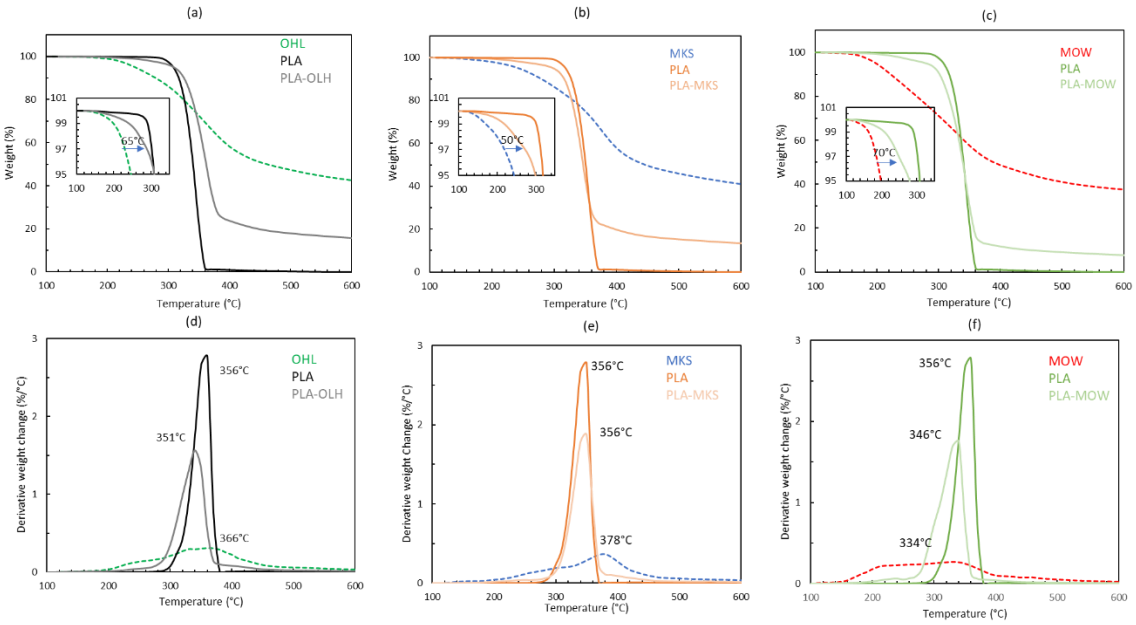

Figure D-4. TGA and DTG of PLA, lignin and PLA-lignin blend of OLH, MKS and MOW

Table D-3. Tensile properties of PLA and its lignin derived blends at 30 wt. % lignin contents [a].

Sample	Tensile Strength (MPa)	Modulus (GPa)	Strain at break (%)
PLA	63 (1.18)	1.1 (0.02)	6.9 (0.11)
PLA-OLH	43 (1.26)	1.1 (0.03)	5.1 (0.36)
PLA-MKS	35 (0.34)	1.2 (0.02)	3.5 (0.10)
PLA-MOW	24 (0.71)	1.1 (0.04)	2.7 (0.31)

[a] Standard deviation in parenthesis

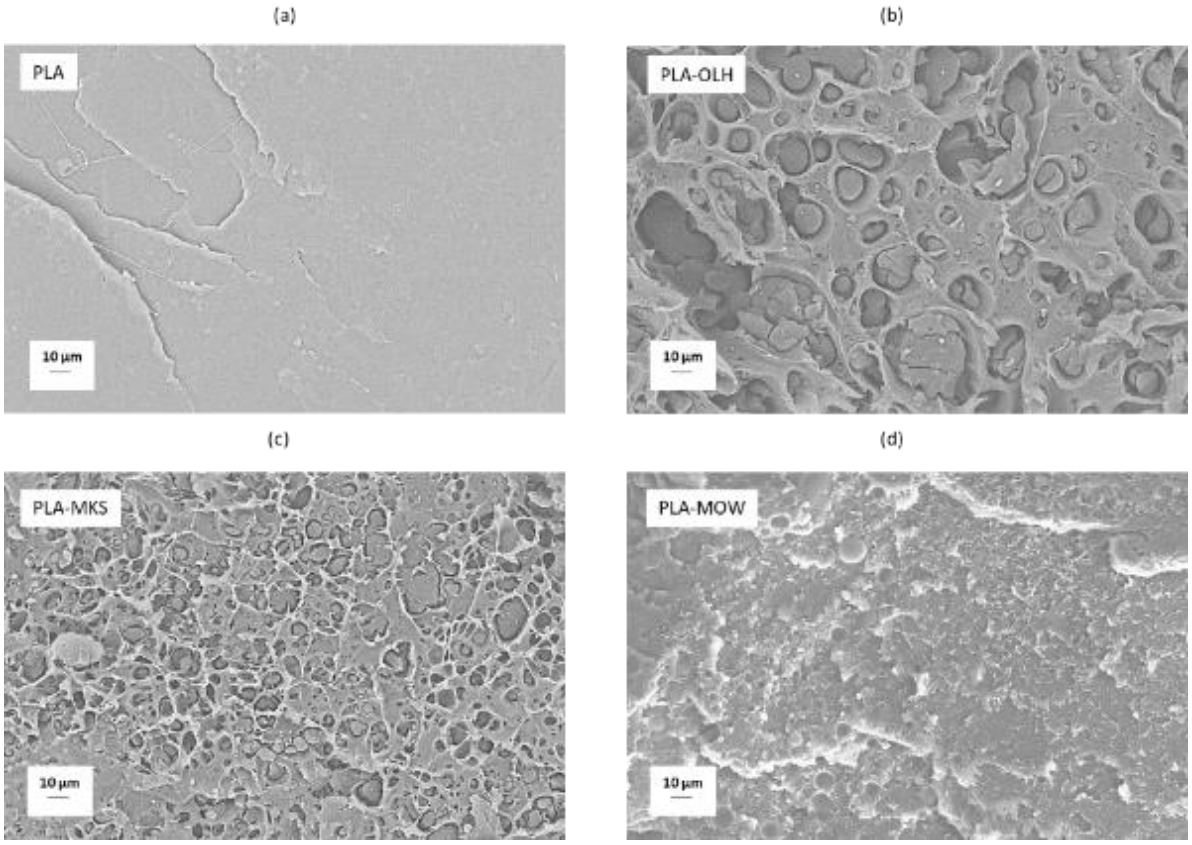

Figure D-5. Micrographs of tensile fractured surfaces the samples. (a) PLA, (b)PLA-OLH, (c) PLA-MKS and (d) PLA-MOW showing aggregates of lignin in random locations.

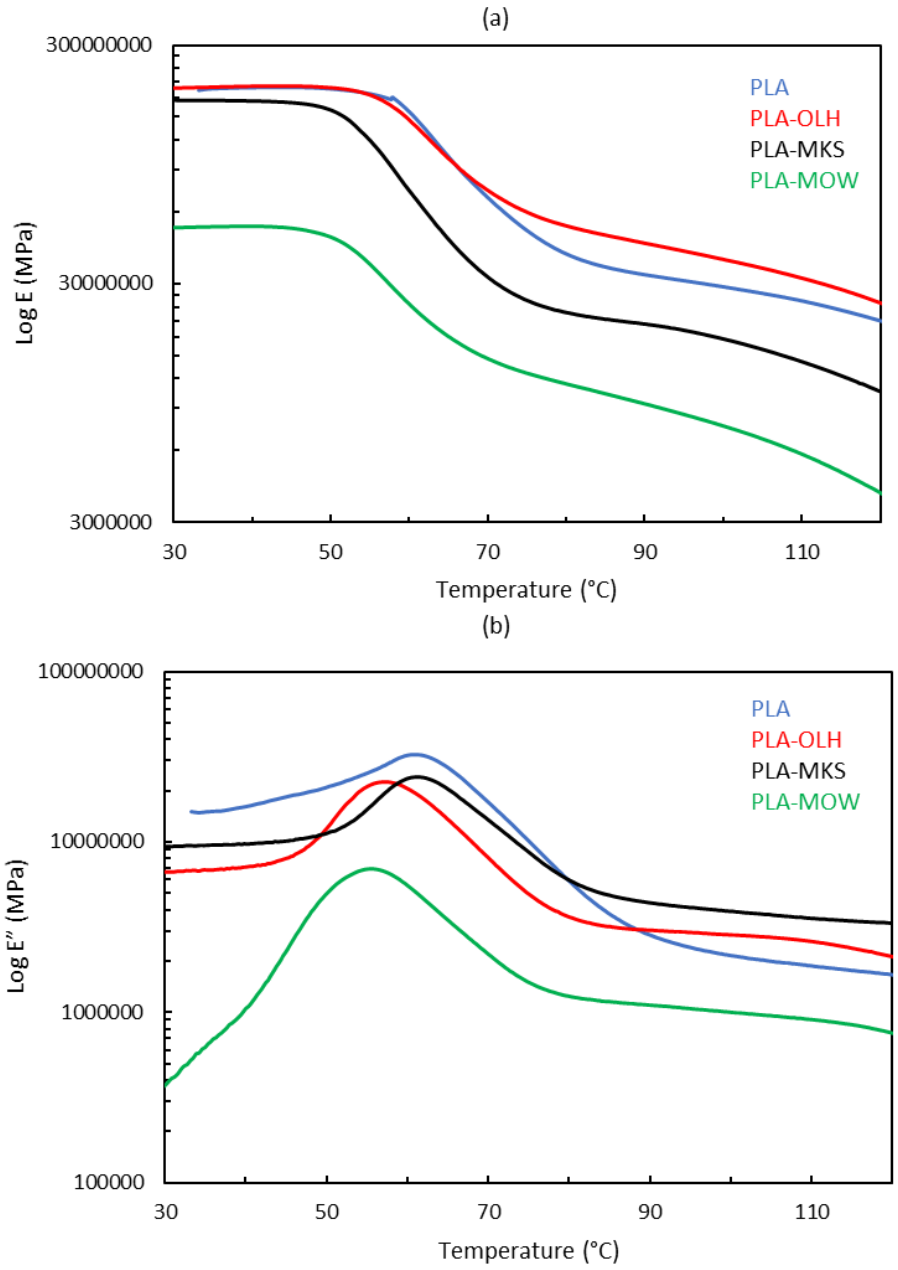

Figure D-6. Storage modulus E and loss modulus E" data for neat PLA and PLA-lignin derived blends at 1 Hz.

CHAPTER 6
CONCLUSION

6.1. Conclusions

Lignin is the second most abundant organic material from plant biomass and is relatively inexpensive. Using lignin as a low-cost feedstock in renewable polymeric blends provides an important near-term boost to the economics of biomass processing industries. Developing high-performance polymers from lignin is attractive, but often requires additional lignin purification and significant functionalization followed by copolymerization. Often, the additional processing steps do not offer favorable cost-to-performance ratio of the lignin-derivatives. This work analyzed lignin sourced from various biomass such as oak, pine, and wheat straw and studied the effects of these lignin chemistries on the properties of commodity plastics such as ABS, recycled PET, and bio-derived PLA. The goal of this study was the development of sustainable high-performance plastics from thermoplastic blends of lignin without chemical modification.

In chapter 2, we have discussed successful development of a path for loading lignin to a high-performance engineering thermoplastic matrix (ABS) without the usual deleterious effects on mechanical properties under reactive condition. A thermoplastic ABS resin containing nearly 30 wt.% lignin was formulated to exhibit properties like those of neat resin by incorporating 10 wt.% PEO (with respect to lignin fractions). The developed partial renewable polymer showed excellent properties when reinforced with short carbon fibers at 20 volume % and meets performance criteria as lightweight automotive materials for enhanced fuel economy.

In chapter 3, we have presented modification of engineering polyethylene terephthalate (PET) polyester matrix waste through plasticization with renewable tall oil fatty acid (TOFA). This plasticization improves the processability of PET and broadens applications of PET scraps from the manufacturing floor. We accomplished a reduction of PET processing temperature from 270-285°C to 240°C. This helps to improve the recycling of the waste and enable the processing of PET With biopolymers (i.e. lignin). This is an alternative way to recycle polyester waste that would have ended up in landfill and caused environmental hazard.

In chapter 4, we demonstrate that lignin dispersion and interfacial interaction can be controlled in recycled PET/lignin alloys through thermal pretreatment of lignin. Addition of renewable plasticizer at 10 wt.% relative to PET helped to soften PET below its normal processing temperature to avoid further degradation of lignin during mixing. Thermal treatment of lignin decreases aliphatic hydroxyl group, minimizes lignin-lignin intermolecular interactions and improves lignin thermal stability. Relative tensile failure stress of lignin-PET alloys with respect to that of the PET matrix improves by 15 % by thermal pretreatment of lignin for the composition with 30 wt. % lignin.

In chapter 5, we summarize specific interactions of three technical lignins with polylactic acid (PLA) matrix. Lignin functionalities were analyzed and its effects on the blend properties were assessed. For example, aliphatic hydroxyl and carboxylic acid groups' decomposition affect thermal stability of the PLA-lignin blends. Other factors such as

lignin purity, poor dispersion of lignin during mixing, foaming of materials were found to impact the blends properties as well.

In summary, we addressed our principal goal by evaluating diverse ways to develop thermoplastic-lignin blends. We added compatibilizer to help with dispersion. The proposed solution of modifying industrial resin (ABS) and its composite products by incorporating a significant quantity of lignin offers to reduce the carbon footprint through the direct use of these partially renewable plastics and the production of lighter weight automotive materials for enhanced fuel economy. Therefore, the results shown here have significant potential for beneficial economic and societal impacts. We also used processing aid to reduce processing temperature to avoid lignin degradation. TOFA shows a potential as a renewable and cost-effective plasticizer for post-industrial PET wastes. Our formulations use lignin, a low-cost renewable resource, post-industrial PET waste destined for landfills, and renewable plasticizer TOFA, a low-priced byproduct from pulping industries to develop a renewable alloy with well dispersed lignin domain and moderate mechanical performance. This work highlights development of renewable thermoplastics based on lignin and sustainable industrial waste PET, offering a path for high-volume utilization of lignin in a value-added form. Finally, we evaluated different lignin to elucidate how lignin source and chemistry are important in the performance of the blends. This study can help to establish a library of available lignin and work with lignin manufacturers to deliver homogeneous consistent lignin for thermoplastic-lignin development toward lignin valorization. Overall, this research provides an economic way to valorize lignin and address environmental benefits. This work will lead to future publications.

6.2. Future research

The idea to use unmodified lignin as a feedstock for polymeric materials is attractive for economic reasons. This work shows that different polymers can be used in the development of thermoplastic-lignin alloys. There are several areas that open the opportunities for future research and pave the way for industrial production of the thermoplastic-lignin materials.

We need to continue screening of the lignins for its best compatibility with a preferred host matrix and finding lignin source that is homogenous and structurally consistent by working with lignin manufacturing companies. Lignin purity will be another area to expand on as it could be a deciding factor to improve thermal stability of lignin and subsequent blends by removing low molecular weight unstable compounds during processing of lignin.

Current state-of-the-art high-performance polymers from lignin requires additional lignin modification that is cost intensive. One can investigate if lignin modification can be made economically viable and scalable to deliver low-cost lignin derivatives. Additionally, one can explore 3D printing of the lignin-thermoplastic blends as additive manufacturing is gaining momentum and industrial interest. Developing renewable polymeric materials that are readily printable will be beneficial to commercial applications.

Last but not the least, a cost model for different lignin and suitable matrix system for target application can establish pathway for commercialization and large-scale manufacturing. The model must include costs associated with lignin isolation, matrix modification, if any, and reactive processing of thermoplastic-lignin blends.

VITA

Kokouvi was born in Lome, TOGO (West Africa). He obtained his bachelor's in science in Material Science and Engineering from the University of Tennessee, Knoxville (UTK) in 2010. He remained at UTK to work toward his M.S. in Polymer Engineering under Dr. Gajanan Bhat direction. He studied cellulose-based carbon fiber for his M.S. thesis. He also focused on processing and characterization of nonwoven materials. After receiving his M.S., Kokouvi joined the Carbon and Composites Group at Oak Ridge National Laboratory (ORNL) working with Dr. Amit Naskar. His research involved alternative low-cost carbon fiber precursor development, polymer matrix composites, and recovery of carbon composites from recycled tires for energy application. In Fall 2015, Kokouvi joined the Bredesen Center for Interdisciplinary Research and Graduate Education to pursue his PhD in Energy Science and Engineering under the guidance of Dr. Amit Naskar. He worked on the development of renewable polymeric materials. He is currently doing his research at the Center for Renewable Carbon (CRC) at UTK.